Karlsruhe Institute of Technology

# Squeezed Light Emitting Diode

# Supraleiter-Leuchtdioden Heterostruktur als Quelle von gequetschtem Licht

Diploma Thesis of


Paul Sebastian Baireuther

At the Department of Physics
Institut für Theorie
der Kondensierten Materie


Reviewer: Prof. Dr. Jörg Schmalian
Second reviewer: Prof. Dr. Kurt Busch

Duration: 16. June 2011 – 16. July 2012

Als Ansichtsexemplar genehmigt von

. . . . . .

Karlsruhe, den 16.07.2012, Prof. Dr. Jörg Schmalian

# Erklärung zur Selbständigkeit

Hiermit erkläre ich, die vorliegende Arbeit selbstständig angefertigt und dabei nur die angegebenen Quellen und Hilfsmittel verwendet zu haben.

. . . . . .

Karlsruhe, den 16.07.2012, Paul Baireuther

# Contents

# 1. Introduction

Confluence of two established materials or technologies often leads to the emergence of qualitatively new phenomena. One of the best known examples is the resonant circuit. It consists of an inductor and a capacitor and has properties that neither of its parts has by itself. Or as Aristoteles put it: "The whole is more than the sum of its parts."

Two of the most exciting classes of materials are semiconductors and superconductors. Semiconductors are *the* foundation of all our modern technology. They are the raw material for transistors, diodes, MOSFETs and many other ingredients of modern technology. Computers, mobile phones, remote controls and uncountable other devices require these semiconductor based building blocks. A basic building block of semiconductor electronics is a p-n junction or diode. It consists of a heterostructure of a electron-doped semiconductor and a hole-doped semiconductor. If the bandstructure of a diode has a direct band gap in the vicinity of the interface, an electron that tunnels from the conduction band of the electron-doped side to the valence band of the hole doped-side releases its excess energy via emission of a photon [Rou07]. (This process can also happen in reverse which is the principle of a solar cell.) Therefore light emitting diodes (LEDs) provide a beautiful man made electron-photon coupling. Superconductors, while currently less visible in our everyday life (mostly because they need extensive cooling), are often considered a foundation for future technologies. In medicine they are the key element to build ultra strong magnets which are needed for magnetic resonance imaging. And there is more to them than zero resistivity. They exhibit quantum mechanical properties on a macroscopic scale. The ground state of a superconductor, first described by Bardeen, Cooper, and Schrieffer in 1957 [BCS57], is a macroscopic coherent state extending over the entire sample size and has a well defined phase. It consists of a superposition of entangled electron pairs, called Cooper pairs. One of the most remarkable effects in superconductor-non superconductor heterostructures is that, under certain circumstances, Cooper pairs can tunnel into the non superconducting materials and survive there long enough to induce superconductivity by proximity. As a consequence, these materials become a superconductor themselves, while at the same time keeping some of their original properties.

Naturally, this remarkable injection property of superconductors has triggered a plethora of experiments and theoretical considerations that investigated a large variety of superconductor-non superconductor heterostructures. Arguably the most important of these are Josephson junctions [Jos62] consisting of two superconductors separated by an insulating layer. They are the basis for superconducting quantum interference devices (SQUIDs).

Over a long time all systems that where investigated were solely based on electric charge and current. However, about ten years ago, people started to wonder what happens if one brings superconductivity together with light emitting structures such as a light emitting diode. If the Cooper pairs can tunnel deep enough and survive long enough in the LED, would they couple to the emitted photons? And if this is indeed the case, which unusual properties would the emerging light have? A first guess would be coherent light, which is well known from lasers, since a superconductor is described by state. However, laser light is described by coherent *single* photon states and superconductors by coherent *two* electron states. In quantum optics literature one finds that the concept of two photon coherent states is known under the term squeezed light. The idea of squeezing dates back to Schrödinger [Sch26]. If one considers a pair of conjugated variables, than the product of their variances satisfies Heisenberg's uncertainty principle. If this uncertainty is not equally distributed between the two variables, the system is in a squeezed state. In analogy to position and momentum in an oscillator the electric field of light can be described by a pair of conjugated variables, called quadrature amplitudes. Their choice is not unique. If there exists at least one pair of quadrature amplitudes for which the uncertainty is not equally distributed, we talk about squeezed light. The first extensive discussion of squeezed light didn't take place before 1968 [KS68]. The interest in squeezed light increased about two decades ago, when high precission measurement devices, such as interferometers, had reached a precission where reducing quantum fluctuations became an important issue. This can be achieved using squeezed light. The idea has caused great interested in the field, and triggered the search for a suitable source. However, to our knowledge, so far there exist no generic source capable of direct production of squeezed light. The most popular method is spontaneous parametric down conversion (SPDC) [BW70] and relies on the conversion of an existing light beam into squeezed light. Unfortunately the efficiency rate of SPDC is very low.

In this thesis we propose that a superconductor-LED-superconductor heterostructure may be such a generic source of squeezed light. In 2002 Eiichi Hanamura suggested a similar heterostructure for an increased photon emission rate [Han02], and conjectured that it might be a source of entangled photon pairs. Experimentally a light emitting diode with a superconductor attached to one side was first realized a couple of years later [HTA$^+$08], and supported Hanamura's idea of increased photon emission rate. This experiment in turn triggered subsequent theoretical investigations [ASTH09], [RNK10], [HNK09] and [GHN11]. In this work we consider a LED with two superconducting contacts, and focus

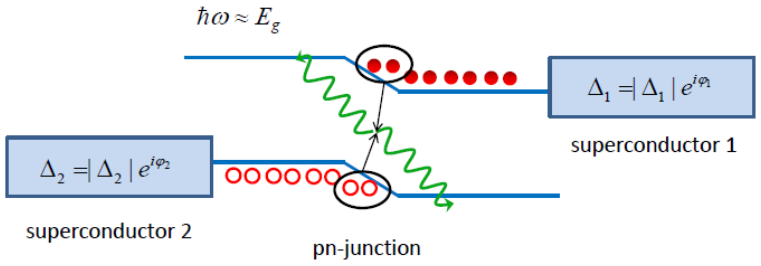


Figure 1.1.: Superconductor-Light Emitting Diode-Superconductor heterostructure

on the properties of the emitted light. Since we want to investigate if the presence of the superconductors leads to the emission of squeezed light, we treat the phases of the superconducting leads accurately. We show that the relative phase between the superconductors is inherited by the emitted photon pairs. We derive an effective photon description that exhibits a photon-photon coupling with a rotating phase. Such a coupling is known as parametric amplifier [GM65] and causes the squeezing of light. We explicitly calculate the variance in the quadrature amplitudes to show that a high degree of squeezing can

be achieved. Finally we conclude by demonstrating that we can utilize the relative phase to control how the uncertainty ellipse is orientated in a diagram where the x- and y-axes display the magnitudes of a pair of quadrature amplitudes.

## 1.1. Outline

This work is structured as follows: We begin with a review of experimental work to demonstrate that Cooper pairs can probe deeply into a light emitting diode, reach the region where the photon production takes place, and has an impact on the photon emission. We then discuss previous theoretical work on similar problems to give an overview about the state of the art and in what respect our work is different and new. In chapter 3 we introduce and discuss the fundamental concepts that are relevant for our analysis. In the subsequent chapter we explain how a light emitting diode is modeled and how we include the superconducting leads. Chapter 5 is the main part of this work. We first discuss the spontaneous photon emission of a normal light emitting diode and investigate which effect higher order corrections have. Then we derive an expression from which the properties of the emitted photons become obvious. Due to the superconductivity it contains a term that acts as a parametric amplifier, which is responsible for the squeezing of light. In the last section we show that the emitted light is squeezed and that we can control the orientation of the uncertainty ellipse with respect to a particular pair of quadrature amplitudes.

# 2. Review

## 2.1. Experiments

In this section we review experimental work that investigates superconductor- semiconductor junctions. We focus on two sets of consecutive papers [ITA$^+$10], [TIA$^+$10] and [SKH$^+$11], [HTA$^+$08], [SHK$^+$10]. Before we start the discussion we present some experimental results regarding a superconductor-semiconductor-superconductor Josephson junction from [SAT$^+$06]. Subsequently we review the first set of papers, which is centered around the investigation of the proximity effect in a p-n-junction. In the third part of this section we focus on the second set. It investigates the photon emission rather than just electric currents.

### 2.1.1. Proximity Effect in Semiconductors

When a superconductor is attached to a non-superconductor with mobile charge carriers, including semiconductors, Cooper pairs can tunnel from the superconductor into the non-superconductor. The characteristic length scale on which the Cooper pairs leak into an attached material is proportional to the third root of the electron density in the non-superconducting material $\xi \approx (n_{el})^{1/3}$ [SKH$^+$11]. Therefore, if one wants to induce superconductivity into semiconductors the latter should be highly doped. Below we summarize an experiment in which the electron density exceeds $3 \cdot 10^{19}\text{cm}^{-3}$. Another very important factor is that the lattices of the superconducting and the non-superconducting materials have to match in order to ensure a good ohmic contact. For this reason, as of today, no experiments where a superconductor was attached to a p-doped semiconductor have been reported. In the experiment that was reviewed in [SAT$^+$06] a n-doped layer is inserted between two Niobium contacts. Niobium becomes a superconductor below 9 Kelvin. Naively we would expect a roughly linear I-V curve, for not too high voltages, because the semiconductor is a limiting factor for the current. At room temperature this is true. At temperatures somewhat below the critical temperature of Niobium however the I-V curve exhibits a jump at zero bias voltage. This is because the induced Cooper pairs make the semiconductor superconducting. In the experiment this is shown in figure 2.1, where the temperature was 0.7 Kelvin. This experiment shows that superconductivity can indeed be induced into a semiconductor.

### 2.1.2. Proximity Effect in a p-n junction with bias voltage

In this subsection we discuss two more or less equivalent papers [TIA$^+$10] and [ITA$^+$10] that report experimental findings about a hybrid of Josephson junction and pn junction.

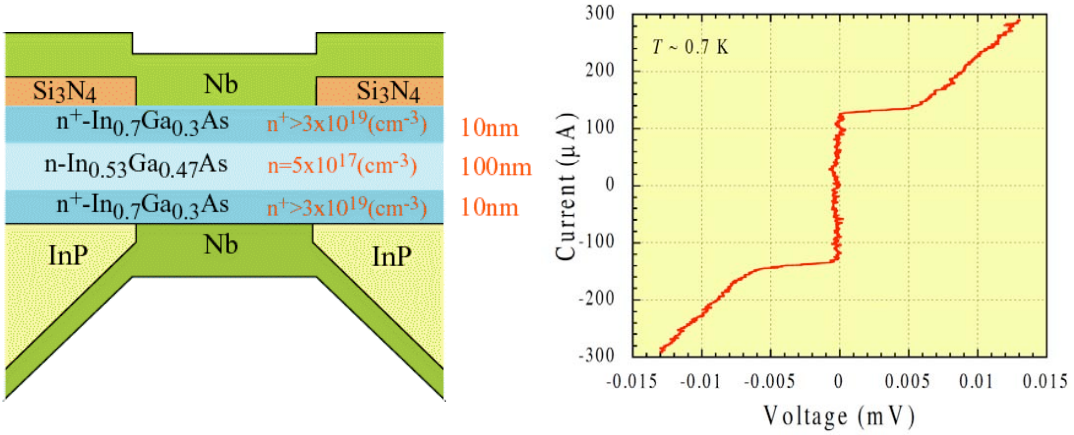


Figure 2.1.: Proximity Effect - Source [SAT+06]

Two niobium electrodes are attached to the n-side of a highly doped p-n junction (see figure 2.3). The niobium electrodes together with the n-doped semiconductor form a Josephson junction and the presence of the p-doped semiconductor creates a depletion layer at the p-n interface. Together with a bias voltage this allows to control the effective width of the n-doped side and thus the current in the Josephson junction. There are two different

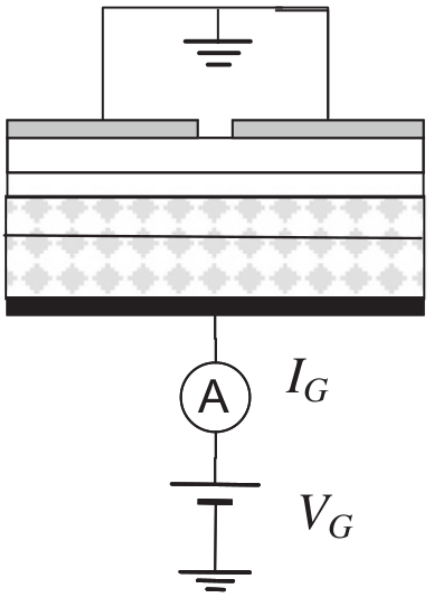


Figure 2.2.: Measurement Setup - Source [TIA+10]

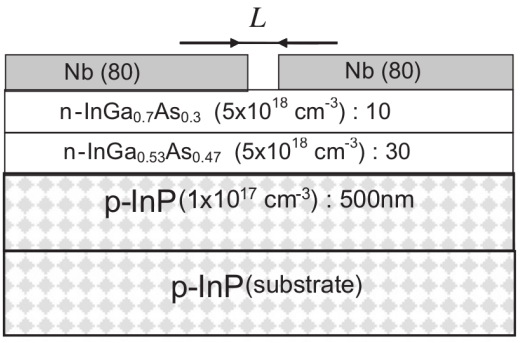


Figure 2.3.: Schematic Sample Structure- Source [TIA+10]

currents that can be measured in this setup. The Josephson current between superconducting leads and the current which is injected by a bias voltage applied between gold- and the superconducting lead. A schematic picture of the setup is shown in figure 2.2. Well below the superconducting temperature of niobium the system exhibits a supercurrent. In figure 2.4 "Shapiro steps (AC Josephson effect) indicate that the Nb-InGaAs-Nb junction is a Josephson junction and the supercurrent depends on the phase difference of the superconductors." [TIA+10]

A particularly important question for the realization of Cooper pair based LEDs is, whether Cooper pairs can tunnel deep enough into the semiconductor and reach the p-n interface.

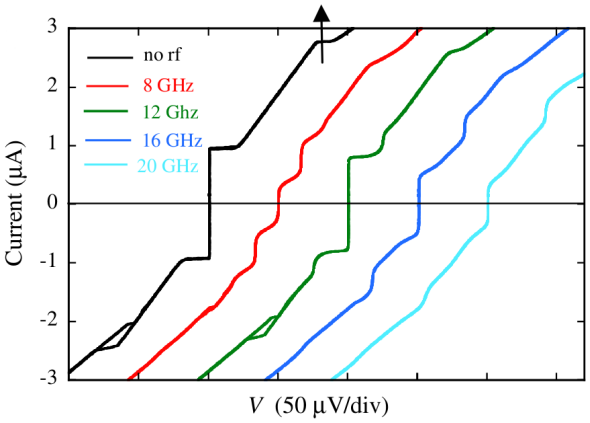


Figure 2.4.: Supercurrent with and without microwave irradiation - Source [TIA$^+$10]

This is important because the photon production takes place in the region around the interface. Experimental evidence [ITA$^+$10] and [TIA$^+$10] suggest that they in fact do so. The logic is the following: The width of the depletion layer dependents on the bias voltage. Forward bias reduces the width of the depletion layer, thereby increasing the widths of the non depleted regions. Since the proximity effect is proportional to the third root of the electron density, a supercurrent can not exist in the carrier depletion region of a diode. Therefore, if the critical supercurrent is increasing under the application of a forward bias, it is direct evidence that Cooper pairs are present in the vicinity of the depletion layer. In figure 2.5 the critical current between the two superconducting leads is plotted over the bias voltage. In region I the current induced by the bias voltage is negligible ($\sim 0.1nA$). Hence the bias voltage results in a field effect, that changes the width of the depletion layer. In this region the critical current increases almost linearly with bias voltage. This is direct evidence, that the proximity effect probes the semiconductor up to the depletion layer. Another nice plot from a different paper [SKH$^+$11] with the same conclusion is shown in

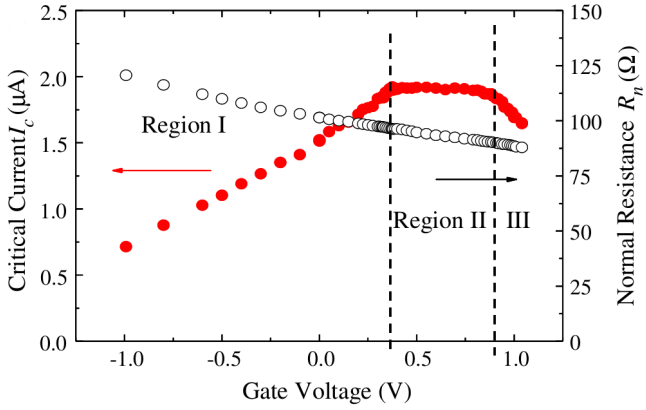


Figure 2.5.: Critical current - Source [TIA$^+$10]

Fig. 2.6. The physics in the other two regions at higher bias voltage is less thoroughly understood. What is known is that in region II the injected current increases by about two orders of magnitude. Why this leads results in a bias voltage independent critical current is not fully understood. A possible explanation is that for a bias that corresponds to the gap of the p-n junction the width of the depletion layer has shrunken to zero. In region III the injected current is a finite fraction of the critical current ($\sim 0.5\%$). In figure 2.5 we see that the critical current decreases rapidly in this region. H. Takayanagi et al argue that this is due to the injected nonequilibrium carriers. But the issue more subtle. Injected holes

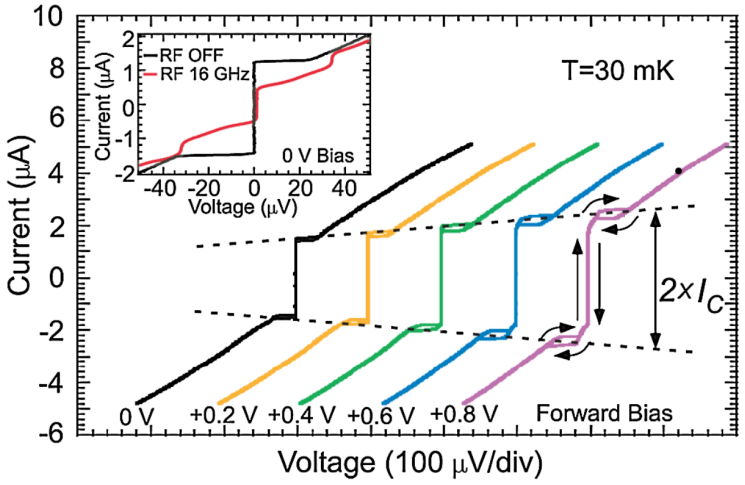


Figure 2.6.: Proximity Effect - Source [SKH+11]

from the p-side diffuse to the p-n junction where they recombine with electrons from the n-side which often results in the emission of photons. These photons have energies much higher than the binding energy of Cooper pairs. Therefore photons break Cooper pairs. The real damage to the Cooper pairs however is done by the resulting 'hot' electrons which break many other Cooper pairs. (see figure 2.7). H. Takayanagi et al [SKH+11] named

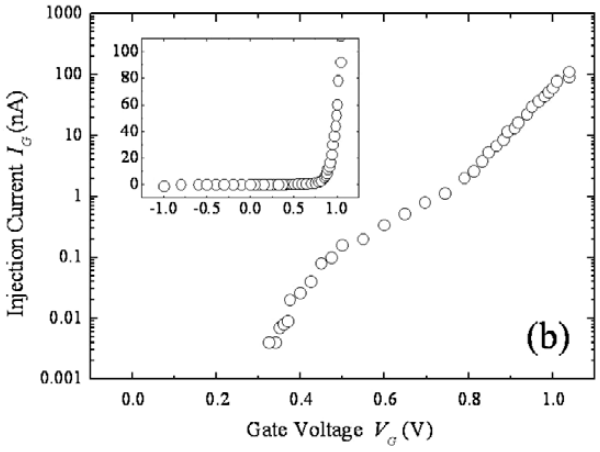


Figure 2.7.: Injected current due to bias voltage - Source [SKH+11]

the ratio of injected holes to break Cooper pairs the recombination efficiency (RE). Based on the assumption that without the photon production the critical current would continue to increase linearly with the forward bias voltage (see figure 2.9), they extrapolate the recombination efficiently to be as high as 700 in region II. With even higher bias voltages it decreases rapidly to the steep increase of injected holes.

### 2.1.3. Superluminescence

In this subsection we discuss a slightly more complicated experiment. The sample is almost the same as in [TIA+10], [ITA+10] but this time the measurement setup includes photon detectors (see figure 2.10). A schematic sketch of the recombination process of Cooper pairs with normal holes as well as an effective band structure is shown in figure 2.14. There are three major processes happening, when the n-side of a LED is attached to a superconductor. Non-radiative recombination, radiative recombination of normal carriers with normal holes and radiative recombination of Cooper pairs with normal holes. Each

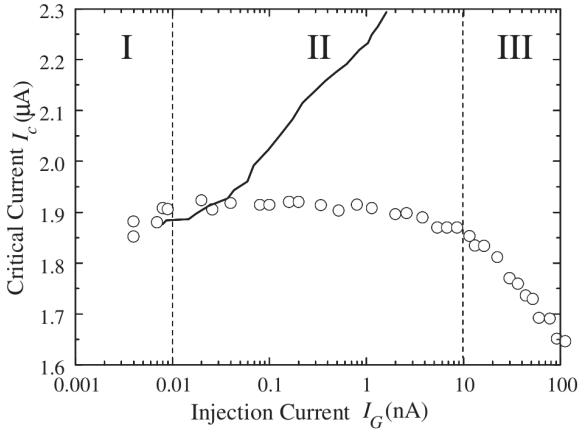


Figure 2.8.: Critical current II - Source [TIA+10]

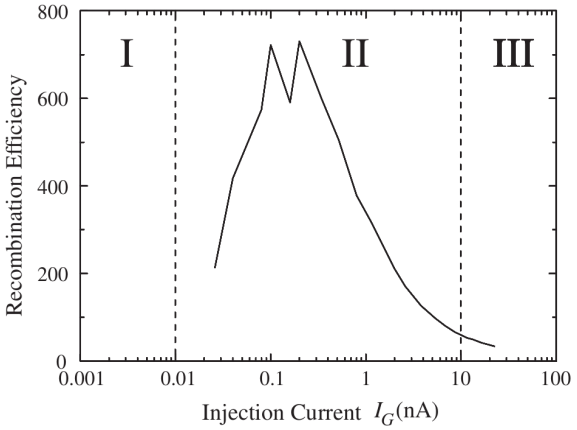


Figure 2.9.: Recombination efficiency - Source [TIA+10]

process has a specific rate $\tau^{-1}$. The total recombination time is given by $1/\tau_{LED} = 1/\tau_{rad} + 1/\tau_{nonrad}$. The radiative recombination time has a normal and a superadiative component that is phenomenologically described by

$$\frac{1}{\tau_{rad}} = \frac{1}{\tau_{rad}^{normal}} + A\frac{\Delta^2(T)}{T}\exp\Big(-\frac{2L}{\xi(T)}\Big), \tag{2.1}$$

which we cited from [ASTH09]. Here $\Delta$ is the gap of the superconductor, $L$ is the width of the n-doped layer and $\xi$ is the correlation length of the Cooper pairs. From the experimental data (fig. 2.13) we see that the recombination time rapidly decreases if the temperature is lowered below the critical temperature of the superconducting lead. This means two things. First, the Cooper pairs actually do contribute to a significant percentage of the recombinative current and second the recombination time of the Cooper pairs is much shorter than the usual recombination times in a LED. In [SKH+11] the ratio of Cooper pair to normal electron recombination is estimated to be almost 1:2 at 3K. This is also known by the term 'superluminescence'. In order to understand this term it is important to know that all the measurements where made at a fixed current through the junction. Therefore there exists an upper limit on the luminescence given by the number of electrons passing the junction. Therefore, the relevant term in this section is the efficiency, rather than the luminescence. In [HTA+08] an increase in the luminescence as a function of the temperature was observed below the critical temperature of the superconducting

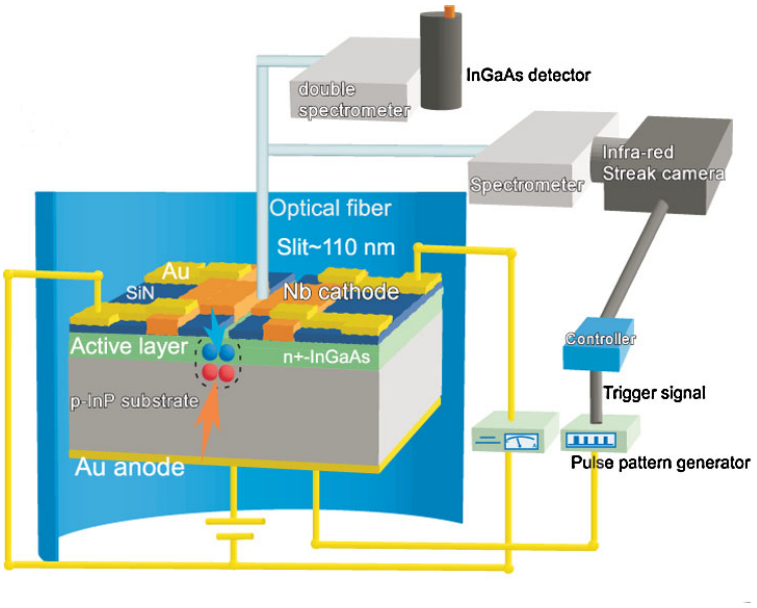


Figure 2.10.: Experimental setup - Source [SKH+11]

lead (fig. 2.15). In a follow up paper [SHK+10] this is explained by an increase of the quantum efficiency. This makes sense if the non-radiative recombination dominates over the radiative recombination. Namely, if the efficiency of the normal conducting state is well below 50 percent. If it were at 80 percent or higher, there would be little room for improvement. Thus, since the recombination time of Cooper pairs with normal holes is much shorter than the recombination time of normal electrons with holes, the efficiency

$$\eta = \frac{1/\tau_{rad}}{1/\tau_{rad} + 1/\tau_{nonrad}} \approx \frac{\tau_{nonrad}}{\tau_{rad}} \quad (\text{for } \tau_{rad} \gg \tau_{nonrad}) \tag{2.2}$$

increases below the critical temperature. In contrast to this observation in [SKH+11], published by the same group, there is no sign of the superluminescence observed in the earlier two papers (fig. 2.16). Nevertheless the recombination time still decreases as discussed in the previous section. The authors of [SKH+11] explain this by claiming that the quantum efficiency $\eta$ of the LED used in the last paper is already very high at temperatures above the critical temperature. This implies that the efficiency

$$\eta = \frac{1/\tau_{rad}}{1/\tau_{rad} + 1/\tau_{nonrad}} \approx 1 \quad (\text{for } \tau_{rad} \ll \tau_{nonrad}) \tag{2.3}$$

can't be increased very much anymore. Summarizing the experimental data shows that it is in general possible to build a Cooper pair based light emitting diode using the proximity effect. It has been shown that the Cooper pairs can tunnel all the way into the p-n interface and that they participate in the photon production. In fact the data suggest that the recombination rate of Cooper pairs with normal holes is about twice as high as for normal electrons. The only experimental challenge that remains is to induce superconductivity to the p side of the junction. This challenge lies in precise matching of lattices and is no fundamental obstacle.

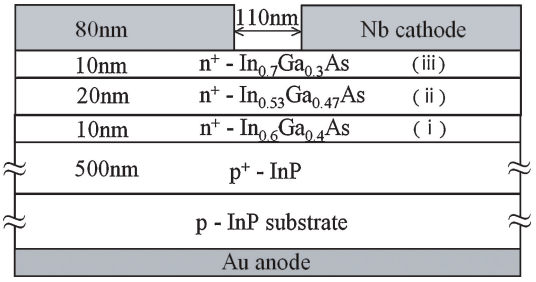


Figure 2.11.: Schematic sketch of sample - Source [HTA+08]

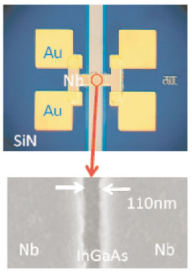


Figure 2.12.: Photo of sample - Source [SKH+11]

## 2.2. Theory

In this section we review theoretical work on setups that are similar to ours. The initial idea to a superconducting light emitting diode was put forward by Eiichi Hanamura in 2002 [Han02]. In response to this paper seven years later Asano *et.al.* published a paper to explain first experiments with proximity induced superconducting light emitting diodes. They considered the situation where the n-side of a LED is coupled to a superconductor [ASTH09] and the p-side to a normal conductor. Around the same time Leo P. Kouwenhoven et al started a set of three consecutive papers which they call Josephson light-emitting diode [RNK10], [HNK09], and [GHN11].

### 2.2.1. The initial idea by Eiichi Hanamura

In 2002 Hanamura proposed a superconducting p-i-n junction (see figure 2.17). Specifically he suggested for the p-type superconductor ($La_{2-x}Sr_xCuO_4$), for the n-type superconductor ($Nd_{2-x}Ce_xCuO_4$) and ($La_2CuO_4$ or $Nd_2CuO_4$) for the insulating layer. When a voltage is applied to such a sp-i-sn junction as shown in figure 2.17 electron Cooper pairs from the n-type superconductor and hole Cooper pairs from the p-type superconductor tunnel balistically into the insulating layer. In this layer they recombine with each other. A schematic band structure is given in figure 2.18. Both radiative and non-radiative processes possible. The paper only discusses the radiative processes. There are two distinct processes how an electron Cooper pair recombines with an hole Cooper pair. In one case the Cooper pair split up in two electrons and two holes. One of the electron recombines with one of the holes by emitting a photon. The remaining unpaired electron and hole can carry away both energy and momentum. Therefore the frequency of the emitted photon can take any value below the difference in chemical potentials of the n- and p-Cooper pair level. Also the emission angle is arbitrary. The other process, in which an electron Cooper pair recombines with a hole Cooper pair, is quite distinct. First, all photons have exactly the energy of the chemical potential difference and second the momentum of the two emitted photons sum up to zero. Together with the conservation of angular momentum this

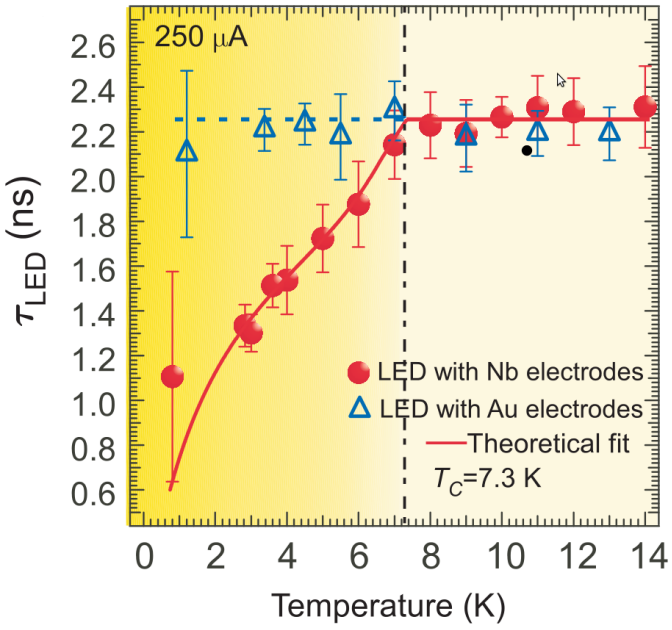


Figure 2.13.: Recombination times - Source [SKH+11]

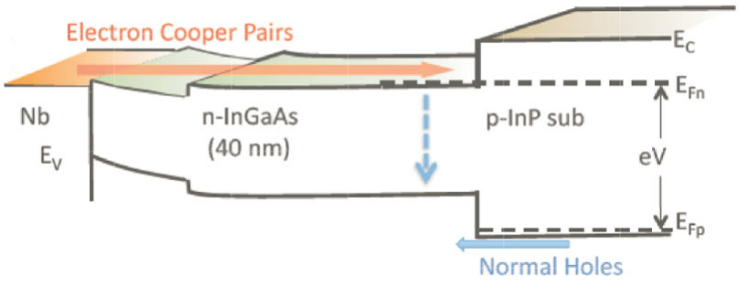


Figure 2.14.: Schematic bandstructure - Source [SKH+11]

means that the two photons of such a pair have the same chirality. Hence, the emitted photon-pair is strongly entangled with respect to a single photon basis. The sharp peak at the resonance frequency in the photon spectrum is a clear signature of the pair emission process that is accessible experimentally. The paper also discusses the realization of a laser that emits pulses of entangled photons and technical problems in the experimental realization but this is beyond the scope of this thesis.

### 2.2.2. Next to leading order contributions to the luminescence

In 2009 Asano and collaborators theoretically investigated the emission spectrum of a forward biased p-n junction which has a superconductor coupled to the n-doped side [ASTH09]. The bandstructure of such a setup is schematically shown in figure 2.19. The study is done in a second order (fourth order in the coupling constant) perturbation theory in the electron-photon interaction. Their approach to calculate the luminescence, i.e. the photon emission rate, is to calculate the short time average of the photon number

$$N_{ph} = \sum_{\mathbf{q}} a^{\dagger}_{\mathbf{q}} a_{\mathbf{q}} \tag{2.4}$$

in a zero photon state

$$|\chi_0\rangle = |0\rangle \otimes |N\rangle \otimes |P\rangle. \tag{2.5}$$

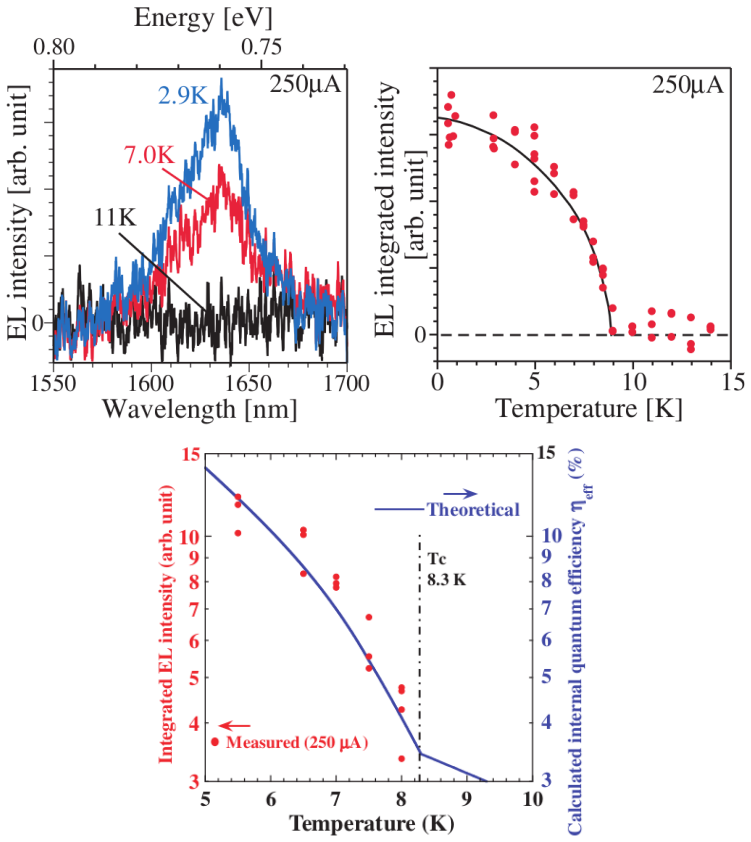


Figure 2.15.: Superluminescense - Source [HTA+08] and [SHK+10]

In this product state $|N\rangle$ describes the n-type superconductor and $|P\rangle$ the p-type superconductor. We denote the time average of the expectation value of the luminescence by $\overline{\langle N_{ph}(1)\rangle}$. Therefore it is comparable to calculate the luminescence in a stationary state and then setting the photon number in the system to zero to get rid of the absorption process as it is done in this thesis. In leading order perturbation theory they get

$$\overline{\langle N_{ph}(1)\rangle} = 2\pi \sum_{\mathbf{k},\mathbf{q},\sigma} |B_{\mathbf{k},\mathbf{q}}|^2 f^p_{\mathbf{k}-\mathbf{q}} \Big( u_k^2 f_k^n \delta(\tilde{w} - E_k) + v_k^2 (1 - f_k^n) \delta(\tilde{w} + E_k) \Big), \tag{2.6}$$

as we do, too. $B$ is the electron-photon coupling constant, $f^x$ are the Fermi distribution functions, $E_k$ the Bogoliubov quasi particle energies and $\tilde{w}$ the photon frequency minus the gap. In order to allow energy from the perturbation to leave the system they introduce an artificial relaxation time $\tau$. In next to leading order they obtain

$$\overline{\langle N_{ph}(2)\rangle} =\sim |B|^4 \sum_{\mathbf{k}} \left( \frac{f_k^n(1-f_k^n)}{(E_k - \mathrm{i}/\tau)^2} + \frac{f_k^n(1-f_k^n)}{(E_k + \mathrm{i}/\tau)^2} + \frac{(f_k^n)^2 + (1-f_k^n)^2}{E_k^2 + (1/\tau)^2} \right) \frac{|\Delta|^2}{E_k^2}. \tag{2.7}$$

When we carry out the last summation by rewriting it as an integral times the density of states we see that in the limes of vanishing relaxation rate the luminescence is proportional to the density of states in the superconductor divided by the superconducting gap. Therefore, since the density of states of a superconductor diverges above and below the gap and because the superconducting gap is usually one of the smallest scales in a problem the luminescence is greatly enhanced in comparison to a normal light emitting diode. The fact that the next to leading order terms dominate over the leading order renders perturbation theory useless one sums up an infinite series of diagrams to regularize the results. In their paper Asano et al choose a more physical approach. First they employ elastic impurity

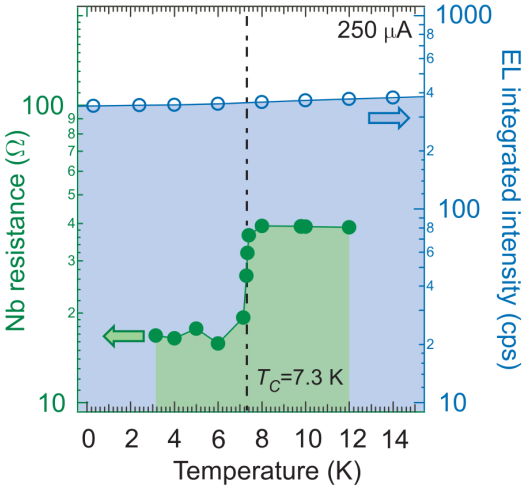


Figure 2.16.: Recombination times and efficiency rate - Source [SKH+11]

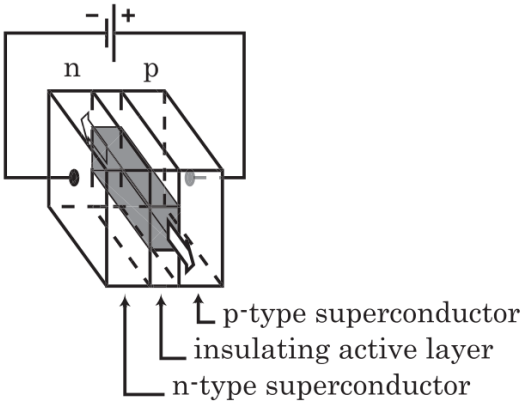


Figure 2.17.: Setup - Source [Han02]

scattering and then inelastic scattering. The results are plotted in figure 2.20. Figure a) shows the elastic case and figure b) the inelastic case. The scattering rate in the inelastic case depends on temperature and vanishes at zero temperature. Typical mechanisms for inelastic scattering is electron-phonon or electron-photon scattering. In the elastic case at high damping they predict a monotonous behavior of the luminescence. However for low damping the curve acquires a maximum slightly below the critical temperature and then converges to a finite value as in the high damping cases when the temperature approaches zero. In the inelastic case the situation is quite different, since the scattering rate decreases with decreasing temperature, going to zero when the temperature reaches zero Kelvin. Therefore all curves coincide at zero temperature. At low damping they predict the same anomalous behavior as in the elastic case. Finally they modify their model to describe a more realistic situation including the proximity effect and tunneling into a quantum dot in order to model experimental data. Their final formula (for $T < T_c$) is

$$\overline{\langle N_{ph}(2)\rangle} \approx |B|^4 \mathcal{N}_0 \Gamma \sum_{\mathbf{q},\sigma} \frac{|\Delta|^2 \tau^2 \mathrm{e}^{-2L_w/\xi_T}/T}{(w_q - w_0)^2 + \Gamma^2}, \tag{2.8}$$

where $\Gamma = t_w^2 \mathcal{N}_0$ and $t_w$ is the transfer integral between the quantum well and the semiconductor. This behavior is indeed qualitatively confirmed by experiments [SKH+11]. Summarizing Asano and collaborators found that the presence of Cooper pairs in the n side of a light emitting diode leads to an enhanced photon emission rate in the next to lead-

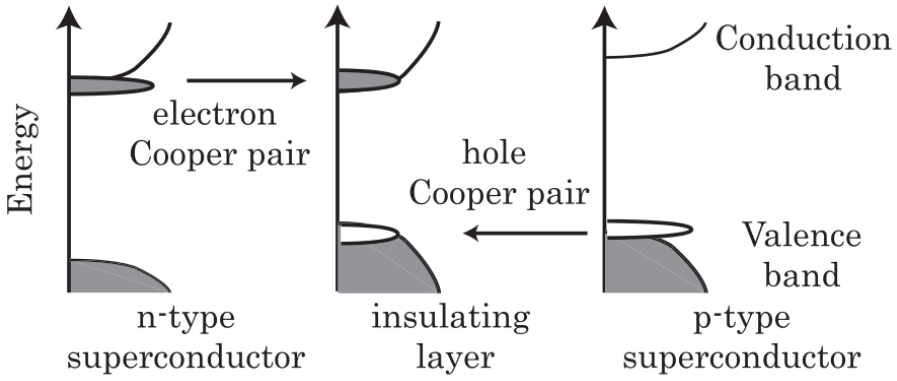


Figure 2.18.: Bandstructure - Source [Han02]

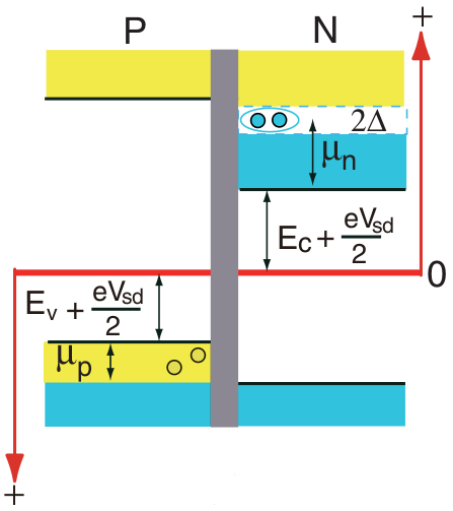


Figure 2.19.: Schematic bandstructure - Source [ASTH09]

ing order contribution. Physically they attribute this to the fact that the superconducting state is almost unaltered if a Cooper pair is removed.

### 2.2.3. Josephson light emitting diode

In the years 2009-2011 Recher *et.al.* cooperated on a set of papers [RNK10], [HNK09], and [GHN11] that investigate an optical quantum dot with two levels. The quantum dot is embedded into a p-n junction which has superconducting leads are attached to the conduction band of the n-side and the valence band of the p-side. A bias voltage close to the band gap of the semiconductors is applied in forward direction to stimulate the emission of light. A schematic sketch of their model is shown in figure 2.21. They distinguish between two types of emitted photons which they call blue and red. Blue photon emission is due to the Cooper pair exchange between the two superconducting leads. This means a single photon is emitted from the recombination of a Cooper pair. We note that this should be suppressed, strictly speaking it violates momentum conservation. However blue photons don't come in pairs and therefore are of no interest for this thesis. For our considerations the much more interesting part of their work outlined is the production of what they call red photons which have a frequency of $w \approx$ eV, because it allows for the production of entangled photon pairs. Their Hamiltonian for one isolated level of the quantum dot is

$$H_D^c = \epsilon_c \sum_\sigma c_\sigma^\dagger c_\sigma + \Delta_c c_\uparrow^\dagger c_\downarrow^\dagger + \Delta_c^* c_\downarrow c_\uparrow + U n_\uparrow n_\downarrow,$$

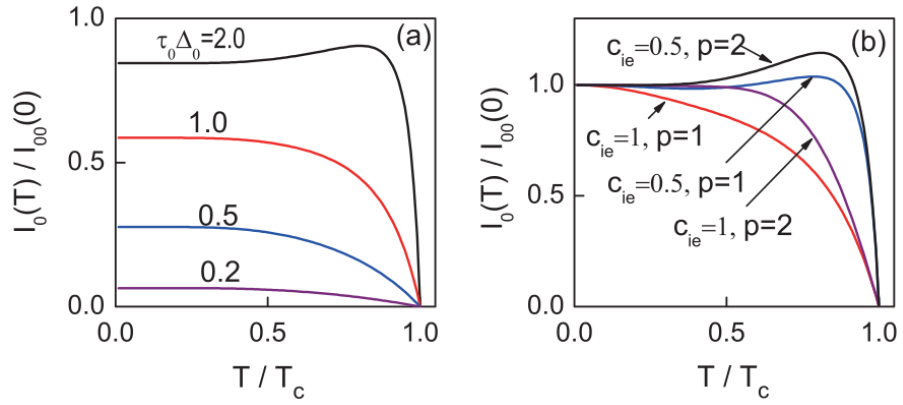


Figure 2.20.: Luminescence intensity - Source [ASTH09]

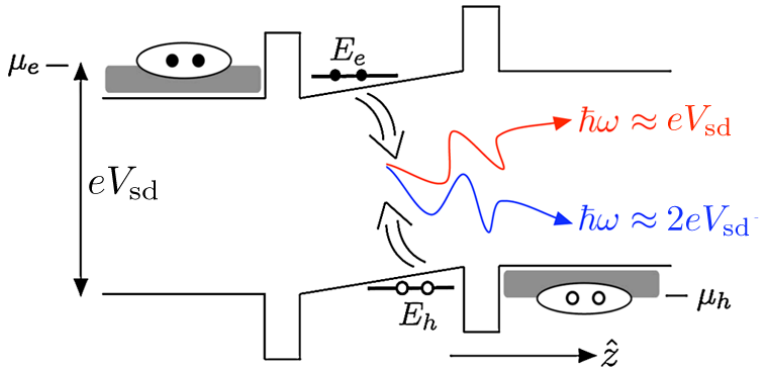


Figure 2.21.: Schematic bandstructure - Source [RNK10]

where $U$ is the onside Coulomb repulsion. Diagonalization reveals two degenerate doublet states and two non degenerated singlet sates:

$$
\begin{aligned}
|g\rangle &= -\mathrm{e}^{-\mathrm{i}\phi}|u||0\rangle + |v|c_\uparrow^\dagger c_\downarrow^\dagger|0\rangle && \text{ground state} \\
|\uparrow\rangle &= c_\uparrow^\dagger|0\rangle && \text{degenerated intermediate state} \\
|\downarrow\rangle &= c_\downarrow^\dagger|0\rangle && \text{degenerated intermediate state} \\
|e\rangle &= -\mathrm{e}^{-\mathrm{i}\phi}|v||0\rangle + |u|c_\uparrow^\dagger c_\downarrow^\dagger|0\rangle && \text{excited state}
\end{aligned}
$$

The factors $u$ and $v$ as well as the relative phase $\phi$ are the usual factors from the Bogoliubov transformation. In order to describe the physical processes however it is more convenient to use the language of occupation number states instead of eigenstates. There are two major circles of transition between different number states. One in which the total system has even parity (see figure 2.22) and one where the system has odd parity (figure 2.23). There are also transitions that change the parity but these are much slower than the two cycles just mentioned. This is because radiative recombination does not change the parity of the quantum dot. So in oder to change the parity of the system an photon must be emitted and at the same time a Bogoliubov quasi-particle must be created in one of the superconducting leads. The rate $r$ of the parity changing processes,

$$r = \Gamma_{ph}\Gamma_e/|\Delta_e|, \tag{2.9}$$

is approximately given by the ratio of the recombination rate of electrons with holes $\Gamma_{ph}$ times the tunneling rate between the superconducting leads with the quantum dot $\Gamma_e$ divided by the Cooper pair binding energy $|\Delta_h|$. The different transitions that emit photons

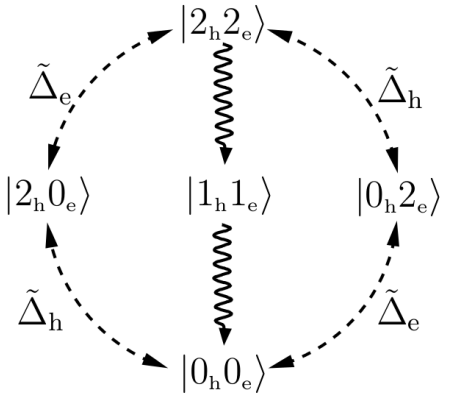


Figure 2.22.: Even parity cycle - Source [HNK09]

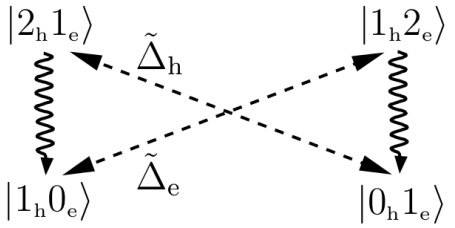


Figure 2.23.: Odd parity cycle - Source [HNK09]

result in sharp peaks in the photon spectrum. From the transitions that do not conserve parity results a continuous spectrum of emitted photons. This is because the Bogoliubov quasi-particle which is created along the way can carry an arbitrary amount of energy. The full emission spectrum is shown in figure 2.24. The dotted line depicts the spectrum with non-superconducting leads. The continuous tail due to the slow second order processes is separated from the peaked emission spectrum by the energy of the lowest Bogoliubov quasi-particle in the leads which is the superconducting gap $|\Delta|$. It is enlarged in the inset. At this point it is remarkably that the total intensity of the continuous spectrum in the non-superconducting case is comparable to the total intensity of the three peeked lines of the superconducting case. This is surprising, since in other theoretical papers a tremendous enhancement of the luminescence was predicted [ASTH09]. In order to create

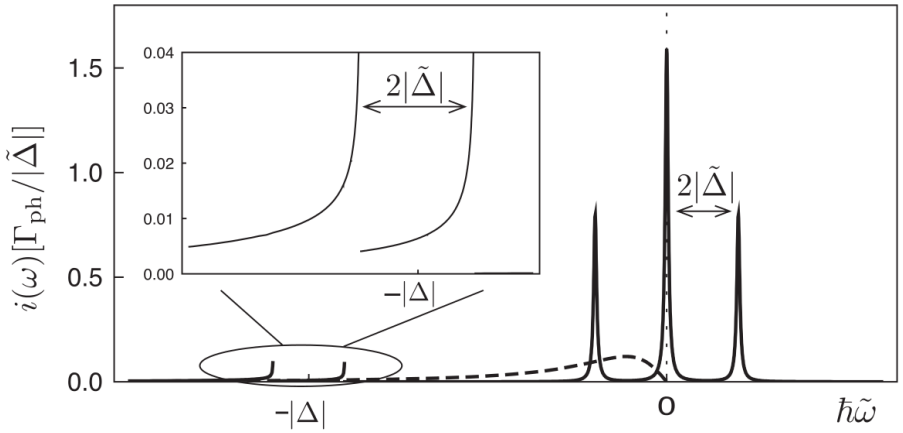


Figure 2.24.: Emission spectrum - Source [RNK10]

a constant electron emission using the cycle shown in figure 2.22, the fully occupied state, the empty state and one of the transition states have to be close to degeneracy. This can

be achieved by applying on site voltages that are individually tuned for the two levels of the quantum dot. A schematic experimental setup is shown in figure 2.25. In their paper

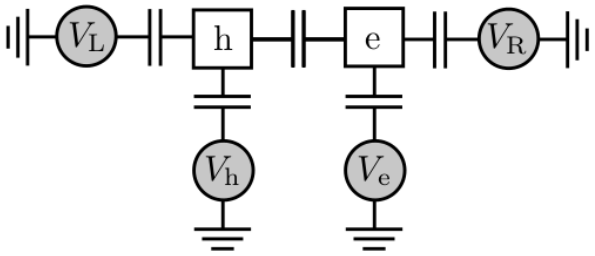


Figure 2.25.: Experimental setup for onside energy control - Source [HNK09]

they choose these states to be $|0_h 0_e\rangle$,$|0_h 2_e\rangle$, and $|2_h 2_e\rangle$. Finally they discuss the nature of entangled two photon emission depicted in figure 2.26. Another remarkable side note is

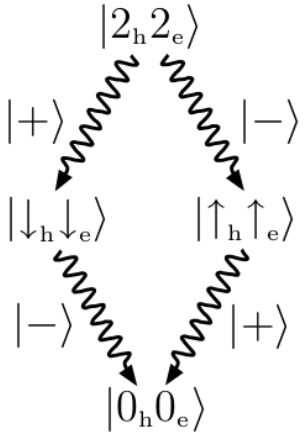


Figure 2.26.: Entangled two photon emission - Source [HNK09]
The key feature to note here is that the emission time of the second photon is much shorter than the emission time for the first photon. First from the $|2_h 2_e\rangle$ state a photon with a + or - circular polarization is emitted and forms a temporary intermediate state with the remaining electron hole pair. Then, before any other processes can alter the spins of the remaining electron and hole, a second photon with the opposite chirality is emitted. Thus a pair of fully entangled photons is produced. The predicted emission spectra is depicted in figure 2.27.

that the two entangled photons have in general different energies. The reason is that in order to emit the first photon two Cooper pairs have to be split up, resulting in a photon with an energy that is four times the induced superconducting gap smaller than the applied voltage. The second photon on the other hand has exactly this amount on top of the applied voltage. This is depicted in by the two full lines at + and - 4 in figure 2.27. Note that this does not affect the entanglement of the photon pair, since polarization and energy are uncorrelated. Summarizing Recher and collaborators have shown that a optical quantum dot with injected Cooper pairs is capable of emitting entangled photon pairs. The energy of the photons in such a pair is slightly different by twice the Cooper pair binding energy. In contrast to Asano and collaborators they do not predict an enhanced photon emission rate.

To conclude this section we elaborate how our work is different from what has been done in the theoretical papers discussed in this section. In contrast to Recher and collaborators we do not investigate a quantum dot but continuous leads. We expect that this widens the

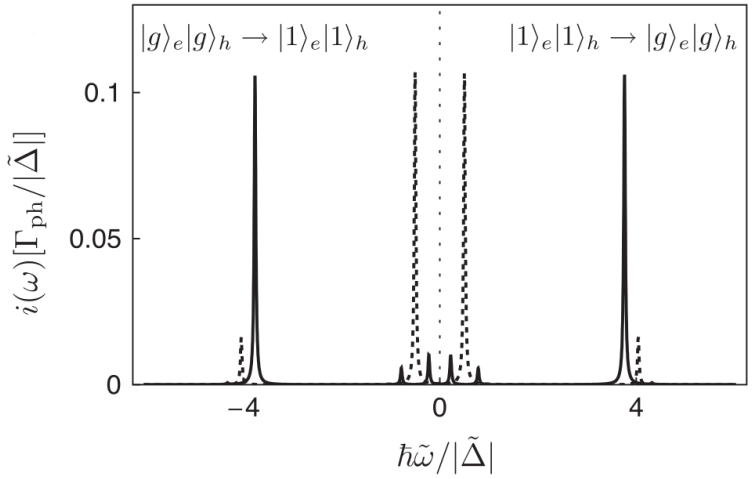


Figure 2.27.: Emission spectrum of coherent two photon production - Source [RNK10]

peaks in the photon spectrum and increases the emission rate. Also it is not clear, why a quantum dot - an effectively zero dimensional object, should conserve momentum. In terms of the model our work is more similar to the paper of Asano et. al. but we consider superconducting leads on both sides of the LED. This leads to qualitatively different physics, because Cooper pairs can recombine with Cooper holes. Hence, the emitted photon pairs inherit the coherence of the Cooper pairs and the relative phase of the two superconducting leads. Also we focus on the qualitative properties of the emitted photons, such as squeezing, rather instead of the emission rate.

# 3. Fundamentals

In this chapter we introduce fundamental concepts that form the backbone of this thesis and define many of the terms that we use throughout the whole work. We begin with a section about the formalism of Bardeen-Cooper-Schrieffer (BCS) theory. Subsequently we discuss the proximity effect that describes how superconductors affect attached non-superconducting materials. The third chapter is about squeezed light and finally in the last section we discuss the concept of entanglement.

## 3.1. BCS Theory

The BCS theory is a mean-field approach to phonon mediated electron-electron interaction. In this section we closely follow derivation from Bruus and Flensberg 'Many Body Quantum Theory in Condensed matter physics' Chapter 18 [BF04]. Starting point of this theory is a Hamiltonian

$$H - \mu N = \sum_{\mathbf{k}\sigma} \xi_{\mathbf{k}} c^\dagger_{\mathbf{k}\sigma} c_{\mathbf{k}\sigma} + \sum_{\mathbf{k}\mathbf{k}'} V_{\mathbf{k}\mathbf{k}'} c^\dagger_{\mathbf{k}\uparrow} c^\dagger_{-\mathbf{k}\downarrow} c_{-\mathbf{k}'\downarrow} c_{\mathbf{k}'\uparrow} \tag{3.1}$$

with an effective electron-electron interaction which is mediated by phonons. In a superconductor this interaction is attractive and the origin of Cooper pairing. The quartic electron-electron interaction term makes practical calculations complicated. In the BCS approach a mean field approximation is chosen to reduce the problem to a quadratic Hamiltonian

$$H_{\mathrm{BCS}} - \mu N = \sum_{\mathbf{k}\sigma} \xi_{\mathbf{k}} c^\dagger_{\mathbf{k}\sigma} c_{\mathbf{k}\sigma} - \sum_{\mathbf{k}} \Delta_{\mathbf{k}} c^\dagger_{\mathbf{k}\uparrow} c^\dagger_{-\mathbf{k}\downarrow} - \sum_{\mathbf{k}} \Delta^*_{\mathbf{k}} c_{-\mathbf{k}\downarrow} c_{\mathbf{k}\uparrow}, \tag{3.2}$$

where the mean field

$$\Delta_{\mathbf{k}} \equiv - \sum_{\mathbf{k}'} V_{\mathbf{k}\mathbf{k}'} \langle c_{-\mathbf{k}'\downarrow} c_{\mathbf{k}'\uparrow} \rangle = |\Delta_{\mathbf{k}}| \mathrm{e}^{\mathrm{i}\phi_{\mathbf{k}}} \tag{3.3}$$

is called order parameter. Such a quadratic Hamiltonian can always be diagonalized with a Bogoliubov transformation. Hence, the approximation is to neglect fluctuations in the order parameter $\Delta_{\mathbf{k}}$. This approximation is well justified, because Cooper pairs form a state with macroscopic occupation number. As we know from statistics the fluctuations in such a system behave as $1/\sqrt{N}$ which makes this an excellent approximation.

The unique ground state of the BCS Hamiltonian is a state where the number of Cooper pairs is undetermined. The coefficients $u_{\mathbf{k}}$ and $v_{\mathbf{k}}$ are called coherence factors. The $|v_{\mathbf{k}}|^2$ describe the probability of the state $(-\mathbf{k}\downarrow, k\uparrow)$ to be occupied and it's $\mathbf{k}$-dependence is such that most of the states with $k < k_F$ are filled and most of the others empty. The BCS ground state is

$$|\mathrm{BCS}\rangle = \prod_{\mathbf{k}} (u_{\mathbf{k}} + v_{\mathbf{k}} c^\dagger_{\mathbf{k}\uparrow} c^\dagger_{-\mathbf{k}\downarrow})|0\rangle. \tag{3.4}$$

Minimizing $\langle \mathrm{BCS}|H_{\mathrm{BCS}}|\mathrm{BCS}\rangle$ with respect to $u_{\mathbf{k}}$ and $v_{\mathbf{k}}$ gives the following coefficients:

$$\begin{aligned} u_{\mathbf{k}} &\equiv |u_{\mathbf{k}}| e^{i\chi_{\mathbf{k}}}, & v_{\mathbf{k}} &\equiv |v_{\mathbf{k}}| e^{i\chi_{\mathbf{k}}}, \\ e^{i\chi_{\mathbf{k}}} &\equiv \sqrt{e^{i(\phi_{\mathbf{k}}+\pi)}}, & e^{-i\chi_{\mathbf{k}}} &\equiv \sqrt{e^{-i(\phi_{\mathbf{k}}+\pi)}}, \\ |u_{\mathbf{k}}| &= \sqrt{\frac{1}{2}\Big(1 + \frac{\xi_{\mathbf{k}}}{E_{\mathbf{k}}}\Big)}, & |v_{\mathbf{k}}| &= \sqrt{\frac{1}{2}\Big(1 - \frac{\xi_{\mathbf{k}}}{E_{\mathbf{k}}}\Big)}. \end{aligned} \tag{3.5}$$

The transformation that diagonalizes the BCS Hamiltonian is called Bogoliubov transfor-

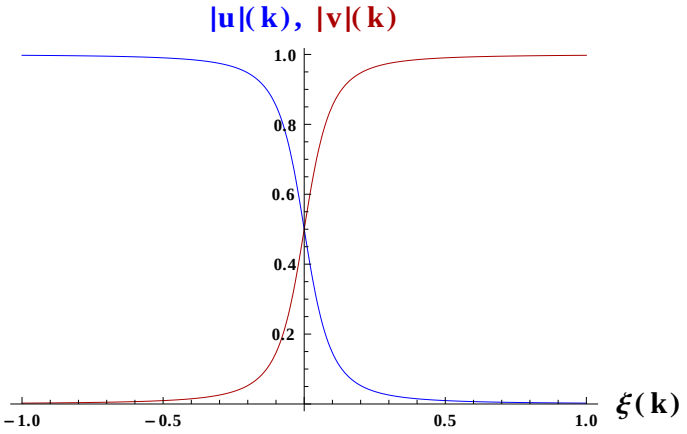


Figure 3.1.: Coherence factors with order parameter $\Delta$=0.01

mation. The easiest way to preform the Bogoliubov transformation is to use the Nambu notation which we discuss in the appendix A.3. The resulting transformations are

$$\begin{aligned} \gamma_{\mathbf{k}\uparrow} &= u^*_{\mathbf{k}} c_{\mathbf{k}\uparrow} + v_{\mathbf{k}} c^\dagger_{-\mathbf{k}\downarrow}, & c_{\mathbf{k}\uparrow} &= u_{\mathbf{k}} \gamma_{\mathbf{k}\uparrow} - v_{\mathbf{k}} \gamma^\dagger_{-\mathbf{k}\downarrow}, \\ \gamma^\dagger_{-\mathbf{k}\downarrow} &= -v^*_{\mathbf{k}} c_{\mathbf{k}\uparrow} + u_{\mathbf{k}} c^\dagger_{-\mathbf{k}\downarrow}, & c^\dagger_{-\mathbf{k}\downarrow} &= v^*_{\mathbf{k}} \gamma_{\mathbf{k}\uparrow} + u^*_{\mathbf{k}} \gamma^\dagger_{-\mathbf{k}\downarrow}. \end{aligned} \tag{3.6}$$

The fermionic quasiparticles that are associated with $\gamma^\dagger_{\mathbf{k}\sigma}$ are excitations of the BCS ground state and are superposition of particles and holes. They are called Bogoliubons or Bogoliubov quasiparticles. There is a excitation gap which is the absolute value of the order parameter. Below this energy there are no excitation. All these properties become obvious from the diagonalized form of the Hamiltonian

$$H_{\mathrm{BCS}} - \mu N = \sum_{k\sigma} E_{\mathbf{k}} \gamma^\dagger_{\mathbf{k},\sigma} \gamma_{\mathbf{k},\sigma} + \mathrm{const}, \tag{3.7}$$

where

$$E_{\mathbf{k}} \equiv \sqrt{\xi^2_{\mathbf{k}} + |\Delta_{\mathbf{k}}|^2} \tag{3.8}$$

is the quasiparticle energy. We see that the bogoliubons are free fermions and hence their distribution function is the Fermi-Dirac distribution.

## 3.2. Proximity Effect

When a superconductor is brought in good contact with a non superconducting material, Cooper pairs tunnel into the non superconducting material. In the vicinity of the contact this leads to a finite density of Cooper pairs in the non superconducting material. If we write an effective Hamiltonian for the non superconducting material with induced Cooper pairs unusual correlations will occur resulting in terms like in BCS theory. Therefore the diagonalized effective Hamiltonian will have a gap in the excitation spectrum, which we call induced gap. A formal derivation with a microscopic theory is difficult and involved. There is however a trick that allows for a simple description based on Ginsburg Landau theory [PF05]. Instead of considering for example a superconductor-normal metal junction we take a system consisting of two superconductors. Those superconductors have slightly different critical temperatures $T_1$ and $T_2$. The actual temperature defined to be right in between those critical temperatures. We label those superconductors and there corresponding critical temperatures I and II with ($T_I < T < T_{II}$). Hence, before the contact is established superconductor I is not superconducting while superconductor II is. Upon contact Cooper pairs diffuse from SCII into SCI and induce an order parameter in the vicinity of the junction. This induced order parameter is in general much smaller than the order parameter in SCII but reaches relatively far into SCI ($\sim$ 100nm). The space dependence of the order parameter shown qualitatively by the dotted line in figure 3.2. The key idea is that we can describe both sides of the setup by the same theory. The Ginsburg Landau equations (3.9) for a superconductor in 1D are well known and we simply state

$$\xi^2\Big(\mathrm{i}\partial_x + \frac{2\pi}{\phi_0}A\Big)^2\psi - \psi + \psi|\psi|^2 = 0, \tag{3.9}$$

where $\xi$ is the coherence length, $\phi_0$ is the flux quantum and $A$ the vector potential. Choosing an appropriate gauge we can prepare the order parameter $\psi$ to be a real number. Further, for small fields the term quadratic in the vector potential is negligible, hence

$$-\xi^2\partial_x^2\psi - \psi + \psi^3 = 0. \tag{3.10}$$

First we consider the SCII half space. The boundary at the SCI-SCII interface,

$$\frac{1}{\Psi}\partial_x\Psi = \frac{1}{b}, \tag{3.11}$$

is different from the usual Ginsburg-Landau boundary conditions of a superconductor-vacuum interface. The parameter $b$ is a phenomenological parameter that must be put in and describes how deep the Cooper pairs penetrate into SCI. Together with the boundary condition on the other side of the SCII $\partial_x\psi(\infty) = 0$ and the deep in the bulk condition $\Psi(\infty) = 1$ the behavior of the order parameter in SCII is

$$\Psi(x > 0) = \tanh\left(\frac{x-c}{\sqrt{2}\xi_{II}}\right) \quad \text{with} \quad \sinh\left(\frac{-\sqrt{2}c}{\xi}\right) = \frac{\sqrt{2}b}{\xi}. \tag{3.12}$$

In SCI the order parameter is much smaller than 1, therefore the Ginsburg Landau equation simplify to

$$-\xi_I^2\partial_x^2\psi - \psi = 0. \tag{3.13}$$

Together with the condition that the induced order parameter vanishes deep inside SCI $\Psi(-\infty) = 0$ the solution reads

$$\Psi(x < 0) = \Psi_N(0)\mathrm{e}^{x/\xi_n}. \tag{3.14}$$

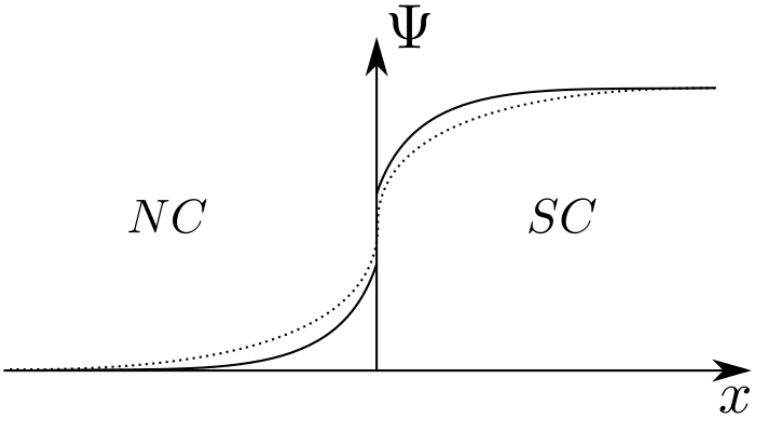


Figure 3.2.: Order parameter at a normal conductor - super conductor junction, the full line is in the Ginsburg Landau approximation and the dotted line the exact microscopic result

In a more realistic model, we would have to consider a more complicated approach to model the non superconducting material. The good news is that the only thing that needs to be done is adjust $\xi_n$ for a qualitative description. In general there are two limits. The clean limit,

$$\xi_n = \frac{v_F}{2\pi T}, \tag{3.15}$$

and the dirty limit,

$$\xi_n = \sqrt{\frac{v_F l}{6\pi T}}, \tag{3.16}$$

which is applicable in the case of a light emitting diode between superconductors, because of the doped leads. In equation (3.16) $v_F$ is the fermi velocity and $l$ is the mean free path. The definition of dirty is that the mean free path is shorter than the coherence length.

## 3.3. Coherent Light

There are many applications for coherent light, commonly known as LASER light. The nice feature besides the temporal and spatial coherence is the phenomenon of being a minimal uncertainty state. Let $a$ be a photon annihilation operator. An eigenstate $|\alpha\rangle$ of this operator is called a coherent state and fulfills

$$a|\alpha\rangle = \alpha|\alpha\rangle \tag{3.17}$$

The operator that creates a coherent state with amplitude $\alpha$ from the vacuum is called unitary displacement operator $D(\alpha)$:

$$|\alpha\rangle = \mathrm{e}^{\alpha a^\dagger - \alpha^* a}|0\rangle \equiv D(\alpha)|0\rangle. \tag{3.18}$$

An important concept are the quadrature components

$$\begin{aligned} a &\equiv a_1 + \mathrm{i}a_2 \qquad & a_i &= a_i^\dagger, \\ \alpha &\equiv \alpha_1 + \mathrm{i}\alpha_2 \qquad & \alpha_i &\in \mathbb{R}. \end{aligned} \tag{3.19}$$

The name derives from the fact that the amplitudes associated with this operators having a phase difference of $\pi/2$. They are hermitian. "The physical significance of the quadrature

phase-amplitudes lies in their close connection to experimental techniques; they are the complex-amplitude operators for fields -the quadrature phases - that are directly accessible to measurement and experimental manipulation. The quadrature phases are accessible because they describe the physical process of putting amplitude and phase modulation on a carrier signal and because they are the quantities detected by phase-sensitive detection, techniques such as heterodyning." [CS85]. Usually quadrature operators are chosen to be dimensionless, such that $[a_1, a_2] = \mathrm{i}/2$. For a coherent state such operators have

$$\langle \Delta a_1^2 \rangle = \langle \Delta a_2^2 \rangle = \frac{1}{4}. \tag{3.20}$$

Coherent states are suitable to model ideal classical photon sources (such as coherent laser light). This concept can be generalized from single-mode to multi-mode coherent states. As an example

$$a|\alpha\beta\rangle = \alpha|\alpha\beta\rangle, \qquad \text{and} \qquad b|\alpha\beta\rangle = \beta|\alpha\beta\rangle \Rightarrow |\alpha\beta\rangle \qquad = D(\alpha)D(\beta)|0\rangle. \tag{3.21}$$

## 3.4. Squeezed Light

In general light is an electromagnetic wave. The electric field component,

$$\mathbf{E}(x,t) = \mathcal{E}(b\mathrm{e}^{-\mathrm{i}wt} + b^\dagger \mathrm{e}^{\mathrm{i}wt})\hat{\epsilon}, \tag{3.22}$$

has a positive and a negative frequency part. The photon creation and annihilation operators can be thought of being in the interaction picture, because the main phase has been removed. We can now introduce a pair of conjugated hermitian operators

$$A = \frac{1}{2}(b + b^\dagger) \qquad B = \frac{1}{2\mathrm{i}}(b - b^\dagger). \tag{3.23}$$

They are called quadrature amplitudes because they modulate field components that are orthogonal to each other (have a $\pi/2$ phase difference). With this definitions we can rewrite the electric field

$$\mathbf{E}(x,t) = 2\mathcal{E}(A\cos(wt) + B\sin(wt))\hat{\epsilon}. \tag{3.24}$$

It is important to notice that this choice of quadrature amplitudes is not unique. Different choices of quadrature amplitudes,

$$\tilde{A}(\varphi) + \mathrm{i}\tilde{B}(\varphi) = (A + \mathrm{i}B)\mathrm{e}^{-\mathrm{i}\varphi/2}, \tag{3.25}$$

can be parametrized by an angle $\varphi$ whose meaning we will discuss later on. Each quadrature amplitudes has an uncertainty. Coherent light is a special case in which the uncertainty is equal in both modes for any choice of $\varphi$. In case of squeezed light this is by definition not the case. There exists one angle $\varphi_{\max}$ for which the difference in uncertainty between the two quadrature amplitudes is maximal and another angle $\varphi_0$ the uncertainty is equally spread. We can understand this best by looking at the quadrature phase diagram in figure 3.3. The left hand side graph shows a coherent state, the right hand side a squeezed state. The transformation (3.25) into another quadrature basis corresponds to a rotation of the coordinate system, which is equivalent to a rotation of the ellipse around it's center. From this picture we understand why there is a quadrature basis in which the uncertainty is the same in each phase and one where the difference is maximal. The latter is the main axis system of the ellipse. If we consider an ideal squeezed state the product of the uncertainties of any of the two uncertainty modes is the same as for a coherent

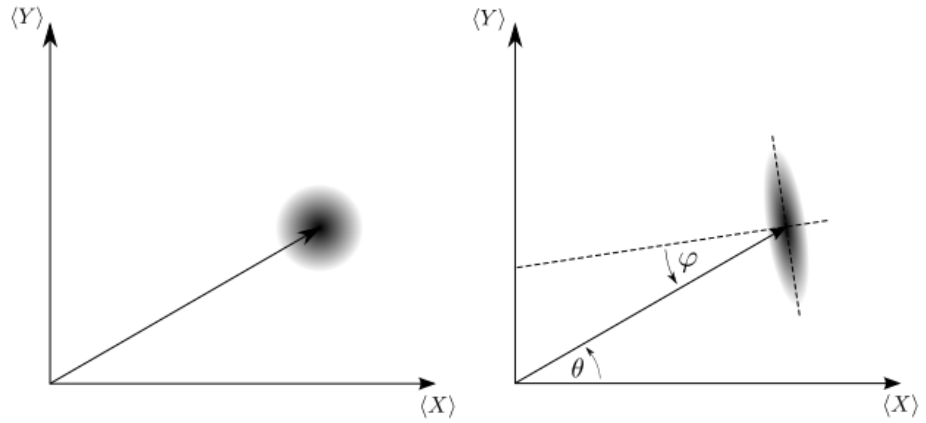


Figure 3.3.: left:coherent state, right: squeezed state

state. Further, if we choose the quadrature modes to fall together with the main axes of the uncertainty ellipse we can characterize an ideal squeezed state by

$$\langle \Delta A^2 \rangle \langle \Delta B^2 \rangle = \frac{1}{16} \qquad \text{where} \qquad \langle \Delta A^2 \rangle < \frac{1}{4} \quad \text{or} \quad \langle \Delta B^2 \rangle < \frac{1}{4}. \tag{3.26}$$

or vice versa. We will now let this intuitive approach behind and deal with squeezed states in a more mathematical way. For further details we suggest [Yue76] and [CS85], [SC85]. Much of the remainder of this section is based on this papers. Mathematically a squeezed state is constructed by acting with the so called squeezing operator $S(r, \varphi)$ onto a coherent state. The coherent state is prepared by the so called displacement operator $D(s, \theta)$. For a single mode the explicit expression reads

$$|\psi(r, \varphi; s, \theta)\rangle = S(r, \varphi) D(s, \theta) |0\rangle. \tag{3.27}$$

The real number $s$ describes the magnitude of displacement. In figure 3.3 this corresponds to the length of the arrow. The phase angle $\theta$ controls how the amplitude of the coherent state is distributed between the two quadrature amplitudes. The squeezing is also parametrized by two real parameters, the squeezing factor r and the squeezing phase $\varphi$. The squeezing factor determines the eccentricity of the ellipse and the squeezing phase its rotation relative to the quadrature axes.

### 3.4.1. Squeezed Vacuum

A special case of squeezed light is the so called squeezed vacuum

$$|0(r, \varphi)\rangle \equiv S(r, \varphi) |0\rangle \tag{3.28}$$

It's created by acting with a squeezing operator,

$$S(r, \varphi) \equiv \mathrm{e}^{\frac{1}{2} r (a^2 \mathrm{e}^{-2\mathrm{i}\varphi} - (a^\dagger)^2 \mathrm{e}^{2\mathrm{i}\varphi})} \tag{3.29}$$

on a coherent state that does not contain any photons. By definition this is the same as the Fock vacuum. As with the coherent states we can readily generalizes this concept to two modes:

$$\begin{aligned} S(r, \varphi) &\equiv \mathrm{e}^{r (a_+ a_- \mathrm{e}^{-2\mathrm{i}\varphi} - a_+^\dagger a_-^\dagger \mathrm{e}^{2\mathrm{i}\varphi})} \\ |0(r, \varphi)\rangle &\equiv S(r, \varphi) |0_+ 0_-\rangle. \end{aligned} \tag{3.30}$$

Using a text book operator relation, we can factorize the squeezing operator into

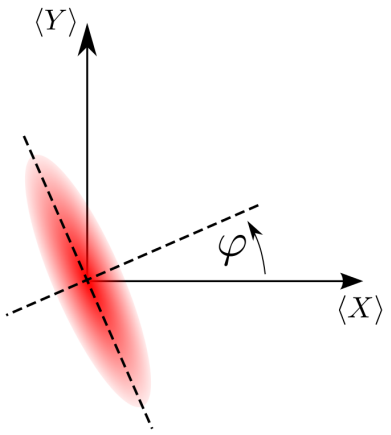


Figure 3.4.: Squeezed Vacuum

$$S(r,\varphi)|0\rangle \equiv \big(\cosh(r)\big)^{-1} \mathrm{e}^{-a_+^\dagger a_-^\dagger \mathrm{e}^{2\mathrm{i}\varphi}\tanh(r)} \mathrm{e}^{-(a_+^\dagger a_+ + a_-^\dagger a_-)\ln(\cosh(r))} \mathrm{e}^{a_+ a_- \mathrm{e}^{-2\mathrm{i}\varphi}\tanh(r)}$$
$$= \big(\cosh(r)\big)^{-1} \sum_{n=0}^{\infty} \mathrm{e}^{2\mathrm{i}n\varphi} (-\tanh(r))^n |n_+ n_-\rangle \equiv |0(r,\varphi)\rangle. \tag{3.31}$$

This will prove helpful later when we investigate the entanglement of the squeezed vacuum in the next subsection.

### 3.4.2. Entanglement of squeezed states

This section we discuss the entanglement of pure states of bipartite bosonic systems ($H = H_+ + H_-$). We show that the squeezed vacuum (3.30) is the maximal entangled state at any given energy and that the entanglement does not depend on the squeezing phase $\varphi$. A measure of the entanglement of a state is to calculate the von Neumann entropy,

$$S = -\mathrm{Tr}(\rho_+ \ln(\rho_+)), \tag{3.32}$$

of the reduced density-matrix of one of the subsystems. For a state which is not entangled, i.e. which can be written as a product state $|n\rangle_+ \otimes |n\rangle_-$, it is zero. A detailed discussion can be found in [Kha09] chapter 14.5. From (3.31) it is straightforward to show that the entanglement is independent of $\varphi$. The density matrix of the squeezed vacuum is

$$\rho_{+-} = |0(r,\varphi)\rangle\langle 0(r,\varphi)|. \tag{3.33}$$

Tracing over the "−" subsystem leads to the reduced density matrix of the "+" subsystem:

$$\rho_+ = \sum_{k=0}^{\infty} {}_-\langle k|\rho_{+-}(r,\varphi)|k\rangle_- = \frac{1}{\cosh^2(r)} \sum_{n=0}^{\infty} \tanh^{2n}(r)|n\rangle_{++}\langle n| = \rho_+(r). \tag{3.34}$$

For a pure state of a bipartite system a criterion for maximal entanglement at a given energy is that the reduced density matrix has the following form:

$$\rho_+ = \frac{1}{Z}\exp(-\tau H_+), \qquad Z = \mathrm{Tr}\exp(-\tau H_+). \tag{3.35}$$

For a proof we refer to the literature [Kha09]. And indeed we find that (3.34) can be brought into this form via the following reparametrization:

$$\rho_+ = \frac{1}{Z_+(\tau)} \mathrm{e}^{-\tau a_+^\dagger a_+}, \qquad \mathrm{e}^{-\tau/2} \equiv \tanh(r), \qquad Z_+(\tau) = \mathrm{Tr}(\mathrm{e}^{-\tau a_+^\dagger a_+}). \tag{3.36}$$

Therefore the squeezed vacuum is the maximal entangled state at any given (fixed) energy.

# 4. Modeling

In this chapter we motivate and justify the model we use to describe a superconductor-pn-superconductor heterostructure. We begin with a general discussion of a normal light emitting diode (LED) which is followed by a section that covers the effect of the attached superconductors.

## 4.1. Model of a normal light emitting diode

A pn-junction consists of a p- and a n-doped semiconductor which have a common interface. There are two energy scales in the problem. First the semiconductor gap which is of the order of 0.5-4 electron volt. And second, the energy it takes to excite donor electrons to the conduction band or respectively to excite valence electrons to the acceptor level. This second energy is much smaller, on the order of 0.01 - 0.1 electron volt which corresponds to 1-10 kelvin. Thus at small but finite temperatures some of the donor electrons are excited into the conduction band of the n-doped semiconductor. On the p-side some of the valence band electrons are excited into the acceptor states which leaves holes in the valence band. Because of this the chemical potential which is depicted by the dotted line

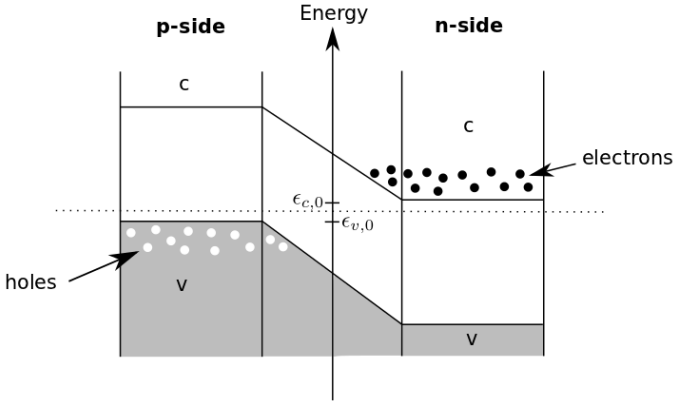


Figure 4.1.: Unbiased pn-junction

in figure 4.1 is between the donor level energy and the conduction band on the n-side and in between the valence band and the acceptor levels on the p-side. In a pn-junction without bias voltage there can only be one uniform chemical potential. Therefore the

bands bend at the interface. Physically this bending corresponds to a charge separation which causes a voltage. This voltage is called diffusion voltage $V_d$ and we can understand it as follows: The electrons in the n-doped side and the holes on the p-doped side are called majority carriers. Holes in the n-side and electrons in the p-side are called minority carriers. The majority carriers can move balistically and carry the vast majority current if the pn-junction is under forward bias. The minority carriers that are much rarer behave diffusively and recombine with majority carriers quickly. Therefore, by random movement there is a constant electron based current into the p-side where the electrons annihilate with holes and and by the same argument also a hole based current going the opposite way. A a consequence the region of the interface is depleted of carriers and forms an insulating layer called depletion layer. This depletion layer is usually on the order of several hundred nanometers. Since the system is an open circuit this causes a positive charge to accumulate on the n-side and a negative charge in the p-side. (figure 4.2). The

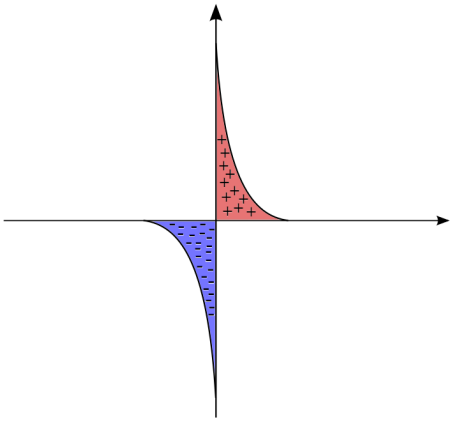

Figure 4.2.: Charge separation in depletion layer

resulting electric field induces currents in the opposite ways that compensate the diffusion currents. Those currents are mediated by minority carriers which are produced by the diffusion voltage. Hence, a dynamical equilibrium is established in the vicinity of the pn-interface. In order to operate a pn-junction a bias voltage is necessary. Either forward bias, which is positive voltage applied to the p-side and negative voltage applied to the n-side or backward bias which is the opposite. Backward bias is of no interest to understand the light emitting diode. Forward bias counteracts the diffusion voltage. If the forward bias becomes of the order of the diffusion voltage electrons from the n-side flow into the conduction band of the p-side. There they quickly recombine with holes. At the same time holes from the p-side flow into the valence band of the n-side where they recombine with electrons. This leads to a finite overall current that is carried by the majority carriers in each part of the junction. Due to this dynamical equilibrium understanding the chemical potential under bias is a non trivial task. The reason is that because the system is out of equilibrium electrons and holes have separate chemical potentials in each part of the system. This is schematically shown in figure 4.5 by the dotted lines.

A light emitting diode is a forward biased pn-junction which has two important properties. The interface between the p- and the n-doped semiconductor allows interband tunneling without changing the momentum (direct band-gap). And the band-gap is of the order of a few electron volt. The first property takes into consideration that the dispersion relation of photons is linear and extremely steep. If there is no direct band-gap phonons are necessary to fulfill momentum conservation which strongly suppresses the photon emission rate. The second property is only necessary to ensure that the emitted photons are in or close to the visible spectrum that ranges from 1.65 to 3.1 eV.

The most important thing to note is that the photon production (figure 4.5) takes place in a narrow layer right at the interface of p- and n-side. This layer is often called active region or active layer (figure 4.3). It is usually rather thin on the order of 100nm and the carrier density is low. Therefore we can model the light emitting diode by a model for this layer. The p- and n-bulk serve as reservoirs that are represented by chemical potentials. Despite

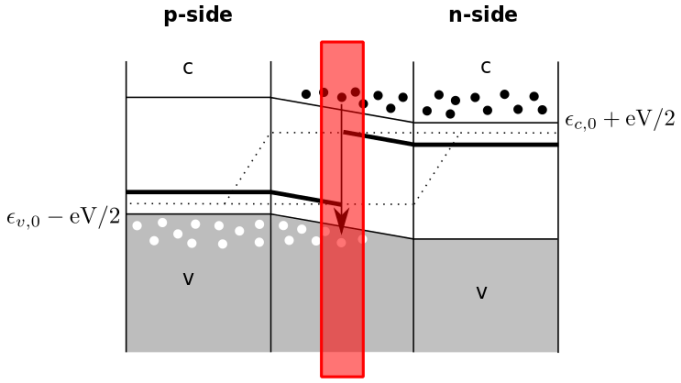


Figure 4.3.: Biased pn-junction, red: active layer of light emitting diode

the fact that the active layer is rather thin we assume that we can model it by two bands. This means we assume that we can use periodic boundary conditions. As a consequence our interaction term will fulfill momentum conservation. In a more quantitative calculation we would have to consider corrections that result form momentum change in the direction perpendicular to the layer. In comparison to the active layer the p- and n-doped leads are huge and we can treat them as being semi infinite. They form a electron-, respectively hole-bath which we can approximate as being in equilibrium at all times, yet at different chemical potentials. In the model Hamiltonian those leads are used to keep the electron occupations in the active layer constant and are encoded in the separate conduction and valence band chemical potentials. The effective model for the active layer is sketched in figure 4.4. So far we did not talk about the interaction which produces or absorbs

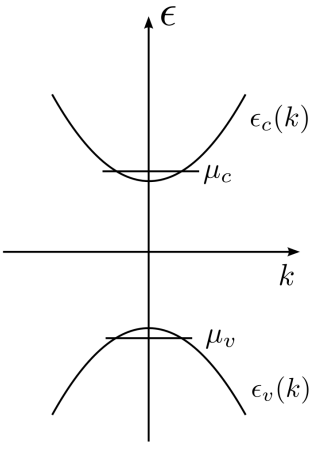


Figure 4.4.: Chemical potentials in active layer

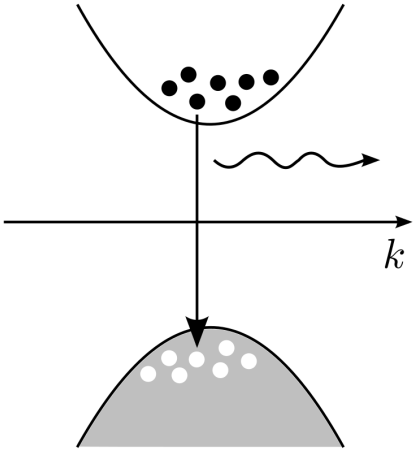


Figure 4.5.: Photon emission in active layer

photons. The easiest approach to understand the coupling of electrons to light is via first quantization using the principle of minimal coupling

$$\mathbf{p}_i \to \mathbf{p}_i - q\mathbf{A}(x_i). \tag{4.1}$$

In equation 4.1 $p_i$ is the momentum of the $i$th and electron, $q = -\mathrm{e}$ is the electron charge and $\mathbf{A}(x_i)$ is the vector potential at the position of this electron. Thus the electron photon coupling is part of the kinetic energy term in the Hamiltonian. The term quadratic in the vector potential is small for not too strong radiation fields and we will neglect it. In the Coulomb gauge $\nabla \cdot \mathbf{A} = 0$ the electron photon interaction energy is then given by

$$H_T = \frac{\mathrm{e}}{m} \mathbf{A}(x_i) \cdot \mathbf{p}_i. \tag{4.2}$$

Since the active layer is thin and assuming that it's area is not too large the long wave length approximation, also known as dipole approximation, is valid. Essentially this means that the vector potential is assumed constant over the volume of the device and the individual coordinates of the electrons do not matter $x_i \to x$. The electron photon Hamiltonian becomes

$$H_T = \frac{\mathrm{e}}{m} \mathbf{A}(x) \cdot \mathbf{p}_i. \tag{4.3}$$

Next we rewrite this first order electron-photon Hamiltonian in second quantization. This is accomplished in two steps. First we quantize the vector potential $\mathbf{A}$ in terms of photon creation and annihilation operators $b_{\lambda\mathbf{q}}$:

$$\mathbf{A}(x) = \sum_{\mathbf{q},\lambda} \frac{2\pi}{V|q|} \Big( b_{\lambda\mathbf{q}} \hat{\epsilon}_\lambda \mathrm{e}^{\mathrm{i}q\cdot x} + b^\dagger_{\lambda\mathbf{q}} \hat{\epsilon}_\lambda \mathrm{e}^{-\mathrm{i}q\cdot x} \Big). \tag{4.4}$$

Here $\lambda$ is the polarization index, $\mathbf{q}$ the photon momentum, $\hat{\mathrm{e}}_\lambda$ the unit polarization vectors and $V$ the macroscopic volume of the system. For clarity we choose a convention to label the momentum vectors. The letter $q$ is reserved primarily for photon momenta, $k$ for conduction electron momenta and $p$ for valence electrons momenta. Also, for clarity we don't use bold letters but merely note that those letters always have vectorial nature. If nothing else is mentioned they are usually assumed to be three dimensional. The same is true for the spatial coordinates $x$ and $r$. In a second step we introduce the fermionic creation $c^\dagger$, $v^\dagger$ and annihilation operators $c$, $v$ for the conduction ($c$) and valence ($v$) electrons. We get

$$\begin{aligned} \hat{\epsilon}_\lambda \mathrm{e}^{\mathrm{i}q\cdot\hat{x}} &= \langle k|\hat{\epsilon}_\lambda \mathrm{e}^{\mathrm{i}q\cdot\hat{x}}|p\rangle c^\dagger_k v_p & (4.5)\\ &= \int \mathrm{d}^{\dim} r \, \langle k|r\rangle \vec{\epsilon}_\lambda \mathrm{e}^{\mathrm{i}q\cdot r} \langle r|p\rangle c^\dagger_k v_p \\ &= 2\pi\delta(k-p-q)\, \vec{\mathrm{e}}_\lambda c^\dagger_k v_p. & (4.6) \end{aligned}$$

Here make two approximations. We allow only interband scattering because only this type of scattering involves photons and we allow only energy conserving terms. Terms where a valence electron goes to the conduction band, which costs energy, and a photon is emitted rather than absorbed are thus neglected. This is similar to the commonly used rotating wave approximation. All together the electron-photon interaction in second quantized form is given by

$$H_T = \frac{-\mathrm{e}}{m} \sum_{k,q,\lambda} \frac{2\pi}{V|q|} \Big( b_{\lambda q} c^\dagger_k v_{k-q} \vec{\epsilon}_\lambda \cdot (k-q) + b^\dagger_{\lambda q} v^\dagger_{k-q} c_k \vec{\epsilon}_\lambda \cdot k \Big), \tag{4.7}$$

where $\frac{\mathrm{e}}{m}$ is the ration between electron charge and electron mass. This model looks very nice but is much too complicated for analytical techniques. Therefore we use a simplified version,

$$H_T = \sum_{k,q} \Big( g b_q c^\dagger_k v_{k-q} + g^* b^\dagger_q v^\dagger_{k-q} c_k \Big), \tag{4.8}$$

where $g$ is simply a constant for our further analysis. Despite the total disregard of the momentum dependency of the coupling constant we can justify this model since the focus of this thesis is on the qualitative nature of the emitted photons. Firstly, the angular dependent intensity is of little interest. Secondly, most of the emitted photons have approximately the energy of the semiconductor gap which confines the length of the photon momenta to a small interval. And thirdly, in comparison to a metal we have only a low electron density in the conduction band of the n-side and a only few holes in the valence band of the p-side. As a consequence only a small range of electron momenta is important. All together this means that the momentum dependency of the coupling constant is not very important for the things we are interested in. Now we know everything to write down our model:

$$\begin{aligned} H - \mu_c N_c - \mu_v N_v = &\sum_k (\epsilon_{c,k} - \mu_c) c_k^\dagger c_k + \sum_p (\epsilon_{v,p} - \mu_v) v_p^\dagger v_p + \sum_q w_q b_q^\dagger b_q \\ &+ g \sum_{k,q} b_q c_k^\dagger v_{k-q} + g^* \sum_{k,q} b_{-q}^\dagger v_{q-k}^\dagger c_{-k}. \end{aligned} \tag{4.9}$$

The conduction and valence band have the usual parabolic shape which is an approximation for any band structure with an extremum for small momenta $k$ and $p$, respectively. The photons have a linear dispersion relation. Thus, we have:

$$\epsilon_{c,k} = \epsilon_{c,0} + \frac{k^2}{2m_c}, \qquad \epsilon_{v,p} = \epsilon_{v,0} - \frac{p^2}{2m_v}, \qquad w_q = c|q|, \qquad k, p, q \in \mathbb{R}^{\dim}, \tag{4.10}$$

with $c$ being the speed of light. Here $m_c$ and $m_v$ are the effective masses of electrons in the conduction respectively hole band. For simplicity in the following we assume that $m_c = m_v = m$.

## 4.2. Superconducting leads

So far our model describes a normal light emitting diode. The exciting new physics however is caused by putting superconducting leads on both sides of the diode. Then, via proximity effect, Cooper pairs tunnel into the diode. If the diode is very thin they can tunnel all the way into the active region where the photon production takes place. In section 3.2 we give a more detailed discussion of this effect which is called proximity effect. For the purpose of modeling it is sufficient for us to know that the proximity effect induces a gap in the density of states in the semiconductor which is called induced order parameter. This means that the leads describing the p- and n-doped sides acquire BCS type order parameter terms $\Delta_{c,k}$ and $\Delta_{v,p}$. For clarity we group the full model Hamiltonian minus the energy from the chemical potentials in four pieces

$$H - \mu_c N_c - \mu_v N_v \equiv (H_{0,c} - \mu_c N_c) + (H_{0,v} - \mu_v N_v) + H_{0,ph} + H_T. \tag{4.11}$$

In contrast to the non superconducting case the leads are described by

$$\begin{aligned} H_{0,c} - \mu_c N_c &= \sum_{m,\sigma} (\epsilon_{c,m} - \mu_c) c_{m,\sigma}^\dagger c_{m,\sigma} - \sum_m \Delta_{c,m} c_{m,\uparrow}^\dagger c_{-m,\downarrow}^\dagger - \sum_m \Delta_{c,m}^* c_{-m,\downarrow} c_{m,\uparrow}, \\ H_{0,v} - \mu_v N_v &= \sum_{n,\sigma} (\epsilon_{v,n} - \mu_v) v_{n,\sigma}^\dagger v_{n,\sigma} - \sum_n \Delta_{v,n} v_{n,\uparrow}^\dagger v_{-n,\downarrow}^\dagger - \sum_n \Delta_{v,n}^* v_{-n,\downarrow} v_{n,\uparrow}, \end{aligned} \tag{4.12}$$

and we need to include spin indices $\sigma$. The free photon Hamiltonian

$$H_{0,ph} = \sum_q w_q b_q^\dagger b_q, \tag{4.13}$$

remains unchanged. By the inclusion of superconductivity in principle the photon operators should be equipped with a chirality index. However, we neglect effects such as spin-orbit coupling and hence from spin and momentum conservation it is clear that the photons in photon pairs have the same chirality. The tunneling or interaction term,

$$H_T = g \sum_{k,q,\sigma} b_q c^\dagger_{k,\sigma} v_{k-q,\sigma} + g^* \sum_{k,q,\sigma} b^\dagger_{-q} v^\dagger_{q-k,\bar{\sigma}} c_{-k,\bar{\sigma}}, \tag{4.14}$$

also remains unchanged but is now equipped with spin indices $\sigma$ in a spin conserving way. The spin index can take the values $\pm\frac{1}{2}$. A spin index with a bar denotes the opposite spin, $\bar{\sigma} = -\sigma$. The order parameters,

$$\Delta_{c,k} \equiv \sum_{k'} V_{k,k'} \langle c_{-k'\downarrow} c_{k'\uparrow} \rangle \approx \Delta_c, \qquad \Delta_{v,k} \equiv \sum_{k'} V_{k,k'} \langle v_{-k'\downarrow} v_{k'\uparrow} \rangle \approx \Delta_v, \tag{4.15}$$

do in principle depend on momentum. In what follows we consider s-wave superconductors, where it is a good approximation to ignore this and replace it by a constant.

We use the following list of (anti-)commutation relations throughout the entire thesis:

$$\begin{aligned}
\{c_{\mathbf{k}}, c^\dagger_{\mathbf{k}'}\} &= \delta_{\mathbf{k}\mathbf{k}'} & \{c_{\mathbf{k}}, c_{\mathbf{k}'}\} &= 0 & \{c^\dagger_{\mathbf{k}}, c^\dagger_{\mathbf{k}'}\} &= 0 \\
\{v_{\mathbf{p}}, v^\dagger_{\mathbf{p}'}\} &= \delta_{\mathbf{p}\mathbf{p}'} & \{v_{\mathbf{p}}, v_{\mathbf{p}'}\} &= 0 & \{v^\dagger_{\mathbf{p}}, v^\dagger_{\mathbf{p}'}\} &= 0 \\
[b_{\mathbf{q}}, b^\dagger_{\mathbf{q}'}] &= \delta_{\mathbf{q}\mathbf{q}'} & [b_{\mathbf{q}}, b^\dagger_{\mathbf{q}'}] &= 0 & [b_{\mathbf{q}}, b^\dagger_{\mathbf{q}'}] &= 0 \\
\{c_{\mathbf{k}}, v^\dagger_{\mathbf{p}}\} &= 0 & [c_{\mathbf{k}}, b^\dagger_{\mathbf{q}}] &= 0 & [v_{\mathbf{p}}, b^\dagger_{\mathbf{q}}] &= 0
\end{aligned} \tag{4.16}$$

The first three lines are obvious consequences of the particles being fermions or bosons. The last line considers how different particle species commute or anti commute with each other. Fermions do commute with bosons because they are truly different particles which can not transform into each other one by one. The situation for fermions is less clear. A nice argument can be found in Landau Lifshitz 'Quantenmechanik' §64 and §65. Their argumentation is that it does not matter for theories where the two types of fermions can not transform into each other. In theories as for example certain relativistic theories where the two fermions could represent different inner states of a more complex particle, the have to anticommute.

# 5. Evaluation

## 5.1. Luminescence

In this section we discuss the spontaneous photon emission of a light emitting diode (LED). We show that it is sufficient to only consider the leading order in the coupling constant $|g|$. Before we start explicit calculations we discuss the term luminescence on a general level and give a relation to experiments. As any diode a light emitting diode needs a forward bias to be operated. Hence, we deal with a nonequilibrium problem. Therefore we use the Keldysh formalism [Kel65]. On the same general level we then elaborate the subtle procedure of introducing stationarity. By stationarity we mean that the luminescence is constant in time. This requires careful checking of the physics before employing the technical machinery. In the second part of the section we introduce and justify approximations that we use throughout all calculations. With this preparation we derive the leading order and find that the luminescence depends on the chemical potentials and the photon density of states in an intuitive way. The next to leading order contribution gives a finite contribution that describes an effective interaction between the conduction and the valence electrons that is mediated by virtual photons. In a third step we sum up an infinite number of diagrams in the random phase approximation (RPA). As a result we see that the higher order corrections only give quantitative corrections of the leading order term. In the last subsection we discuss the special case where the electron bands are reduced to single levels.

### 5.1.1. General notes on luminescence

In this subsection we discuss what luminescence is and how it can be calculated using the Keldysh formalism. In our discussion we follow the arguments in [KRB09]. The key observable of a light emitting diode is the luminescence $L$. It is defined as the change in the photon number of the system

$$L(t) \equiv \frac{\mathrm{d}}{\mathrm{d}t} n_{\mathrm{ph}}(t). \tag{5.1}$$

In general it consists of three contributions. Spontaneous photon emission, stimulated photon emission and photon absorption. A light emitting diode needs a bias voltage in order to be operated. Hence, we have to deal with a nonequilibrium problem. The Keldysh formalism is suitable to treat such problems. We begin by deriving a nice working

expression. First we rewrite equation 5.1 in a symmetrized way

$$L(t) \equiv \Big(\partial_{t_1} + \partial_{t_2}\Big) \sum_q \langle b_q^\dagger(t_1) b_q(t_2)\rangle \Big|_{t_2 \to t_1 \equiv t} \tag{5.2}$$

The nice thing about this slightly more complicated expression is that the expectation value is precisely the definition of the lesser photon Green's function $D_q^<(t_1,t_2) \equiv -\mathrm{i}\langle b_q^\dagger(t_1) b_q(t_2)\rangle$. This allows us to rewrite the luminescence in a nifty way that allows us to exploit theoretical literature most easily

$$L(t_1) \equiv \Big(\partial_{t_1} + \partial_{t_2}\Big) \sum_q \mathrm{i} D_q^<(t_1,t_2) \Big|_{t_2 \to t_1}. \tag{5.3}$$

The calculation of the time derivative of $D_q^<$ is still non trivial but now we can do it in a systematic perturbative way. The equations of motion for the lesser Green's function, which we derive below, are known as the Kadanoff-Baym equations and can be found for instance in [KB62]. The starting points are two versions of the Dyson equation of the photon propagator in Keldysh formalism

$$\begin{aligned} D_q(t_1,t_2) &= d_q(t_1,t_2) + \int_C \mathrm{d}s_1 \mathrm{d}s_2\, d_q(t_1,s_1)\Pi_q(s_1,s_2) D_q(s_2,t_2), \\ D_q(t_1,t_2) &= d_q(t_1,t_2) + \int_C \mathrm{d}s_1 \mathrm{d}s_2\, D_q(t_1,s_1)\Pi_q(s_1,s_2) d_q(s_2,t_2), \end{aligned} \tag{5.4}$$

where we denoted the integration over the Keldysh contour by $\int_C$. The lower-case $d_q(t_1,t_2)$ is the photon propagator in the decoupled system. In appendix A.2 we discuss the Keldysh formalism in more detail. Next we use the Langreth theorem of analytic continuation [Lan76] to go to real time. In the real time language the lesser photon propagators read

$$\begin{aligned} D_q^<(t_1,t_2) = d_q^<(t_1,t_2) + \int_{-\infty}^{\infty} \mathrm{d}t_1' \mathrm{d}t_2' \Big[ & d_q^T(t_1,t_1')\Pi_q^T(t_1',t_2') D_q^<(t_2',t_2) \\ & - d_q^T(t_1,t_1')\Pi_q^<(t_1',t_2') D_q^{\tilde{T}}(t_2',t_2) \\ & - d_q^<(t_1,t_1')\Pi_q^>(t_1',t_2') D_q^<(t_2',t_2) \\ & + d_q^<(t_1,t_1')\Pi_q^{\tilde{T}}(t_1',t_2') D_q^{\tilde{T}}(t_2',t_2) \Big], \end{aligned} \tag{5.5}$$

$$\begin{aligned} D_q^<(t_1,t_2) = d_q^<(t_1,t_2) + \int_{-\infty}^{\infty} \mathrm{d}t_1' \mathrm{d}t_2' \Big[ & D_q^T(t_1,t_1')\Pi_q^T(t_1',t_2') d_q^<(t_2',t_2) \\ & - D_q^T(t_1,t_1')\Pi_q^<(t_1',t_2') d_q^{\tilde{T}}(t_2',t_2) \\ & - D_q^<(t_1,t_1')\Pi_q^>(t_1',t_2') d_q^<(t_2',t_2) \\ & + D_q^<(t_1,t_1')\Pi_q^{\tilde{T}}(t_1',t_2') d_q^{\tilde{T}}(t_2',t_2) \Big]. \end{aligned} \tag{5.6}$$

Equations (5.5) and (5.6) allow us to write down the equations of motion. At this point it becomes clear why we did the formal trick of symmetrizing the time derivative and why we did all previous steps for both versions of the Dyson equation. Acting with $\partial_{t_1}$ on the first equation and with $\partial_{t_2}$ on the second boils down to calculating time derivatives of *free* Green's functions instead of fully dressed ones. This is trivial, since free Green's function are the solution to the free Schrödinger equation

$$\begin{aligned} \big(\mathrm{i}\partial_t - H_0(-\mathrm{i}\nabla_x, x, t)\big) d^<(x,t,x',t') &= 0, \\ \big(\mathrm{i}\partial_t - H_0(-\mathrm{i}\nabla_x, x, t)\big) d^>(x,t,x',t') &= 0, \\ \big(\mathrm{i}\partial_t - H_0(-\mathrm{i}\nabla_x, x, t)\big) d^T(x,t,x',t') &= \delta(x-x')\delta(t-t'), \\ \big(\mathrm{i}\partial_t - H_0(-\mathrm{i}\nabla_x, x, t)\big) d^{\tilde{T}}(x,t,x',t') &= -\delta(x-x')\delta(t-t'), \end{aligned} \tag{5.7}$$

by definition. In case of the time ordered version with a potential of a delta distribution shape. The Kadanoff-Baym equations read

$$\Big(\mathrm{i}\partial_{t_1} - w_q\Big)D_q^<(t_1,t_2) = \int_{-\infty}^{\infty}\mathrm{d}t_2'\Big[\Pi_q^T(t_1,t_2')D_q^<(t_2',t_2) - \Pi_q^<(t_1,t_2')D_q^{\tilde{T}}(t_2',t_2)\Big],$$
$$\Big(-\mathrm{i}\partial_{t_2} - w_q\Big)D_q^<(t_1,t_2) = \int_{-\infty}^{\infty}\mathrm{d}t_1'\Big[D_q^T(t_1,t_1')\Pi_q^<(t_1',t_2) - D_q^<(t_1,t_1')\Pi_q^{\tilde{T}}(t_1',t_2)\Big], \quad (5.8)$$

where $w_q$ denotes the photon mode with momentum $q$. Subtracting the second from the first equation gives us exactly the formula we defined as the luminescence. Finally we use general relations between the time-ordered and the retarded, advanced, lesser and greater Green's functions which follow from their definitions. All together we get a very general expression for the spontaneous photon emission

$$L(t) = \sum_q \int_{-\infty}^{\infty}\mathrm{d}t'\Big[\Pi_q^R(t,t')D_q^<(t',t) + \Pi_q^<(t,t')D_q^A(t',t) - D_q^R(t,t')\Pi_q^<(t',t) - D_q^<(t,t')\Pi_q^A(t',t)\Big] \quad \text{and} \quad D_q^<(t,t') = 0. \quad (5.9)$$

So far everything is complete general and we have not made any assumptions. The second and the third term in equation (5.9) describe the spontaneous emission and the other two terms contain stimulated emission and absorption. Now comes a subtle step. We want to assume stationarity in order to Fourier transform. By assuming stationarity we mean that each component of the Luminescence does only depend on relative but not on absolute times $f(t,t') = f(t-t')$. However, we will show that it is crucial to check if a stationary state can be reached in the first place. The reason is that as soon as we assume stationarity and that the system was decoupled in the distant past we can use a set of simplified Dyson equations (5.11). But once we have done this there is no way to check whether this stationary state makes sense. Assuming a stationary state exists and the system is described by this state we Fourier transform the equation for the luminescence:

$$L = -\frac{\mathrm{i}}{\pi}\sum_q \int_{-\infty}^{\infty}\mathrm{d}w\Big[\Pi_q^<(w)\mathrm{Im}\Big(D_q^R(w)\Big) - D_q^<(w)\mathrm{Im}\Big(\Pi_q^R(w)\Big)\Big]. \quad (5.10)$$

Let us further assume that in the infinite past the system is decoupled, there are no photons and that the leads are individually described by equilibrium distribution functions. Then the Dyson equations for the stationary state simplify to

$$\begin{aligned} G^A &= \frac{1}{(g^A)^{-1} - \Pi^A} \\ G^R &= \frac{1}{(g^R)^{-1} - \Pi^R}, \\ G^< &= g^< + G^R\Pi^<G^A, \\ G^> &= g^> + G^R\Pi^>G^A. \end{aligned} \quad (5.11)$$

In the following calculation we will omit the photon momentum $q$ and energy arguments $w$ for clarity,

$$L = -\frac{\mathrm{i}}{\pi}\sum_q \int_{-\infty}^{\infty}\mathrm{d}w\Big[\Pi^<\mathrm{Im}\Big(D^R\Big) - D^<\mathrm{Im}\Big(\Pi^R\Big)\Big]$$

and focus on the integrand

$$\begin{aligned} &\Pi^<\mathrm{Im}\Big(D^R\Big) - D^<\mathrm{Im}\Big(\Pi^R\Big) \\ &= \Pi^<\mathrm{Im}\Big(D^R\Big) - d^<\mathrm{Im}\Big(\Pi^R\Big) - D^R\Pi^<D^A\mathrm{Im}\Big(\Pi^R\Big). \end{aligned} \quad (5.12)$$

Together with the assumption that the uncoupled system does not contain any photons $d^< \equiv 0$ and because of $D^R = (D^A)^*$ we can now show that the integrand is infinitesimal if $\Pi_q^R(w)$ has a finite imaginary part:

$$\begin{aligned}
&= \Pi^< \left[ \mathrm{Im}\Big(D^R\Big) - |D^R|^2 \mathrm{Im}\Big(\Pi^R\Big) \right] \\
&= \Pi^< |D^R|^2 \mathrm{Im}\left[ ((D^R)^*)^{-1} - \Pi^R \right] \\
&= \Pi^< |D^R|^2 \mathrm{Im}\left[ ((d^R)^*)^{-1} - (\Pi^R)^* - \Pi^R \right] \\
&= \Pi^< |D^R|^2 \mathrm{Im}\left[ ((d^R)^*)^{-1} \right] \\
&= \lim_{\eta \to 0} \Pi^< \frac{-\eta}{|w - w_q + \mathrm{i}\eta - \Pi_q^R(w)|^2}
\end{aligned} \tag{5.13}$$

The final result vanishes if $\Pi_q^R(w)$ has a finite imaginary part which is the case in any model that describes a real experiment. Hence, the luminescence vanishes

$$L = -\frac{\mathrm{i}}{\pi} \sum_q \int_{-\infty}^{\infty} \mathrm{d}w \Big[ \lim_{\eta \to 0} \Pi_q^<(w) \frac{-\eta}{|w - w_q + \mathrm{i}\eta - \Pi_q^R(w)|^2} \Big]. \tag{5.14}$$

The absorption cancels the spontaneous and the stimulated photon emission. Notice that this result was obtained without saying anything about the system or the kind of nonequilibrium situation. We obtain this result whether the system can reach a stationary state or whether it can not. Generally speaking the system can reach such a stationary state if its absorption rate $A$ is greater than it's induced emission rate $I$. Qualitatively in the limit of low photon densities the corresponding differential equation with spontaneous emission $E$ reads

$$\dot{n}_{ph} = E + (I - A) n_{ph}. \tag{5.15}$$

Both $I$ and $A$ are functions of the electron distribution in the bands. A popular example where it can't reach a stationary state is a laser in a cavity. The level inversion leads to a dominating induced emission ($I > A$). It is therefore crucial that we check whether a stationary state is possible before using Fourier transform and the simplified Dyson equations.

In order to ensure stationarity and to make our calculations simpler we introduce spherical photon detector that encloses the light emitting diode. This detector absorbs all light that exits the light emitting diode immediately. By light we mean all real - as opposed to virtual - photons. We model the detector by the boundary condition $n_{\mathrm{ph}}(t) = 0$. Since both stimulated photon emission and photon absorption require real photons, we observe only spontaneous photon emission. In the following we will continue to use the term luminescence but from now on imply that it is only the spontaneous photon emission. This also has the convenient side effect to ensure that the system always reaches a stationary state. Mathematically having zero photons in the system which is in a stationary state, corresponds to $D_q^<(w) = 0$. The reason is that because we have a stationary state and assume that the photons can be described by a distribution function, we can express the lesser photon propagator as the product of photon occupation number $n_{ph}(w)$ and the photon spectral density $\mathcal{A}_q(w)$ [Alt10]:

$$\mathrm{i}D_q^<(w) = n_{ph}(w)(D_q^A(w) - D_q^R(w)) = n_q(w)\mathcal{A}_q(w). \tag{5.16}$$

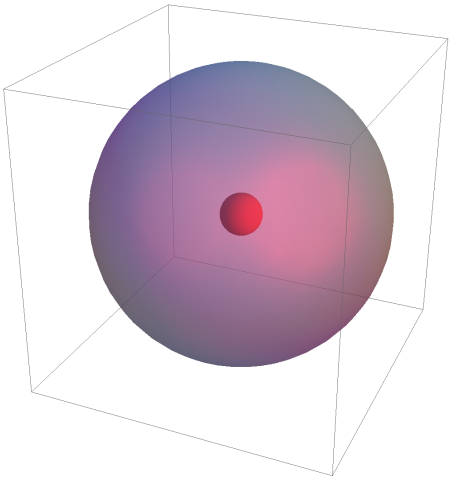

Figure 5.1.: Experimental setup - LED in spherical detector

Both, $n_{ph}$ and $\mathcal{A}_q(w)$ are positive semidefinite numbers, and therefore $D_q^<(w) \geq 0$. The number of photons in the system can be written as

$$n_{ph} = \sum_q \int \mathrm{d}w\, n_{ph}(w)\mathcal{A}_q(w) = \mathrm{i}\sum_q \int \mathrm{d}w\, D_q^<(w) = 0, \tag{5.17}$$

and hence $D_q^<(w) = 0$. The formula for the luminescence simplifies to

$$L^{\mathrm{em}} = -\frac{\mathrm{i}}{\pi}\sum_q \int_{-\infty}^{\infty} \mathrm{d}w\, \Pi_q^<(w)\mathrm{Im}\Big(D_q^R(w)\Big), \tag{5.18}$$

since it now contains only spontaneous photon emission. We indicate this by the superscript "em".

### 5.1.2. Model and assumptions

So far all calculations have been on a very general level. In this subsection we analyze our model (5.19), go to the stationary limit and justify several approximations that we need throughout the rest of the section. We begin with the model Hamiltonian of a light emitting diode

$$H = \sum_k \epsilon_{c,k} c_k^\dagger c_k + \sum_p \epsilon_{v,p} v_p^\dagger v_p + \sum_q w_q b_q^\dagger b_q + g\sum_{k,q} b_q c_k^\dagger v_{k-q} + g^*\sum_{k,q} b_q^\dagger v_{k-q}^\dagger c_k, \tag{5.19}$$

which we derived in section 4.1. Conduction and valence band have a parabolic shape. The photons have a linear dispersion relation, $d$ is the spatial dimension of the system and $c$ the speed of light. The difference in chemical potentials is the applied forward bias $\mu_c - \mu_v = \mathrm{e}V$. It is comparable to the size of the gap between the conduction and the valence band $\Delta\epsilon \equiv \epsilon_{c,0} - \epsilon_{v,0}$. The position of the chemical potentials is chosen so that they both lie within the bands. A typical semiconductor where the chemical potential lies in the band is for example PbTe. The coupling constant $g$ is assumed to be small relative to the energy of the gap. We assume that at some distant time in the past the system was decoupled and that the interaction was switched on over a time scale $\eta^{-1}$. This is encoded in the coupling 'constant'

$$g = g(t) = |g|\mathrm{e}^{\eta t}. \tag{5.20}$$

We chose the switchon to be adiabatic in order to send the switchon parameter to zero later in the calculations. In addition we require that the decoupled state the components of the system where in their individual thermal equilibrium characterized by individual chemical potentials. For simplicity we set the temperature of the two leads to be the same and constant at all times. We totally ignore thermal currents. The free Keldysh Green's functions which are the main building blocks of all calculations are given by

$$\begin{aligned}
g^T_{\mathbf{p}}(w) &= \frac{1}{w-\epsilon_p+\mathrm{i}0} \pm 2\pi\mathrm{i}n_p\delta(w-\epsilon_p),\\
g^<_{\mathbf{p}}(w) &= \pm 2\pi\mathrm{i}n_p\delta(w-\epsilon_p),\\
g^>_{\mathbf{p}}(w) &= -2\pi\mathrm{i}(1\mp n_p)\delta(w-\epsilon_p),\\
g^{\tilde{T}}_{\mathbf{p}}(w) &= -\frac{1}{w-\epsilon_p-\mathrm{i}0} \pm 2\pi\mathrm{i}n_p\delta(w-\epsilon_p),
\end{aligned}$$

$$\begin{aligned}
g^R_{\mathbf{p}}(w) &= \frac{1}{w-\epsilon_p+\mathrm{i}0},\\
g^A_{\mathbf{p}}(w) &= \frac{1}{w-\epsilon_p-\mathrm{i}0},\\
g^K_{\mathbf{p}}(w) &= -2\pi\mathrm{i}(1\mp 2n_p)\delta(w-\epsilon_p).
\end{aligned} \tag{5.21}$$

Their derivation is straightforward and not discussed here. Because the free Green's functions describe parts of the system that are at equilibrium, Fourier transform is legitimate. The upper signs are for fermions the lower for bosons.

Before we go into the calculations we discuss the assumptions that we use during the rest of the section. Whenever one or more assumptions are used this will be denoted by wavy equal lines. The first assumption is that we write $k+q \approx k$. This is justified because the energy of a photon at a given momentum is much greater than the kinetic energy of an electron at the same momentum. Photons with the energy of the gap in the semiconductor have such a small momentum that it is negligible in comparison to the momenta of electrons even at relatively low kinetic energies. As an example an electron with same momentum as a photon at 1 eV has a kinetic energy of $10^{-5}$ eV or $0,1K$. This means that the momentum of the electrons going from the conduction to the valence band $k$ or the other way round is almost conserved. Second, we execute sums over peaked functions by rewriting them as integrals over the given energy variable and a density of states. We assume that this density of states does not vary too much in the region where the integrand is peaked and treat it as a constant. This is legitimate because both electron and photon density of states usually behave as power laws with no divergences at finite energies. Finally, where appropriate, we approximate $\Delta\epsilon_k \approx \Delta\epsilon$, where $\Delta\epsilon_k \equiv \epsilon_{c,k} - \epsilon_{v,k}$ and $\Delta\epsilon = \Delta\epsilon_{k=0}$.

### 5.1.3. Luminescence to leading order in the coupling $|g|$

In this subsection we derive the leading contribution to the photon emission. We show that the spontaneous emission of photons depends on the occupation of the conduction band and the availability of free states in the valence band. Also emission is only possible if there is a finite density of states at the energy of the emitted photons. The leading order is quadratic in the coupling constant $|g|$. The linear order terms vanish due to an odd number of operators of each type, e.g. $\langle c\rangle = 0$. For the same reason all odd orders vanish. We label expressions that are in second order in the coupling by superscript (1)

and expressions in fourth order by superscript (2). The first order luminescence is

$$L^{\mathrm{em}(1)} = -\frac{\mathrm{i}}{\pi}\sum_q \int_{-\infty}^{\infty} \mathrm{d}w\, \Pi^{<(1)}_{ph,q}(w)\mathrm{Im}\Big(d^R_q(w)\Big). \tag{5.22}$$

At the heart of interest is the photon self energy $\Pi^<_q(w)$. We derive it by comparing the perturbative expression of the photon propagator

$$D_q(t_1,t_2) \equiv -\mathrm{i}\sum_{n=0}\frac{(-\mathrm{i})^n}{n!}\int_C \mathrm{d}s_1...\mathrm{d}s_1 \left\langle \hat{T}_c\, H^{\mathrm{int}}_{H_0}(s_1)...H^{\mathrm{int}}_{H_0}(s_n) b_q(t_1) b^\dagger_q(t_2)\right\rangle \tag{5.23}$$

order by order with the Dyson equation:

$$\begin{aligned} D^{(1)}_q(t_1,t_2) &= -\mathrm{i}|g|^2\sum_{k_1}\int_C \mathrm{d}s_{1,2}\, d_q(t_1,s_1) g^c_{k_1}(s_1,s_2) g^v_{k_1-q}(s_2,s_1) d_q(s_2,t_2) \\ &\equiv \int_C \mathrm{d}s_1\mathrm{d}s_2\; d_q(t_1,s_1)\Pi^{(1)}_{ph,q}(s_1,s_2) d_q(s_2,t_2) \end{aligned} \tag{5.24}$$

The leading order self energy

$$\Pi^{(1)}_{ph,q}(s_1,s_2) = -\mathrm{i}|g|^2\sum_k g^c_k(s_1,s_2) g^v_{k-q}(s_2,s_1) = \tag{5.25}$$

is depicted by a self energy bubble which consists of a conduction band propagator (full line) and a valence band propagator (dotted line). Physically it describes a particle-hole excitation and therefore often called polarization operator. In order to calculate the luminescence we need to evaluate the lesser photon self energy. We do this by going to a real time matrix notation that is discussed in appendix A.2. The free Green's function are translational invariant in time and hence depend only on their relative arguments. Therefore we can go to Fourier space and use the explicit expressions from equations 5.21 to evaluate

$$\Pi^{(1)}_{ph,ab,q}(w) = -\mathrm{i}|g|^2\sum_k \int \frac{\mathrm{d}w_1}{2\pi}\; g^c_{ab,k}(w_1) g^v_{ba,k-q}(w_1-w). \tag{5.26}$$

The indices a and b are so called Keldysh indices. For example $a=1$ and $b=2$ denotes that the first time argument lies on the forward and the second on the backward contour. This example $a=1$, $b=1$ is equivalent with the lesser Green's function. The explicit result for the leading order polarization operator is

$$\Pi^{<(1)}_{ph,q}(w) = -2\pi\mathrm{i}|g|^2\sum_k n_{c,k}(1-n_{v,k-q})\delta(w+\epsilon_{v,k-q}-\epsilon_{c,k}). \tag{5.27}$$

With this we can explicitly evaluate the luminescence in leading order

$$\begin{aligned} L^{\mathrm{em}(1)} &= -\frac{\mathrm{i}}{\pi}\sum_q\int_{-\infty}^{\infty}\mathrm{d}w\,\Pi^{<(1)}_{ph,q}(w)\mathrm{Im}\Big(d^R_q(w)\Big) \\ &= 2\pi|g|^2\sum_{k,q} n_{c,k}(1-n_{v,k-q})\delta(w_q+\epsilon_{v,k-q}-\epsilon_{c,k}) \\ &\approx 2\pi|g|^2\sum_k N_{ph}(\epsilon_{c,k}-\epsilon_{v,k}) n_{c,k}(1-n_{v,k}) \\ &\approx 2\pi|g|^2 N_{ph}(\Delta\epsilon)\sum_k n_{c,k}(1-n_{v,k}) \end{aligned} \tag{5.28}$$

where $N_{ph}(w)$ is the photon density of states and $\Delta\epsilon$ the semiconductor gap. The result (5.28) satisfies the physical intuition. The photon emission depends on the filling of the conduction band and the availability of free states in the valence band. Also in order to emit a photon, photon states must be available at the given energy. This is represented by the photon density of states. For a free photon gas the density of states is given by

$$N_{ph}(w) = \Big(\frac{L}{2\pi c}\Big)^d \Omega_d \, w^{d-1}. \tag{5.29}$$

$L$ is the system size, $c$ the speed of light and $\Omega_d$ is the surface of a unit sphere in a space of dimension $d$.

### 5.1.4. Next to leading order correction

In this subsection we discuss the next to leading order corrections to the photon emission, formally given by (5.30)

$$L^{\mathrm{em}(2)} = -\frac{\mathrm{i}}{\pi}\sum_q \int_{-\infty}^{\infty} \mathrm{d}w \Big[\Pi_q^{<(1)}(w)\mathrm{Im}\Big(D_q^{R,(1)}(w)\Big) + \Pi_q^{<(2)}(w)\mathrm{Im}\Big(d_q^R(w)\Big)\Big]. \tag{5.30}$$

It is crucial to be aware what the delta distributions in the free Green's functions 5.21 really mean. They all stem from the limit of vanishing convergence factor

$$\lim_{\eta\to 0^+} \mathrm{Im}\bigg(\frac{1}{w-\epsilon+\mathrm{i}\eta}\bigg) = -\pi\delta(w-\epsilon), \qquad \delta(0)\sim\frac{1}{\eta}. \tag{5.31}$$

Therefore it is important not to mix terms where the convergence factor is still explicitly written with terms where it has been send to zero already. After some algebra we find the following results:

$$\begin{aligned}
D_q^{R,(1)}(w) &= |g|^2\Big(\frac{1}{w-w_q+\mathrm{i}0^+}\Big)^2 \sum_k \frac{n_{v,k-q}-n_{c,k}}{w+\epsilon_{v,k-q}-\epsilon_{c,k}+\mathrm{i}0^+} \\
\Pi_q^{<(1)}(w) &= (-2\pi\mathrm{i})|g|^2 \sum_k n_{c,k}(1-n_{v,k-q})\mathrm{Im}\bigg(\frac{-1/\pi}{w+\epsilon_{v,k-q}-\epsilon_{c,k}+\mathrm{i}0^+}\bigg) \\
\Pi_q^{<(2)}(w) &= 0
\end{aligned} \tag{5.32}$$

In appendices B.2 and B.3 we give a detailed derivation. The second term of equation (5.30), which describes induced emission, vanishes as it should. The term that is left describes virtual processes where a photon is emitted and immediately reabsorbed. These lead to an effective interaction between the two electron bathes. Explicitly it is given by

$$\begin{aligned}
&-\frac{\mathrm{i}}{\pi}\sum_q \int_{-\infty}^{\infty} \mathrm{d}w\, \Pi_q^{<(1)}(w)\mathrm{Im}\Big(D_q^{R,(1)}(w)\Big) \\
&= -2|g|^4 \sum_q \int_{-\infty}^{\infty} \mathrm{d}w \sum_k n_{c,k}(1-n_{v,k-q})\mathrm{Im}\bigg(\frac{-1/\pi}{w+\epsilon_{v,k-q}-\epsilon_{c,k}+\mathrm{i}0^+}\bigg)\times \\
&\qquad \times \mathrm{Im}\bigg(\Big(\frac{1}{w-w_q+\mathrm{i}0^+}\Big)^2 \sum_{k_1} \frac{n_{v,k_1-q}-n_{c,k_1}}{w+\epsilon_{v,k_1-q}-\epsilon_{c,k_1}+\mathrm{i}0^+}\bigg) \\
&\approx -2\pi|g|^4 \frac{\mathcal{N}_{ph}(\Delta\epsilon)}{\Delta\epsilon} \sum_{k,k_1} n_{c,k}(1-n_{v,k})(n_{v,k_1}-n_{c,k_1})\delta(\Delta\epsilon_k-\Delta\epsilon_{k_1}).
\end{aligned} \tag{5.33}$$

Under the assumption that the effective mass of conduction and valence band has the same absolute value we can simplify this equation a little further into its final form

$$\begin{aligned}
= -2\pi|g|^4 \frac{\mathcal{N}_{ph}(\Delta\epsilon)}{\Delta\epsilon} \int \mathrm{d}\epsilon \, \big(\mathcal{N}_F(\epsilon)\big)^2 n_F(\epsilon_{c0}+\epsilon-\mu_c)(1-n_F(\epsilon_{v0}-\epsilon-\mu_v))\times \\
\times (n_F(\epsilon_{v0}-\epsilon-\mu_v)-n_F(\epsilon_{c0}+\epsilon-\mu_c)).
\end{aligned} \tag{5.34}$$

In the equation above $n_F$ are the usual fermi functions and $\mathcal{N}_F(\epsilon) \sim \epsilon^{(d-2)/2}$ is the density of states of a free fermi gas.

### 5.1.5. Higher order corrections

In the last two subsections we discussed the spontaneous photon emission of a light emitting diode in leading and next to leading order. In this subsection we want to investigate if higher order corrections are important and if so what their effect is. We start from the full photo emission term

$$L^{\mathrm{em}} = -\frac{\mathrm{i}}{\pi} \sum_q \int_{-\infty}^{\infty} \mathrm{d}w \, \Pi^<_{ph,q}(w) \mathrm{Im}\Big(D^R_{ph,q}(w)\Big). \tag{5.35}$$

The lesser photon self energy is particularly easy to calculate. Because we have banished all photons from the system $D^< \equiv 0$ there are no higher order corrections to the lesser component of the polarization operator

$$\Pi^<_{ph,q}(w) = \Pi^{<(1)}_{ph,q}(w). \tag{5.36}$$

Details are explained in the appendix B.3. The corrections to the photon propagator are less trivial because they lead to an infinite hierarchy of equations. Using the general expressions

$$\begin{aligned} \Pi^R &= \Pi^T - \Pi^<, \\ G^T_c G^T_v - G^<_c G^>_v &= G^R_c G^A_v + G^<_c G^A_v + G^R_c G^>_v, \end{aligned} \tag{5.37}$$

we find

$$D^R = \frac{1}{(d^R)^{-1} - \Pi^R_{ph}} \qquad \Pi^R_{ph} \sim \int G^R_c \otimes G^A_v + G^<_c \otimes G^A_v + G^R_c \otimes G^>_v, \tag{5.38}$$

for the photon propagator and photon self energy. Similar relations hold for the electron propagators. All together this results in a set of coupled equations that only truncates in very special cases. For clarity we introduced a short hand notation $\otimes$ to denote convolution $\int A \otimes B = \int \mathrm{d}w_1 A(w_1) B(w - w_1)$ and $\tilde{\otimes}$ to denote the correlation integrals $\int A \otimes B = \int \mathrm{d}w_1 A(w_1) B(w_1 - w)$. An easy way to truncate these equations is the random phase approximation

$$D^{R,RPA} = \frac{1}{(d^R)^{-1} - \Pi^{R(1)}_{ph}}. \tag{5.39}$$

This approximation is good if the particle density if fairly high. Usually the small parameter is the number of carriers per atomic volume. Since the photon emission takes place in the depletion layer where the carrier density is not very high the random phase approximation is far from exact. However, since the main effect that we are interested in is the resulting level broadening it is safe to say that such an effect is robust against more sophisticated corrections. The derivation of the lowest order photon self energy is straightforward, yielding

$$\begin{aligned} \Pi^{R(1)}_{ph,q}(w) &= -\mathrm{i}|g|^2 \sum_k \int \frac{\mathrm{d}w_1}{2\pi} \Big( g^R_{c,k}(w_1) g^A_{v,k-q}(w_1 - w) + g^<_{c,k}(w_1) g^A_{v,k-q}(w_1 - w) \\ &\qquad + g^R_{c,k}(w_1) g^>_{v,k-q}(w_1 - w) \Big) \\ &= |g|^2 \sum_k \frac{n_{v,k-q} - n_{c,k}}{w - \epsilon_{c,k} + \epsilon_{v,k-q} + 2\mathrm{i}0^+}. \end{aligned} \tag{5.40}$$

We explain more details in the appendix B.3. The main effect is that the photon propagator gets a finite imaginary component

$$D_q^R(w) \equiv \frac{1}{w - w_q - \Sigma_{ph}^R - \mathrm{i}\Gamma_{ph}^R}. \tag{5.41}$$

The other effect is a shift in the resonance frequency. Both effects are second order in the coupling constant and therefore only lead to small contributions

$$\begin{aligned} D_q^R(w) &\equiv \frac{1}{w - w_q - \Sigma_{ph}^R - \mathrm{i}\Gamma_{ph}^R}, \\ \Sigma_{ph}^{R,(1)} &\equiv \mathrm{Re}\Big(\Pi_{ph,q}^{R(1)}(w)\Big) \sim |g|^2, \\ \Gamma_{ph}^{R,(1)}(w) &\equiv \mathrm{Im}\Big(\Pi_{ph,q}^{R(1)}(w)\Big) \sim |g|^2 N_F(w) \leq 0. \end{aligned} \tag{5.42}$$

All together the luminescence in random phase approximation is

$$\begin{aligned} L^{\text{em, (RPA)}} &= -2|g|^2 \sum_{k,q} n_{c,k}(1 - n_{v,k-q})\mathrm{Im}\Big(D_{ph,q}^{R,RPA}(\epsilon_{c,k} - \epsilon_{v,k-q})\Big) \\ &\approx -2|g|^2 \sum_{k} n_{c,k}(1 - n_{v,k})\times \\ &\qquad \times \int_0^\Gamma \mathrm{d}w_q \mathcal{N}_{ph}(w_q) \frac{\Gamma_{ph}^{R,(1)}(\Delta\epsilon_k)}{(\Delta\epsilon_k - w_q - \Sigma_{ph}^{R,(1)}(\Delta\epsilon_k))^2 + (\Gamma_{ph}^{R,(1)}(\Delta\epsilon_k))^2} \\ &\approx 2\pi|g|^2 \overline{\mathcal{N}_{ph}}(\Delta\epsilon) \sum_k n_{c,k}(1 - n_{v,k}). \end{aligned} \tag{5.43}$$

Here $\overline{\mathcal{N}_{ph}}(\Delta\epsilon)$ refers to the photon density averaged over the interval $(\Delta\epsilon + \Gamma^R, \Delta\epsilon - \Gamma^R)$. Summarizing our analysis we have shown that higher order corrections to the luminescence have only a small quantitative effect and that perturbation theory is well justified.

### 5.1.6. Special case: Two level system

In this subsection we discuss a simplified model

$$H = \epsilon_c c^\dagger c + \epsilon_v v^\dagger v + \sum_q w_q b_q^\dagger b_q + g\sum_q b_q c^\dagger v + g^* \sum_q b_q^\dagger v^\dagger c, \tag{5.44}$$

where the electron bands are replaced by single levels. The absence of a finite level width generates divergences in the next to leading order terms. By summing up an infinite series of diagrams and using random phase approximation the photon mediated interaction gives a finite width to the electron levels and the divergences vanish.

The derivation of the photon emission rate in lowest order is analogous to the derivation in subsection 5.1.3. Previously the nonequilibrium information was encoded in the chemical potentials, here it is simply given by fixed electron occupation numbers $n_c$ and $n_v$. In fact the result

$$\begin{aligned} L^{\mathrm{em}(1)} &= -\frac{\mathrm{i}}{\pi}\sum_q \int_{-\infty}^{\infty} \mathrm{d}w\ \Pi_{ph}^{<(1)}(w)\mathrm{Im}\Big(d_q^R(w)\Big) \\ &= 2\pi|g|^2 \mathcal{N}_{ph}(\epsilon_c - \epsilon_v)\Big[n_c(1 - n_v)\Big] \end{aligned} \tag{5.45}$$

looks very much alike, with the exception that the sum over electron momenta is absent. However, when we go to the next to leading order divergences occur:

$$\begin{aligned}
L^{\mathrm{em}(2)} &= -\frac{\mathrm{i}}{\pi}\sum_q \int_{-\infty}^{\infty} \mathrm{d}w\, \Pi_q^{<(1)}(w)\mathrm{Im}\Big(D_q^{R,(1)}(w)\Big) \\
&= -2|g|^4 \sum_q \int_{-\infty}^{\infty} \mathrm{d}w\, n_c(1-n_v)\mathrm{Im}\bigg(\frac{-1/\pi}{w+\epsilon_v-\epsilon_c+\mathrm{i}0^+}\bigg)\times \\
&\qquad \times \mathrm{Im}\bigg(\Big(\frac{1}{w-w_q+\mathrm{i}0^+}\Big)^2 \frac{n_v-n_c}{w+\epsilon_v-\epsilon_c+\mathrm{i}0^+}\bigg) \\
&\approx 2|g|^4 \mathcal{N}_{ph}(\Delta\epsilon) n_c(1-n_v)(n_v-n_c)\times \\
&\qquad \times \int_{-\infty}^{\infty} \mathrm{d}w\, \mathrm{Im}\bigg(\frac{-1/\pi}{w-\Delta\epsilon+\mathrm{i}0^+}\bigg)\mathrm{Im}\Big(\frac{1}{w+\mathrm{i}0^+}\frac{1}{w-\Delta\epsilon+\mathrm{i}0^+}\Big) \\
&= -\frac{|g|^4}{0^+}\frac{\mathcal{N}_{ph}(\Delta\epsilon)}{\Delta\epsilon}\, n_c(1-n_v)(n_v-n_c).
\end{aligned} \tag{5.46}$$

Mathematically this results from the degenerated photon propagators that link the electron-hole bubbles. In order to fix this problem two steps are necessary. First we renormalize the conduction electron and the valence electron propagators. To do that we sum up an infinite series of diagrams in random phase approximation. The key result is that both obtain a finite imaginary self energy contribution, finite level width. During this step we also introduce a ultraviolet cutoff $\Lambda$ for the photon spectrum. From now on this will implicitly be encoded in the photon density of states $\mathcal{N}_{ph}(\epsilon) \sim \theta(w)\theta(\Lambda - w)$. We than use the renormalized electron propagators to calculate electron-hole bubble. In the second step we renormalize the photon propagator by summing up an infinite series of diagrams in random phase approximation with the renormalized electron-hole bubble. Both steps together remove the divergence. We denote the terms with random phase corrections by "RPA". Additionally we name terms such as the renormalized photon propagator, that do contain random phase approximations with self energies that themself have been renormalized already by RPA+. The fully renormalized expressions are

$$\begin{aligned}
L^{\mathrm{em,\ RPA+}} &= -\frac{\mathrm{i}}{\pi}\sum_q \int_{-\infty}^{\infty} \mathrm{d}w\ \Big(\Pi_{ph,q}^{<(1)}(w)\Big)\mathrm{Im}\Big(D_q^{R,\mathrm{RPA+}}(w)\Big), \\
D^{R,\mathrm{RPA+}} &= \frac{1}{(d^R)^{-1} - \Pi_{ph}^{R,\mathrm{RPA+}}} =
\end{aligned} \tag{5.47}$$

We begin with summing up the geometric series for the RPA corrected electron propagators $G_c$ and $G_v$. The derivation of the valence electron-photon and conduction electron - photon self energy bubbles is analogous the the electron-hole bubble that we discussed earlier and

we state only the results:

$G_c^{\mathrm{RPA}}(w) =$ 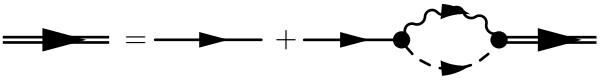

$$
\begin{aligned}
G_c^{R,\mathrm{RPA}}(w) &= \frac{1}{(w-\epsilon_c) + |g|^2(1-n_v)\Big(\int \mathrm{d}w_q \frac{\mathcal{N}_{ph}(w_q)}{w_q - w + \epsilon_v} + \mathrm{i}\pi N_{ph}(w-\epsilon_v)\Big)} \\
G_c^{A,\mathrm{RPA}}(w) &= \frac{1}{(w-\epsilon_c) + |g|^2(1-n_v)\Big(\int \mathrm{d}w_q \frac{\mathcal{N}_{ph}(w_q)}{w_q - w + \epsilon_v} - \mathrm{i}\pi N_{ph}(w-\epsilon_v)\Big)} \\
G_c^{<,\mathrm{RPA}}(w) &= g_c^{<}(w)
\end{aligned}
$$

$G_v^{\mathrm{RPA}}(w) =$ 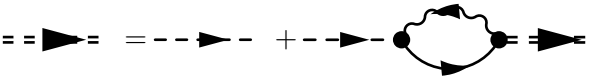

$$
\begin{aligned}
G_v^{R,\mathrm{RPA}}(w) &= \frac{1}{(w-\epsilon_v) - |g|^2 n_c\Big(\int \mathrm{d}w_q \frac{\mathcal{N}_{ph}(w_q)}{w_q + w - \epsilon_c} - \mathrm{i}\pi N_{ph}(\epsilon_c - w)\Big)} \\
G_v^{A,\mathrm{RPA}}(w) &= \frac{1}{(w-\epsilon_v) - |g|^2 n_c\Big(\int \mathrm{d}w_q \frac{\mathcal{N}_{ph}(w_q)}{w_q + w - \epsilon_c} + \mathrm{i}\pi N_{ph}(\epsilon_c - w)\Big)} \\
G_v^{>,\mathrm{RPA}}(w) &= g_v^{>}(w)
\end{aligned}
\tag{5.48}
$$

Before we derive the more complicated higher order self energy bubbles we make some approximations. As before we assume that the photon density of states is sufficiently smooth around $w_q = \Delta\epsilon$. We then exploit that the self energy is proportional to the square of the coupling constant and therefore small. Hence, it is only relevant if $(w - \epsilon_c) \leq |g|^2 N_{ph}(\Delta\epsilon)$. This allows to approximate the self energy as a constant, since the $w$-dependence is not important. The imaginary part of the self energy is denoted by $\Gamma_c^R = \pi|g|^2(1-n_v)N_{ph}(\Delta\epsilon)$ which is in general finite, since $n_v < 1$. Hence, we can neglect the infinitesimal imaginary part of the inverse free propagator. The real part of the self energy is $\Sigma_c^R \equiv |g|^2(1-n_v)\int \mathrm{d}w_q \frac{\mathcal{N}_{ph}(w_q)}{w_q - \Delta\epsilon} \sim |g|^2$ and can be absorbed in the conduction electron level energy $\tilde{\epsilon}_c = \epsilon_c + \Sigma_c^R$. This allows us to write the conduction electron propagator compact form

$$
G_c^{R,\mathrm{RPA}}(w) \approx \frac{1}{(w-\tilde{\epsilon}_c) - \mathrm{i}\Gamma_c^R}. \tag{5.49}
$$

The very same logic applies to the valence electron propagator. To avoid confusions about the location of the poles, we introduce positive constants $\Sigma_c \equiv -\Sigma_c^R = -\Sigma_c^A$ and $\Gamma_c \equiv -\Gamma_c^R = \Gamma_c^A$. Here we have exploited the fact that the imaginary parts of the retarded and advanced propagator have the same absolute value but different signs. Our unified notation is

$$
\begin{aligned}
G_c^{R,\mathrm{RPA}}(w) &\equiv \frac{1}{w - \tilde{\epsilon}_c + \mathrm{i}\Gamma_c}, & G_c^{A,\mathrm{RPA}}(w) &\equiv \frac{1}{w - \tilde{\epsilon}_c - \mathrm{i}\Gamma_c}, \\
G_v^{R,\mathrm{RPA}}(w) &\equiv \frac{1}{w - \tilde{\epsilon}_v + \mathrm{i}\Gamma_v}, & G_v^{A,\mathrm{RPA}}(w) &\equiv \frac{1}{w - \tilde{\epsilon}_v - \mathrm{i}\Gamma_v}.
\end{aligned}
\tag{5.50}
$$

In fact, if we require that $n_c + n_v = 1$, then the conduction and valence electron self energies are identical within the approximations we made so far. With this simplified result we

now derive the photon self energy in random phase approximation

$$\Pi_{ph}^{R,\mathrm{RPA}+}(w) = |g|^2 \left[ \frac{1}{w+\tilde{\epsilon}_v - \tilde{\epsilon}_c + \mathrm{i}(\Gamma_c+\Gamma_v)} + \frac{-n_c}{w+\tilde{\epsilon}_v-\epsilon_c+\mathrm{i}\Gamma_v} + \frac{-(1-n_v)}{w+\epsilon_v-\tilde{\epsilon}_c+\mathrm{i}\Gamma_c} \right]. \tag{5.51}$$

Now that we have removed all divergences we can write down the renormalized expression of the photon propagator

$$\begin{aligned} D_q^{R,\mathrm{RPA}+}(w) &= \frac{1}{w - w_q - |g|^2 \left[ \frac{1}{w+\tilde{\epsilon}_v-\tilde{\epsilon}_c+\mathrm{i}(\Gamma_c+\Gamma_v)} + \frac{-n_c}{w+\tilde{\epsilon}_v-\epsilon_c+\mathrm{i}\Gamma_v} + \frac{-(1-n_v)}{w+\epsilon_v-\tilde{\epsilon}_c+\mathrm{i}\Gamma_c} \right]} \\ &\approx \frac{1}{w - w_q - |g|^2 \left[ \frac{1}{w-\Delta\epsilon+2\mathrm{i}\Gamma} + \frac{-1+n_v-n_c}{w-\Delta\epsilon+\mathrm{i}\Gamma} \right]}. \end{aligned} \tag{5.52}$$

With the full renormalized photon propagator we have all building blocks of the luminescence together and find

$$\begin{aligned} L^{\mathrm{em,\ RPA}+} &= 2|g|^2\, n_c(1-n_v) \frac{1}{\Delta\epsilon} \int_0^{\Lambda} \mathrm{d}w_q \mathcal{N}_{ph}(w_q) \frac{\frac{\frac{1}{2}-n_v+n_c}{\pi(1-n_v)\,\Delta\epsilon N_{ph}(\Delta\epsilon)}}{\left(1-\frac{w_q}{\Delta\epsilon}\right)^2 + \left(\frac{\frac{1}{2}-n_v+n_c}{\pi(1-n_v)\,\Delta\epsilon N_{ph}(\Delta\epsilon)}\right)^2} \\ &\approx 2|g|^2\, n_c(1-n_v)\mathcal{N}_{ph}(\Delta\epsilon) \int_0^{\frac{\Lambda}{\Delta\epsilon}} \mathrm{d}x \frac{\frac{\frac{1}{2}-n_v+n_c}{\pi(1-n_v)\,\Delta\epsilon N_{ph}(\Delta\epsilon)}}{(1-x)^2 + \left(\frac{\frac{1}{2}-n_v+n_c}{\pi(1-n_v)\,\Delta\epsilon N_{ph}(\Delta\epsilon)}\right)^2} \\ &= 2\pi|g|^2\, n_c(1-n_v)\mathcal{N}_{ph}(\Delta\epsilon) \left[ \frac{1}{2} + \frac{1}{\pi} \arctan\left( \pi\,\Delta\epsilon N_{ph}(\Delta\epsilon) \frac{1-n_v}{1-n_v+n_c-\frac{1}{2}} \right) \right]. \end{aligned}$$

In appendices C.1, C.2 and C.3 we give a more detailed derivations. We see that the corrections depend on the dimensionless parameter $\Delta\mathcal{N}_{ph}(\Delta\epsilon)$ which is the product of the photon density of states at the resonance frequency times the gap size. We have used that the ultraviolet cutoff of the photon spectrum is by definition the largest energy in the problem $\frac{\Lambda}{\Delta\epsilon} \gg 1$.

Summarizing we have shown that for a two level system one encounters diverging corrections that are due to resonances between the sharp levels. We resolved this problem by preforming extensive resummation of diagrams in the random phase approximation. In the end the result for the two level system looks very much alike the result of the model with finite bandwidth. As a consequence it is sufficient to consider only the leading order contribution since the higher order terms give only quantitative corrections.

## 5.2. Effective Photon Hamiltonian

In this section we derive an effective photon Hamiltonian for a superconductor-light emitting diode-superconductor heterostructure. It's purpose is to reduce the Hamiltonian in a way that brings the nature of the photon dynamics to the surface. Also it is an expression that is tailored to calculate photon properties with minimal effort and maximal clarity. Technically speaking an effective Hamiltonian is an expression that allows to investigate the properties of a subsystem without evaluating the full Hamiltonian. In our case the subsystem of interest are the photons while we want to integrate out the electrons as far as possible. If a system is at equilibrium the derivation of such an effective Hamiltonian is straightforward. Here however we deal with a nonequilibrium problem which causes considerable problems. While it is not possible to eliminate the fermionic operators entirely we show that we can transform the Hamiltonian into a form that reveals all the qualitative physics of the photon subsystem at a glance. From our final result it is obvious that a superconductor- pn-superconductor system is a source of squeezed light.

In the first two subsections we explain the general concept and all necessary assumptions are introduced and justified. In the third and fourth subsection we derive the effective Hamiltonian of a normal light emitting diode and do some checks. After establishing the credibility of this concept we derive the more involved effective Hamiltonian of the superconductor-pn-superconductor heterostructure.

### 5.2.1. Concept and assumptions

We begin this section with a general discussion about the definition of what we call effective Hamiltonian. This is followed by an outline of the derivation and the necessary assumptions on a general level.

We consider a system of $n+1$ different types of particles. The operators $A$ and $A^\dagger$ belong to the species we are interested in and the operators $B_i$ and $B_i^\dagger$ describe the $n$ other species. Any of the operators can also have additional quantum numbers such as spin and momentum ($A \to A_{\mathbf{k},\sigma}$). Ultimately we are interested in describing experimental observable quantities. In general these can be expressed by expectation values of observables $O(t)$. Hence, any property of the A-particles can be described by expectation values of the following type:

$$\langle O(t)\rangle = \langle f(\hat{A}(t), \hat{A}^\dagger(t), t)\rangle. \tag{5.53}$$

One way to evaluate such an observable is to use the Heisenberg picture were all time dependence is included into the operators. Taking the expectation value corresponds to a trace over the density matrix at a time $t_0$ where Schrödinger and Heisenberg picture fall together by definition. Formally we can define this time to be in the far distant past. There, we assume that the individual parts of the system are decoupled and each subsystem is in its local equilibrium. Therefore at $t_0$ the subsystems can be described by equilibrium distribution functions $n_x$ and the density matrix is well known. Consequently we know exactly how to evaluate expectation values at this time. All that is left to do is to express the time dependent Heisenberg operators by operators at $t_0$. Hence, we write down the Heisenberg equations of motion and formally integrate them,

$$A_H(t) = A_H(t_0) + \mathrm{i}\int_{t_0}^{t} \mathrm{d}t' \,[H_H, A_H(t')]. \tag{5.54}$$

This is the tricky part because an exact solution is possible in special cases only. If the coupling between the subsystems is controlled by a small parameter, which we call coupling constant $|g|$, we can solve the equations of motion perturbatively. The effective

Hamiltonian is an object that replaces the original Hamiltonian in the upper equation (5.54). It can depend explicitly on time and allows us to derive the correct expression for the A-operators,

$$A_H(t) = A_H(t_0) + \mathrm{i}\int_{t_0}^{t} \mathrm{d}t' \left[(H_{\mathrm{eff}})_H(t'), A_H(t')\right] + O(|g|^3) \tag{5.55}$$

up to second order in the coupling constant. In addition, we can trace out the $B_i$ operators in all terms that are of second order in the coupling constant. This formalism is to a certain extend capable of describing non equilibrium situations. Formally we introduce nonequilibrium by adjusting the distribution functions at $t_0$. The only formal limitation is the time scale of the interaction switchon procedure. Non equilibrium phenomena that live on a longer time scale, such as stationary states, are fully accessible. The most general Hamiltonian we can treat by this method is

$$H = wA^\dagger A + \sum_i \epsilon_i B_i^\dagger B_i + gf(A, B_1, B_2, ..., B_n) + \mathrm{h.c.} + O(|g|^2). \tag{5.56}$$

The real numbers $w$ and $\epsilon_i$ are the particle energies of the decoupled system ($g = 0$). The function $f$ describes the coupling between the various species. There are no restrictions necessary since the only requirement we need to derive the effective Hamiltonian is that all couplings are at least linear in the small coupling constant $g$. The technical foundation of the following derivation are the Heisenberg equations of motion. The only approximation we make is to ignore terms of third and higher order in the coupling constant. Technically speaking the effective Hamiltonian is the original Hamiltonian $H$ without all terms that do not contain any operators of the desired species $R$ and with all operators of the species $B_i$ replaced by their expression at time $t_0$. In addition we can evaluate all expectation values of $B_i$ operators if they appear in second order terms. An important subtlety is that the latter is not possible in linear terms without losing vital information about the system. In these terms the fermionic operators at $t_0$ must remain operators and can't be traced out.

In this subsection we have discussed the definition and limitations of the effective Hamiltonian in a very general language. In the following we will be more concrete. The species of interest are the photons $A \to b$ and the other species the electrons $B_1 \to c$ and $B_2 \to v$.

### 5.2.2. Technical subtleties due to non-equilibrium

In this subsection we deal with the subtleties of a system out of equilibrium. We show how it is possible to measure the energy of each subsystem from it's chemical potential and maintain the information about the relative position of the chemical potentials. This will be very useful when we introduce superconductivity later on. The two key concepts are dynamics and statistics. The dynamics of the system are determined by the Hamiltonian $H$ of the system and do not contain any information of the equilibrium or nonequilibrium situation. The information about nonequilibrium is entirely in the statistics. In the easiest case, such as a stationary current between two or more subsystems that are in local equilibrium, the statistics are determined by individual chemical potentials for each subsystems. In equilibrium physics there is only one chemical potential. Since we can always add an absolute energy to the Hamiltonian, in equilibrium the two expressions coincide,

$$[O, H] = [O, H - \mu N_i]. \tag{5.57}$$

Because in equilibrium physics the dynamics are often calculated using $H - \mu N_i$ to evaluate the Heisenberg equations of motion. This is however just accidentally right and out of equilibrium it is crucial that we are very careful. A useful discussion of this topic can be found in [Mah90] in the chapter about superconductivity and electron tunneling. Our

discussion will be in close analogy to what is discussed there an can be found in many other textbooks as well. The conventions we use in this subsection are defined by

$$\begin{aligned} \tilde{H} &\equiv H - \mu_c N_c - \mu_v N_v \qquad & H &\equiv H_0 + H_T \\ N_c &\equiv \sum_{k,\sigma} c^\dagger_{k,\sigma} c_{k,\sigma} & N_v &\equiv \sum_{k,\sigma} v^\dagger_{k,\sigma} v_{k,\sigma}. \end{aligned} \tag{5.58}$$

In this thesis we deal with superconducting leads, hence Bogoliubov transformation is a key technique. Therefore, it is useful to rewrite the Hamiltonian in such a way that it is in the generic form ready for Bogoliubov transformation. This means that the energy in each lead is measured from it's chemical potential. Therefore it is much nicer to work with $\tilde{H}$ instead of $H$. Since the system is out of equilibrium it is important that we ensure that the equations of motion stay unaltered. Technically this means that we must assign an additional phase to the fermionic creation and annihilation operators in the Heisenberg picture. Formally we can absorb this phases into the coupling 'constant', since the interaction terms are the only terms where these phases do not chancel out. This means:

$$H \to \tilde{H} \quad \Rightarrow \quad c(t) \to c(t)\mathrm{e}^{-\mathrm{i}\mu_c t} \qquad v(t) \to v(t)\mathrm{e}^{-\mathrm{i}\mu_v t} \quad \text{or} \quad g \to g(t) \sim \mathrm{e}^{\mathrm{i}(\mu_c - \mu_v)t}. \tag{5.59}$$

The formal reason for this technique is based on the linearity of the commutator $[A + B, C] = [A, C] + [B, C]$. If we know the solution of a linear differential equation and we then add a term to it's derivative that is proportional to the function this simply gives a multiplicative phase

$$\begin{aligned} \frac{\mathrm{d}}{\mathrm{d}t}\big(c_{k,\sigma}\big)_H(t) &= \mathrm{i}[H, c_{k,\sigma}]_H(t) \\ &= \mathrm{i}[\tilde{H}, c_{k,\sigma}]_H(t) + \mathrm{i}\Big[\mu_c N_c + \mu_v N_v, c_{k,\sigma}\Big](t) \\ &= \mathrm{i}[\tilde{H}, c_{k,\sigma}]_H(t) - \mathrm{i}\mu_c\big(c_{k,\sigma}\big)_H(t), \\ \Rightarrow \big(c_{k,\sigma}(t)\big)_H &= \big(c_{k,\sigma}(t)\big)_{\tilde{H}}\, \mathrm{e}^{-\mathrm{i}\mu_c t}. \end{aligned} \tag{5.60}$$

For the valence electrons we find an equivalent result

$$\big(v_{k,\sigma}(t)\big)_H = \big(v_{k,\sigma}(t)\big)_{\tilde{H}}\, \mathrm{e}^{-\mathrm{i}\mu_v t}. \tag{5.61}$$

In the case of superconducting leads there is a small subtlety. In a BCS type Hamiltonian there are terms such as $\Delta_c c^\dagger_\uparrow c^\dagger_\downarrow$. On first sight we might assume that this means that in the Heisenberg picture such terms acquire a phase of $\mathrm{e}^{2\mathrm{i}\mu_c}$. However, the order parameter which is defined as $\Delta_c = \langle c_\downarrow c_\uparrow \rangle$ acquires the opposite phase so that the total phase chancels. Summarizing we have shown how to reformulate the Heisenberg equations of motion in terms of $\tilde{H}$ without losing the information about the relative energy of the different types of particles.

### 5.2.3. Discussion of times scales

Our effective model lives and dies with the correct usage of the various limits and scales. We devote this subsection to the investigation and understanding of those scales and limits. There are four time scales in the problem. Three are obvious and one is quite subtle.

The first question that arises is if the system can reach a stationary nonequilibrium state once we set nonequilibrium initial conditions and then let the system evolve. This seems to be a contradiction by itself because we would exspect either that the system oscillates or that it converges to an equilibrium state. Strictly speaking the system does indeed oscillate. However the period of the oscillation is inverse proportional to the energy spacing

in the density of states in the leads. This time scale goes to infinity with the size of the leads and is the largest of all four time scales in the system. The second largest time scale is the switchon time of the interaction $1/\eta$ which we choose in such a way that the interaction is turned off at the time $t_0$ where Heisenberg and Schrödinger picture coincide. In the adiabatic limit this scale goes to infinity. As a consequence it is crucial that we take the time limits in the right order to ensure the oscillation time of the system remains large in comparison to the switchon time. The third largest time scale is the scale on which measurements take place $\Delta t$. It is the scale over which we must time-average observables to describe the measurable quantities. Finally the shortest time scale is the inverse semiconductor gap which is of the order of femto seconds. In the rest of this section we give evidence that we can indeed switched on the interaction adiabatically, starting from a nonequilibrium initial situation, and reach a stationary nonequilibrium state. The key observable is the luminescence $L(t)$. A time independent constant and finite luminescence is only possible if the system is in a nonequilibrium stationary state. As a demonstration model we choose the light emitting diode without superconductivity (5.19). We start form the general expression of the luminescence,

$$L(t) = \left(\frac{\mathrm{d}}{\mathrm{d}t_1} + \frac{\mathrm{d}}{\mathrm{d}t_2}\right) \sum_q \langle b^\dagger_{H,q}(t_1) b_{H,q}(t_2)\rangle \Big|_{t_2 \to t_1 = t}, \tag{5.62}$$

that we have introduced in section 5.1. Since we derive the explicit expressions of the photon creation and annihilation operators in the Heisenberg picture up to second order in the coupling constant later on (5.81) we immediately write

$$\begin{aligned}\langle b^\dagger_q(t_1) b_q(t_2)\rangle = n_{pk,q} - |g|^2 n_{pk,q} \sum_k (n_{v,k-q} - n_{c,k})(B_{q,k,k-q}(t_2) + B^*_{q,k,k-q}(t_1)) \\ + |g|^2 \sum_k n_{c,k}(1 - n_{v,k-q}) A^*_{q,k,k-q}(t_1) A_{q,k,k-q}(t_2),\end{aligned} \tag{5.63}$$

where we introduced

$$\begin{aligned}A_{q,k,p}(t) &\equiv \int_{t_0}^{t} \mathrm{d}t'\, \mathrm{e}^{\mathrm{i}(w_q - \epsilon_{c,k} + \epsilon_{v,p} - \mathrm{i}\eta)t'}, \\ B_{q_1,k,p,q_2}(t) &\equiv \int_{t_0}^{t} \mathrm{d}t' \int_{t_0}^{t'} \mathrm{d}t''\, \mathrm{e}^{-\mathrm{i}(w_{q_1} - \epsilon_{c,k} + \epsilon_{v,p} + \mathrm{i}\eta)t''} \mathrm{e}^{\mathrm{i}(w_{q_2} - \epsilon_{c,k} + \epsilon_{v,p} - \mathrm{i}\eta)t'}.\end{aligned} \tag{5.64}$$

At the initial time $t_0$ where Heisenberg and Schrödinger picture coincide the interaction is switched of by definition ($\mathrm{e}^{\eta t_0} \approx 0$). This simplifies the evaluation of the coefficients $A$ and $B$ which fulfill

$$\frac{\mathrm{d}}{\mathrm{d}t} B_{q,k,p}(t) = \frac{\mathrm{i}\mathrm{e}^{2\eta t}}{w_q - \epsilon_{c,k} + \epsilon_{v,p} + \mathrm{i}\eta} = A^*_{q,k,p}(t) \frac{\mathrm{d}}{\mathrm{d}t} A_{q,k,p}(t) \equiv X_{q,k,p}(t). \tag{5.65}$$

We notice if $t_1 = t_2$, then $\langle b^\dagger_q(t) b_q(t)\rangle = \langle b^\dagger_{H,q}(t) b_{H,q}(t)\rangle$ which completes the calculation of the time dependent photon number. Finally we plug this result into the definition of the luminescence (5.62) and make use of the fact that the switchon time is much longer than the measurement time ($\mathrm{e}^{\eta t} \approx 1$). We then readily get

$$L = 2|g|^2 \sum_{k,q} \Big(n_{c,k}(1 - n_{v,k-q}) - n_{pk,q}(n_{v,k-q} - n_{c,k})\Big) \frac{\eta}{(w_q - \epsilon_{c,k} + \epsilon_{v,k-q})^2 + \eta^2}. \tag{5.66}$$

From equation (5.66) the most important result is already obvious: The luminescence is independent of time and the system accordingly in a stationary state. It remains to show that the luminescence is finite, i.e. that this stationary state is a nonequilibrium state.

In the adiabatic limit, i.e. when we assume that the switchon speed $\eta$ is much smaller than the energy scale on with the prefactor varies, we can approximate the Lorentzian in equation (5.66) by a delta distribution and obtain

$$L \approx 2|g|^2 \sum_{k,q} \Big( n_{c,k}(1 - n_{v,k-q}) - n_{pk,q}(n_{v,k-q} - n_{c,k}) \Big) \delta(w_q - \epsilon_{c,k} + \epsilon_{v,k-q}). \tag{5.67}$$

This is also where the subtle oscillation time hits in. We can evaluate the delta function only if we have a continuous spectrum of energies. The next physical idea that makes the calculation easier is that the energy of a photon at a given momentum is much greater than the kinetic energy of an electron at the same momentum. Also photons with the energy of the gap in the semiconductor have such a small momentum that it is negligible in comparison to the momenta of electrons even at relatively low energies. This means that the momentum of the electrons going from the conduction to the valence band or the other way round is almost conserved $k^2/(2m) \ll c|k|$ where $c$ is the speed of light. To keep the notation compact we now define $\Delta\epsilon \equiv \epsilon_{c,0} - \epsilon_{v,0}$, and write

$$L \approx 2|g|^2 \mathcal{N}_{ph}(\Delta\epsilon) \sum_{k} \Big( n_{c,k}(1 - n_{v,k}) - n_{pk}(\Delta\epsilon) \left( n_{v,k} - n_{c,k} \right) \Big), \tag{5.68}$$

where $\mathcal{N}_{ph}$ is the photon density of states. This concludes the calculation of the luminescence. We see that the luminescence described by formula (5.68) is in general finite and vanishes only if the initial conditions are chosen in a specific way. If we set the initial number of photons in the system to zero $n_{pk}(\Delta\epsilon) = 0$ we recover the same result that we derived using the Keldysh formalism (5.28). Summarizing, we have shown that using an effective model and by choosing the limits in the appropriate way it is indeed possible to describe a stationary nonequilibrium problem by Heisenberg equations of motion with initial conditions. We will use this order of time scale that we introduced in this section throughout this thesis.

### 5.2.4. Effective photon Hamiltonian for a light emitting diode

To flesh out the ideas of subsection 5.2.1 we discuss the explicit example of a normal light emitting diode. The photons are the species of interest and the conduction and valence electrons are the other two species in the problem. We show that the effect of the bias leads is similar to a parametric photon pump field. The full Hamiltonian is given by

$$\begin{aligned} H = &\sum_k (\epsilon_{c,k} - \mu_c) c_k^\dagger c_k + \sum_p (\epsilon_{v,p} - \mu_v) v_p^\dagger v_p + \sum_q w_q b_q^\dagger b_q \\ &+ g \sum_{k,q} b_q c_k^\dagger v_{k-q} + g^* \sum_{k,q} b_q^\dagger v_{k-q}^\dagger c_k, \end{aligned} \tag{5.69}$$

and is discussed in detail in section 4.1. The first step is to neglect all terms that do commute with the photon operators $b$ and $b^\dagger$. We denote these terms $R$ and the reduced Hamiltonian

$$\tilde{H} = H - R = \sum_q w_q b_q^\dagger b_q + g \sum_{k,q} b_q c_k^\dagger v_{k-q} + g^* \sum_{k,q} b_q^\dagger v_{k-q}^\dagger c_k. \tag{5.70}$$

Next we formally transform this Hamiltonian to the Heisenberg picture:

$$\tilde{H}_H(t) = \sum_q w_q b_{H,q}^\dagger(t) b_{H,q}(t) + g \mathrm{e}^{\mathrm{i}(\mu_c - \mu_v)t} \mathrm{e}^{\eta t} \sum_{k,q} b_{H,q}(t) c_{H,k}^\dagger(t) v_{H,k-q}(t) + h.c.. \tag{5.71}$$

In a third step we replace all fermionic operators such as for example $c_{H,k}(t)$ by expressions in which all fermionic operators are at $t_0$ where the system is decoupled. We choose this

point as the time where Schrödinger and Heisenberg picture fall together $O_H(t_0) \equiv O_S$. Now we easily find the explicit expression using basic commutation relations. They do however contain a term that is of zeroth order in the coupling which prevents us from doing a perturbative expansion right away. An example is given in equation (5.72) for the conduction band electrons, which evolve according to

$$\dot{c}_{H,k} = -\mathrm{i}(\epsilon_{c,k} - \mu_c)c_{H,k} - \mathrm{i}g\mathrm{e}^{(\mu_c-\mu_v)t}\sum_q b_{H,q}v_{H,k-q}. \tag{5.72}$$

We can resolve this problem by defining new operators which we label by an 'I' and that have a different phase such that the zeroth order terms cancel with the time derivative of this phases:

$$c_{H,k} \equiv c_{I,k}\mathrm{e}^{-\mathrm{i}(\epsilon_{c,k}-\mu_c)t}, \qquad v_{H,p} \equiv v_{I,p}\mathrm{e}^{-\mathrm{i}(\epsilon_{v,p}-\mu_v)t}, \qquad b_{H,q} \equiv b_{I,q}\mathrm{e}^{-\mathrm{i}w_q t}. \tag{5.73}$$

Now these new operators,

$$\begin{aligned}
\dot{c}_{I,k} &= -\mathrm{i}g\sum_q b_{I,q}v_{I,k-q}\mathrm{e}^{-\mathrm{i}(w_q-\epsilon_{c,k}+\epsilon_{v,k-q})t},\\
\dot{v}_{I,p} &= -\mathrm{i}g^*\sum_q b^\dagger_{I,q}c_{I,p+q}\mathrm{e}^{\mathrm{i}(w_q-\epsilon_{c,p+q}+\epsilon_{v,p})t},\\
\dot{b}_{I,q} &= -\mathrm{i}g^*\sum_k v^\dagger_{I,k-q}c_{I,k}\mathrm{e}^{\mathrm{i}(w_q-\epsilon_{c,k}+\epsilon_{v,k-q})t},
\end{aligned} \tag{5.74}$$

have the desired property that each time derivative will increase the order in the coupling constant. In a next step we integrate these differential equations. We assume that the tunneling was switched on $g(t) \sim \mathrm{e}^{\eta t}$ in such a way that the system is decoupled at $\mathrm{e}^{\eta t_0} \approx 0$ and fully turned on at $t = 0$. Also we assume that the scale on which the measurement takes place is much shorter than the switchon time, so that the tunneling is constant during the experiment. The experiment takes place around $t = 0$. For we drop the 'I' index in the following. We also introduce a short notation $O_I(t_0) \equiv O_0$ for operators at $t_0$. The solutions of (5.74) are then given by

$$\begin{aligned}
c_k(t) &= c_{k,0} - \mathrm{i}g\sum_q \int_{t_0}^t \mathrm{d}t'\, b_q(t')v_{k-q}(t')\mathrm{e}^{-\mathrm{i}(w_q-\epsilon_{c,k}+\epsilon_{v,k-q}+\mathrm{i}\eta)t'},\\
v_p(t) &= v_{p,0} - \mathrm{i}g^*\sum_q \int_{t_0}^t \mathrm{d}t'\, b^\dagger_q(t')c_{p+q}(t')\mathrm{e}^{\mathrm{i}(w_q-\epsilon_{c,p+q}+\epsilon_{v,k}-\mathrm{i}\eta)t'},\\
b_q(t) &= b_{q,0} - \mathrm{i}g^*\sum_k \int_{t_0}^t \mathrm{d}t'\, v^\dagger_{k-q}(t')c_k(t')\mathrm{e}^{\mathrm{i}(w_q-\epsilon_{c,k}+\epsilon_{v,k-q}-\mathrm{i}\eta)t'}.
\end{aligned} \tag{5.75}$$

It is sufficient to focus on the tunneling terms, since they are the only ones that do not commute with the photon operators and contain fermionic operators. These terms are already linear in the coupling constant and therefore it is sufficient if we expand the fermionic operators in linear order. We obtain

$$\begin{aligned}
c_k(t) &= c_{k,0} + g\sum_q b_{q,0}v_{k-q,0}\frac{\mathrm{e}^{-\mathrm{i}(w_q-\epsilon_{c,k}+\epsilon_{v,k-q}+\mathrm{i}\eta)t}}{w_q - \epsilon_{c,k} + \epsilon_{v,k-q} + \mathrm{i}\eta} + O(|g|^2),\\
v_p(t) &= v_{p,0} - g^*\sum_q b^\dagger_{q,0}c_{p+q,0}\frac{\mathrm{e}^{\mathrm{i}(w_q-\epsilon_{c,p+q}+\epsilon_{v,p}-\mathrm{i}\eta)t}}{w_q - \epsilon_{c,p+q} + \epsilon_{v,p} - \mathrm{i}\eta} + O(|g|^2).
\end{aligned} \tag{5.76}$$

Plugging this into the interaction terms gives the fundamental ingredients of the effective Hamiltonian. Therefore, it is enough if we calculate one of the interaction terms since the

other one is its hermitian conjugate

$$
\begin{aligned}
& g^*(t)\sum_{k,q} b^\dagger_{H,q}(t)v^\dagger_{H,k-q}(t)c_{H,k}(t) \\
&= g^*\mathrm{e}^{\eta t}\sum_{k,q}\mathrm{e}^{\mathrm{i}(w_q-\epsilon_{c,k}+\epsilon_{v,k-q})t}b^\dagger_q(t)v^\dagger_{k-q}(t)c_k(t) \\
&= g^*\mathrm{e}^{\eta t}\sum_{k,q}\mathrm{e}^{\mathrm{i}(w_q-\epsilon_{c,k}+\epsilon_{v,k-q})t}b^\dagger_q(t)v^\dagger_{k-q,0}c_{k,0} \\
&\quad + |g|^2\mathrm{e}^{2\eta t}\sum_{k,q_1,q_2}\frac{\mathrm{e}^{\mathrm{i}(w_{q_1}-w_{q_2})t}\mathrm{e}^{\mathrm{i}(\epsilon_{v,k-q_1}-\epsilon_{v,k-q_2})t}}{w_{q_2}-\epsilon_{c,k}+\epsilon_{v,k-q_2}+\mathrm{i}\eta}v^\dagger_{k-q_1,0}v_{k-q_2,0}b^\dagger_{q_1}(t)b_{q_2,0} \\
&\quad - |g|^2\mathrm{e}^{2\eta t}\sum_{k,q_1,q_2}\frac{\mathrm{e}^{\mathrm{i}(w_{q_1}-w_{q_2})t}\mathrm{e}^{-\mathrm{i}(\epsilon_{c,k}-\epsilon_{c,k-q_1+q_2})t}}{w_{q_2}-\epsilon_{c,k-q_1+q_2}+\epsilon_{v,k-q_1}+\mathrm{i}\eta}c^\dagger_{k-q_1+q_2,0}c_{k,0}b^\dagger_{q_1}(t)b_{q_2,0}. \qquad (5.77)
\end{aligned}
$$

To simplify further we can exploit two things. First, $b_q(t) = b_q(t_0)+O(|g|)$ and second that the distribution functions are known for the decoupled system at $t_0$. The latter permits us to trace out the fermionic operators in all second order terms, which yields

$$
\begin{aligned}
g^*(t)\sum_{k,q} b^\dagger_{H,q}(t)v^\dagger_{H,k-q}(t)c_{H,k}(t) &= g^*\mathrm{e}^{\eta t}\sum_{k,q} b^\dagger_{H,q}(t)\mathrm{e}^{-\mathrm{i}(\epsilon_{c,k}-\epsilon_{v,k-q})t}v^\dagger_{k-q,0}c_{k,0} \\
&\quad + |g|^2\mathrm{e}^{2\eta t}\sum_{k,q}\frac{n_{v,k-q}-n_{c,k}}{w_q-\epsilon_{c,k}+\epsilon_{v,k-q}+\mathrm{i}\eta}b^\dagger_{H,q}(t)b_{H,q}(t). \qquad (5.78)
\end{aligned}
$$

With this we have all building blocks for the effective Hamiltonian

$$
\begin{aligned}
\Big(H_{\mathrm{eff}}\Big)_H(t) &= \sum_q\Big(w_q+|g|^2\mathrm{e}^{2\eta t}X_q\Big)b^\dagger_{H,q}(t)b_{H,q}(t) \\
&\quad + \sum_q\Big(g\mathrm{e}^{\eta t}Y_q(t)b_{H,q}(t)+g^*\mathrm{e}^{\eta t}\mathrm{e}^{\mathrm{i}e\mathrm{V}t}b^\dagger_{H,q}(t)\mathrm{e}^{-\mathrm{i}e\mathrm{V}t}Y^\dagger_q\Big), \qquad (5.79)
\end{aligned}
$$

where we introduced

$$
\begin{aligned}
X_q &= \sum_k(n_{v,k-q}-n_{c,k})\Big(\frac{1}{w_q-\epsilon_{c,k}+\epsilon_{v,k-q}-\mathrm{i}\eta}+\frac{1}{w_q-\epsilon_{c,k}+\epsilon_{v,k-q}+\mathrm{i}\eta}\Big) \\
&= 2\sum_k(n_{v,k-q}-n_{c,k})\frac{w_q-\epsilon_{c,k}+\epsilon_{v,k-q}}{(w_q-\epsilon_{c,k}+\epsilon_{v,k-q})^2+\eta^2},
\end{aligned}
$$

$$
Y_q(t) = \sum_k \mathrm{e}^{\mathrm{i}((\epsilon_{c,k}-\mu_c)-(\epsilon_{v,k-q}-\mu_v))t}c^\dagger_{k,0}v_{k-q,0}. \qquad (5.80)
$$

Notice that $Y(t)$ has still fermionic operators inside. This is a necessary evil and there is no way around it. Nevertheless the effective Hamiltonian allows for a natural understanding of the photon physics and it is immediately obvious that the system works as a photon pump - as a light emitting diode should. I.e. it has the form of an external pump field that pumps photons into the system. In the next subsection we will verify the validity of the expression we have derived here.

### 5.2.5. Comparison with results from the full Hamiltonian

In order to verify the results from the last subsection we proof in this subsection that we can derive the correct expression for the photon operators in second order using the effective Hamiltonian. First we derive the Heisenberg photon annihilation operator by

recursive iteration of the equations of motion of the fermion operators (5.74) and adding the phase that we separated earlier. The explicit expression is

$$b_{H,q}(t) = b_{q,0}\mathrm{e}^{-\mathrm{i}w_q t} - g^* \sum_k \frac{\mathrm{e}^{-\mathrm{i}(\epsilon_{c,k}-\epsilon_{v,k-q}+\mathrm{i}\eta)t}}{w_q - \epsilon_{c,k} + \epsilon_{v,k-q} - \mathrm{i}\eta} v^\dagger_{k-q,0} c_{k,0}$$
$$- \mathrm{i}|g|^2 \frac{\mathrm{e}^{2\eta t}}{2\eta} \sum_k (n_{v,k-q} - n_{c,k}) \frac{1}{w_q - \epsilon_{c,k} + \epsilon_{v,k-q} + \mathrm{i}\eta} \mathrm{e}^{-\mathrm{i}w_q t} b_{q,0} + O(|g|^3). \quad (5.81)$$

Second we derive the same result using the effective Hamiltonian. We begin with the Heisenberg equations of motion,

$$\begin{aligned}\dot{b}_{H,q}(t) &= \mathrm{i}[\big(H_{eff}\big)_H(t), b_{H,q}(t)] \\ &= -\mathrm{i}\Big(w_q + |g|^2 \mathrm{e}^{2\eta t} X_q\Big) b_{H,q}(t) - \mathrm{i}g^* \mathrm{e}^{\eta t} Y^\dagger_q(t) \\ &\quad + \mathrm{i}g\mathrm{e}^{\eta t} \sum_{q_1} [Y_{q_1}(t), b_{H,q}(t)] b_{H,q_1}(t) + \mathrm{i}g^* \mathrm{e}^{\eta t} \sum_{q_1} b^\dagger_{H,q_1}(t) [Y^\dagger_{q_1}(t), b_{H,q}(t)], \end{aligned} \quad (5.82)$$

and separate a phase from the photon operators $b_{H,k}(t) \equiv \mathrm{e}^{-\mathrm{i}w_k t} b_k(t)$. Formal integration of the differential equation gives

$$\begin{aligned} b_q(t) &= b_{q,0} - \mathrm{i}|g|^2 X_q \int_{t_0}^t \mathrm{d}t'\, \mathrm{e}^{2\eta t'} b_{H,q}(t') \mathrm{e}^{\mathrm{i}w_q t'} + \mathrm{i}g \int_{t_0}^t \mathrm{d}t'\, \mathrm{e}^{\eta t'} \sum_{q_1} [Y_{q_1}(t'), b_{H,q}(t')] b_{H,q_1}(t') \mathrm{e}^{\mathrm{i}w_q t'} \\ &\quad + \mathrm{i}g^* \int_{t_0}^t \mathrm{d}t'\, \mathrm{e}^{\eta t'} \sum_{q_1} b^\dagger_{H,q_1}(t') [Y^\dagger_{q_1}(t'), b_{H,q}(t')] \mathrm{e}^{\mathrm{i}w_q t'} - \mathrm{i}g^* \int_{t_0}^t \mathrm{d}t'\, \mathrm{e}^{\eta t'} Y^\dagger_q(t') \mathrm{e}^{\mathrm{i}w_q t'} \\ &= b_{q,0} - \mathrm{i}g^* \int_{t_0}^t \mathrm{d}t'\, \mathrm{e}^{\eta t'} Y^\dagger_q(t') \mathrm{e}^{\mathrm{i}w_q t'} + O(|g|)^2. \end{aligned} \quad (5.83)$$

The terms linear in the coupling do contain commutators of the type $[Y_{q_1}(t), b_{H,q}(t)]$. In order to evaluate them we consider the first order expansion of $b_{H,q}(t)$. When we plug it in the expression from equation (5.83) we get terms such as

$$\begin{aligned} &\sum_{q_1} [Y_{q_1}(t), b_{H,q}(t)] \\ &= -\mathrm{i}g^* \int_{t_0}^t \mathrm{d}t' \mathrm{e}^{\eta t'} \mathrm{e}^{\mathrm{i}w_q t'} \sum_{q_1} [Y_{q_1}(t), Y^\dagger_q(t')] \mathrm{e}^{-\mathrm{i}w_q t} + O(|g|^2) \\ &= -g^* \mathrm{e}^{\eta t} \sum_k \frac{n_{c,k} - n_{v,k-q}}{w_q - \epsilon_{c,k} + \epsilon_{v,k-q} - \mathrm{i}\eta}. \end{aligned} \quad (5.84)$$

We put these results back in the previous expression and doing some algebra and indeed we find the same result (5.81) as obtained by the full Hamiltonian. Hence, we conclude that all expectation values of observables that contain only photon operators can be calculated in second order in the coupling constant using the effective Hamiltonian.

### 5.2.6. Superconductor-pn-superconductor heterostructure

In this subsection we derive the key result of this thesis, the effective photon Hamiltonian for the full superconductor-pn-superconductor heterostructure. We find that it has one term that can be interpreted as a pump field, similar to the effective Hamiltonian of the normal light emitting diode. In addition it has another term that has the form of a parametric amplifier which leads to squeezing.

Starting point is the full model Hamiltonian

$$H - \mu_c N_c - \mu_v N_v \equiv (H_{0,c} - \mu_c N_c) + (H_{0,v} - \mu_v N_v) + H_{0,ph} + H_T. \tag{5.85}$$

A justification of this model can be found in section 4.2. This Hamiltonian consist of four components. Two leads, a free photon Hamiltonian and a tunneling term. The latter describe electron tunneling between the leads and is chosen in a way that each tunneling event is accompanied by either the absorption or the emission of a photon. The explicit expression for the building blocks of the Hamiltonian are

$$\begin{aligned}
H_{0,c} - \mu_c N_c &= \sum_{k,\sigma} (\epsilon_{c,k} - \mu_c) c^\dagger_{k,\sigma} c_{k,\sigma} - \sum_k \Delta_{c,k} c^\dagger_{k,\uparrow} c^\dagger_{-k,\downarrow} - \sum_k \Delta^*_{c,k} c_{-k,\downarrow} c_{k,\uparrow}, \\
H_{0,v} - \mu_v N_v &= \sum_{p,\sigma} (\epsilon_{v,p} - \mu_v) v^\dagger_{p,\sigma} v_{p,\sigma} - \sum_p \Delta_{v,p} v^\dagger_{p,\uparrow} v^\dagger_{-p,\downarrow} - \sum_p \Delta^*_{v,p} v_{-p,\downarrow} v_{p,\uparrow}, \\
H_{0,ph} &= \sum_q w_q b^\dagger_q b_q, \\
H_T &= g \sum_{k,q,\sigma} b_q c^\dagger_{k,\sigma} v_{k-q,\sigma} + g^* \sum_{k,q,\sigma} b^\dagger_q v^\dagger_{k-q,\sigma} c_{k,\sigma}.
\end{aligned} \tag{5.86}$$

The first two equations in (5.86) describe the superconducting leads. The third equation is a free photon Hamiltonian and the tunneling term is shown in the last equation. To make this model accessible to analysis we start with Bogoliubov transformations of the leads. The expressions 3.6 can be found in standard textbooks, for example [BF04]. Next we preform the Bogoliubov transformation

$$\begin{aligned}
c_{k,\sigma} &= u_{c,\sigma k} \gamma_{k,\sigma} + \bar{\sigma} v_{c,\sigma k} \gamma^\dagger_{-k,\bar{\sigma}}, \\
c^\dagger_{k,\sigma} &= u^*_{c,\sigma k} \gamma^\dagger_{k,\sigma} + \bar{\sigma} v^*_{c,\sigma k} \gamma_{-k,\bar{\sigma}}, \\
v_{p,\sigma} &= u_{v,\sigma p} \gamma_{p,\sigma} + \bar{\sigma} v_{v,\sigma p} \gamma^\dagger_{-p,\bar{\sigma}}, \\
v^\dagger_{p,\sigma} &= u^*_{v,\sigma p} \gamma^\dagger_{p,\sigma} + \bar{\sigma} v^*_{v,\sigma p} \gamma_{-p,\bar{\sigma}}.
\end{aligned} \tag{5.87}$$

The new operators $\gamma$ which are defined in equations (5.87) fulfill the usual fermionic anti-commutation relations. Hence, the transformed Hamiltonian of the leads,

$$\begin{aligned}
H_{0,c} - \mu_c N_c &= \sum_{k,\sigma} E_{c,k} \gamma^\dagger_{c,k,\sigma} \gamma_{c,k,\sigma} + \text{const}, \\
H_{0,v} - \mu_v N_v &= \sum_{p,\sigma} E_{v,p} \gamma^\dagger_{v,p,\sigma} \gamma_{v,p,\sigma} + \text{const},
\end{aligned} \tag{5.88}$$

have the structure of free Fermi gases. The quasiparticle energies

$$\begin{aligned}
E_{c,k} &= \sqrt{(\epsilon_{c,k} - \mu_c)^2 + |\Delta_{c,k}|^2}, \\
E_{v,p} &= \sqrt{(\epsilon_{v,p} - \mu_v)^2 + |\Delta_{v,p}|^2},
\end{aligned} \tag{5.89}$$

are on the order of the superconducting gap and above. The most important property of the resulting quasiparticles is that all commutation relations between the two types of fermions and the boson (4.16) remain invariant with the new fermions. The interaction on the other hand needs to be rewritten in terms of the Bogoliubov quasiparticle operators, too. Each term of the interaction leads to four new terms in the transformed picture. With the index convention that we have chosen we can add pairs of terms from the photon

absorption and photon emission part together. The result is

$$\begin{aligned}
&gb_q c^\dagger_{k,\sigma} v_{k-q,\sigma} \\
&= gb_q u^*_{c,\sigma k} u_{v,\sigma(k-q)} \gamma^\dagger_{c,k,\sigma} \gamma_{v,k-q,\sigma} + gb_q v^*_{c,\sigma k} v_{v,\sigma(k-q)} \gamma_{c,-k,\bar\sigma} \gamma^\dagger_{v,q-k,\bar\sigma} \\
&+ gb_q \bar\sigma u^*_{c,\sigma k} v_{v,\sigma(k-q)} \gamma^\dagger_{c,k,\sigma} \gamma^\dagger_{v,q-k,\bar\sigma} + gb_q \bar\sigma v^*_{c,\sigma k} u_{v,\sigma(k-q)} \gamma_{c,-k,\bar\sigma} \gamma_{v,k-q,\sigma},
\end{aligned} \tag{5.90}$$

$$\begin{aligned}
&g^* b^\dagger_{-q} v^\dagger_{q-k,\bar\sigma} c_{-k,\bar\sigma} \\
&= -g^* b^\dagger_{-q} v_{c,\sigma k} v^*_{v,\sigma(k-q)} \gamma^\dagger_{c,k,\sigma} \gamma_{v,k-q,\sigma} - g^* b^\dagger_{-q} u_{c,\sigma k} u^*_{v,\sigma(k-q)} \gamma_{c,-k,\bar\sigma} \gamma^\dagger_{v,q-k,\bar\sigma} \\
&\quad - g^* b^\dagger_{-q} \sigma v_{c,\sigma k} u^*_{v,\sigma(k-q)} \gamma^\dagger_{c,k,\sigma} \gamma^\dagger_{v,q-k,\bar\sigma} - g^* b^\dagger_{-q} \sigma u_{c,\sigma k} v^*_{v,\sigma(k-q)} \gamma_{c,-k,\bar\sigma} \gamma_{v,k-q,\sigma}.
\end{aligned} \tag{5.91}$$

The fully transformed Hamiltonian is now ready to be addressed by perturbation theory. The only terms which are not diagonal are the interaction terms and those are proportional to the coupling constant.

$$\begin{aligned}
H = &\sum_{k,\sigma} E_{c,k} \gamma^\dagger_{c,k,\sigma} \gamma_{c,k,\sigma} + \sum_{p,\sigma} E_{v,p} \gamma^\dagger_{v,p,\sigma} \gamma_{v,p,\sigma} + \sum_q w_q b^\dagger_q b_q + \text{const} \\
&+ \sum_{k,q,\sigma} A_{q,k,\sigma} \gamma^\dagger_{c,k,\sigma} \gamma_{v,k-q,\sigma} + \sum_{k,q,\sigma} B_{q,k,\sigma} \gamma_{c,k,\sigma} \gamma_{v,q-k,\bar\sigma} + \text{h.c.}
\end{aligned} \tag{5.92}$$

The prefactors,

$$\begin{aligned}
A_{q,k,\sigma} &= gb_q u^*_{c,\sigma k} u_{v,\sigma(k-q)} - g^* b^\dagger_{-q} v_{c,\sigma k} v^*_{v,\sigma(k-q)}, \\
B_{q,k,\sigma} &= \sigma g b_{-q} v^*_{c,\sigma k} u_{v,\sigma(k-q)} + \sigma g^* b^\dagger_q u_{c,\sigma k} v^*_{v,\sigma(k-q)},
\end{aligned} \tag{5.93}$$

contain the coefficients from the Bogoliubov transformations, the coupling constant and most importantly the photon operators. Hence, this prefactors are operators which do in general not commute with other operators. Most importantly this Hamiltonian is in the form discussed in the general part of section 5.2.1. Hence, it is now possible to calculate an effective photon Hamiltonian. The Heisenberg equations of motion of the quasiparticles follow immediately from the commutation with the transformed Hamiltonian,

$$\begin{aligned}
\dot\gamma_{H,c,k,\sigma}(t) = &-\mathrm{i} E_{c,k} \gamma_{H,c,k,\sigma}(t) \\
&- \mathrm{i} \sum_q A_{H,q,k,\sigma}(t) \gamma_{H,v,k-q,\sigma}(t) + \mathrm{i} \sum_q B^\dagger_{H,q,k,\sigma}(t) \gamma^\dagger_{H,v,q-k,\bar\sigma}(t), \\
\dot\gamma_{H,v,p,\sigma}(t) = &-\mathrm{i} E_{v,p} \gamma_{H,v,p,\sigma}(t) \\
&- \mathrm{i} \sum_q A^\dagger_{H,q,q+p,\sigma}(t) \gamma_{H,c,q+p,\sigma}(t) - \mathrm{i} \sum_q B^\dagger_{H,q,q-p,\bar\sigma}(t) \gamma^\dagger_{H,c,q-p,\bar\sigma}(t).
\end{aligned} \tag{5.94}$$

As we have discussed in subsection 5.2.4, a phases,

$$\begin{aligned}
\gamma_{c,k,\sigma}(t) &\equiv \mathrm{e}^{\mathrm{i}E_{c,k}t} \gamma_{H,c,k,\sigma}, \\
\gamma_{v,p,\sigma}(t) &\equiv \mathrm{e}^{\mathrm{i}E_{v,p}t} \gamma_{H,v,p,\sigma}, \\
b_q(t) &\equiv \mathrm{e}^{\mathrm{i}w_q t} b_{H,q},
\end{aligned} \tag{5.95}$$

have to be separated from the Heisenberg operators in order to do recursive integration. With this newly defined operators the time derivative of the annihilation and creation operators is linear in the coupling constant. This allows us to do the same analysis as in

the case without superconductivity and we get

$$\begin{aligned}
\gamma_{c,k,\sigma}(t) &= \gamma_{c,k,\sigma,0} - \mathrm{i}\sum_q \gamma_{v,k-q,\sigma,0}\int_{t_0}^{t}\mathrm{d}t'\, A_{q,k,\sigma}(t')\mathrm{e}^{\mathrm{i}(E_{c,k}-E_{v,k-q})t'} \\
&\quad + \mathrm{i}\sum_q \gamma^\dagger_{v,q-k,\bar\sigma,0}\int_{t_0}^{t}\mathrm{d}t'\, B^\dagger_{q,k,\sigma}(t')\mathrm{e}^{\mathrm{i}(E_{c,k}+E_{v,q-k})t'} + O(|g|^2), \\
\gamma_{v,k,\sigma}(t) &= \gamma_{v,k,\sigma,0} - \mathrm{i}\sum_q \gamma_{c,q+k,\sigma,0}\int_{t_0}^{t}\mathrm{d}t'\, A^\dagger_{q,q+k,\sigma}(t')\mathrm{e}^{\mathrm{i}(E_{v,k}-E_{c,q+k})t'} \\
&\quad - \mathrm{i}\sum_q \gamma^\dagger_{c,q-k,\bar\sigma,0}\int_{t_0}^{t}\mathrm{d}t'\, B^\dagger_{q,q-k,\bar\sigma}(t')\mathrm{e}^{\mathrm{i}(E_{v,k}+E_{c,q-k})t'} + O(|g|^2).
\end{aligned} \tag{5.96}$$

The interaction is already linear in the coupling, therefore it is sufficient if we abort the recursion after the leading order, yielding

$$\begin{aligned}
&\sum_{q,k,\sigma} A_{H,q,k,\sigma}(t)\gamma^\dagger_{H,c,k,\sigma}\gamma_{H,v,k-q,\sigma} \\
&= \sum_{q,k,\sigma}\tilde A_{q,k,\sigma}(t)\gamma^\dagger_{c,k,\sigma,0}\gamma_{v,k-q,\sigma,0} \\
&\quad + \mathrm{i}\sum_{q,k,\sigma}\big(n_{v,k-q,\sigma}-n_{c,k,\sigma}\big)\tilde A_{q,k,\sigma}(t)\int_{t_0}^{t}\mathrm{d}t'\,\tilde A^\dagger_{q,k,\sigma}(t'), \\
&\sum_{q,k,\sigma} B_{H,q,k,\sigma}(t)\gamma_{H,c,k,\sigma}(t)\gamma_{H,v,q-k,\bar\sigma}(t) \\
&= \sum_{q,k,\sigma}\tilde B_{q,k,\sigma}(t)\gamma_{c,k,\sigma,0}\gamma_{v,q-k,\bar\sigma,0} \\
&\quad + \mathrm{i}\sum_{q,k,\sigma}(n_{c,k,\sigma}+n_{v,q-k,\bar\sigma}-1)\tilde B_{q,k,\sigma}(t)\int_{t_0}^{t}\mathrm{d}t'\,\tilde B^\dagger_{q,k,\sigma}(t').
\end{aligned} \tag{5.97}$$

In this notation we have absorbed all time-dependence into the operator valued coefficients $\tilde A_{q,k,\sigma}(t)$ and $\tilde B_{q,k,\sigma}(t)$, which are explicitly given by

$$\begin{aligned}
\tilde A_{q,k,\sigma}(t) &= g u^*_{c,\sigma k}u_{v,\sigma(k-q)}\mathrm{e}^{-\mathrm{i}(\tilde w_q - E_{c,k}+E_{v,k-q})t}b_q(t) \\
&\quad - g^* v_{c,\sigma k}v^*_{v,\sigma(k-q)}\mathrm{e}^{\mathrm{i}(\tilde w_{-q}+E_{c,k}-E_{v,k-q})t}b^\dagger_{-q}(t), \\
\tilde B_{q,k,\sigma}(t) &= \sigma g v^*_{c,\sigma k}u_{v,\sigma(k-q)}\mathrm{e}^{-\mathrm{i}(\tilde w_{-q}+E_{c,k}+E_{v,q-k})t}b_{-q}(t) \\
&\quad + \sigma g^* u_{c,\sigma k}v^*_{v,\sigma(k-q)}\mathrm{e}^{\mathrm{i}(\tilde w_q - E_{c,k}-E_{v,q-k})t}b^\dagger_q(t).
\end{aligned} \tag{5.98}$$

To make the notation more compact we also introduce a new variable that is the difference of photon frequency and bias voltage $\tilde w \equiv w - \mu_c + \mu_v = w - \mathrm{eV}$. Putting it all together we can write the effective Hamiltonian in the compact form

$$\begin{aligned}
\big(H_{\mathrm{eff}}\big)_H &\equiv \sum_q (w_q + |g|\mathrm{e}^{2\eta t}X_q)b^\dagger_{H,q}b_{H,q} \\
&\quad + \sum_q\Big(g\mathrm{e}^{\eta t}\mathrm{e}^{\mathrm{i}e\mathrm{V}t}Y_q(t)b_{H,q} + g^*\mathrm{e}^{\eta t}\mathrm{e}^{-\mathrm{i}e\mathrm{V}t}b^\dagger_{H,q}Y^\dagger_q(t)\Big) \\
&\quad + \sum_q\Big(g^2\mathrm{e}^{2\eta t}\mathrm{e}^{2\mathrm{i}e\mathrm{V}t}Z_q b_{H,-q}b_{H,q} + (g^*)^2\mathrm{e}^{2\eta t}\mathrm{e}^{-2\mathrm{i}e\mathrm{V}t}Z^\dagger_q b^\dagger_{H,q}b^\dagger_{H,-q}\Big),
\end{aligned} \tag{5.99}$$

that highlights the general structure and qualitative behavior. The details are encoded in the coefficients $X_l$, $Y_l$ and $Z_l$ we discuss later on. We can see all the qualitative photon physics from equation (5.99). The effective Hamiltonian consist of three parts that

correspond to different aspects of the superconductor-ph-superconductor junction. The first part, which is diagonal, is just the photon energy renormalized by the interaction and of little interest. The second term describes the effect of the device being a source of normal, non entangled photons. It has the same structure as the light emitting diode without superconductivity. The effect of the leads is described as the effect of an external field producing single photons at a constant rate. Most exciting and promising is the third term. It has the form of a an ideal parametric amplifier and produces entangled photon pairs. Entanglement is meant in the sense that the emitted photon pairs have opposite momentum and same chirality. In fact, if the linear terms would not contain fermionic operators it would be immediately clear that such a system produces squeezed light [Yue76]. In section 5.3 we will show that the system is indeed a source of squeezed light. In the remainder of this section we discuss the coefficients that appear in the effective Hamiltonian. We have abbreviated the parameters from the Bogoliubov transformation with the Greek letters

$$\begin{aligned}
\alpha_{q,k,\sigma} &\equiv |u_{c,\sigma k}|^2 |u_{v,\sigma(k-q)}|^2, \\
\beta_{q,k,\sigma} &\equiv |v_{c,\sigma k}|^2 |v_{v,\sigma(k-q)}|^2, \\
\chi_{q,k,\sigma} &\equiv u^*_{c,\sigma k} v^*_{c,\sigma k} u_{v,\sigma(k-q)} v_{v,\sigma(k-q)}, \\
\delta_{q,k,\sigma} &\equiv |v_{c,\sigma k}|^2 |u_{v,\sigma(k-q)}|^2, \\
\zeta_{q,k,\sigma} &\equiv |u_{c,\sigma k}|^2 |v_{v,\sigma(k-q)}|^2.
\end{aligned} \tag{5.100}$$

The correction to the frequency $w_q \to w_q + |g|^2 \mathrm{e}^{2\eta t} X_q$ is a real number, as it should for the effective Hamiltonian to be hermitian. This correction therefore is only of quantitative interest and does not lead to any interesting physical properties. For sake of completeness we state the explicit expression for the coefficient $X_q$ that results from the execution of the time integrals

$$\begin{aligned}
X_q = \sum_{k,\sigma} \left(n_{v,k-q,\sigma} - n_{c,k,\sigma}\right) \Bigg( & \frac{\alpha_{q,k,\sigma}}{\tilde{w}_q - E_{c,k} + E_{v,k-q} - \mathrm{i}\eta} + \frac{\alpha_{q,k,\sigma}}{\tilde{w}_q - E_{c,k} + E_{v,k-q} + \mathrm{i}\eta} \\
& - \frac{\beta_{-q,k,\sigma}}{\tilde{w}_q + E_{c,k} - E_{v,k+q} + \mathrm{i}\eta} - \frac{\beta_{-q,k,\sigma}}{\tilde{w}_q + E_{c,k} - E_{v,k+q} - \mathrm{i}\eta} \Bigg) \\
+ \sum_{k,\sigma} (1 - n_{v,q-k,\bar{\sigma}} - n_{c,k,\sigma}) \Bigg( & \frac{\zeta_{q,k,\sigma}}{\tilde{w}_q - E_{c,k} - E_{v,q-k} + \mathrm{i}\eta} + \frac{\zeta_{q,k,\sigma}}{\tilde{w}_q - E_{c,k} - E_{v,q-k} - \mathrm{i}\eta} \\
& - \frac{\delta_{-q,k,\sigma}}{\tilde{w}_q + E_{c,k} + E_{v,-q-k} - \mathrm{i}\eta} - \frac{\delta_{-q,k,\sigma}}{\tilde{w}_q + E_{c,k} + E_{v,-q-k} + \mathrm{i}\eta} \Bigg).
\end{aligned} \tag{5.101}$$

The operator valued coefficient $g\mathrm{e}^{\eta t}\mathrm{e}^{\mathrm{ieV}t} Y_q(t)$ is the most troublesome of the three coefficients. It does have an explicit time dependence and contains fermionic quasiparticle operators. The time dependence is however very weak compared to $\mathrm{e}^{\mathrm{ieV}t}$ since the energy of the quasiparticles is several orders of magnitude smaller than the bias voltage eV. Physically this coefficient controls the amplitude of single photon emission and is only of

quantitative interest. In explicit form it is

$$\begin{aligned} Y_q(t) \equiv \sum_{k,\sigma} \Big( & u^*_{c,\sigma k} u_{v,\sigma(k-q)} \mathrm{e}^{\mathrm{i}(E_{c,k}-E_{v,k-q})t} \gamma^\dagger_{c,k,\sigma,0} \gamma_{v,k-q,\sigma,0} \\ & - v^*_{c,\sigma k} v_{v,\sigma k+q} \mathrm{e}^{-\mathrm{i}(E_{c,k}-E_{v,k+q})t} \gamma^\dagger_{v,k+q,\sigma,0} \gamma_{c,k,\sigma,0} \\ & + \sigma v^*_{c,\sigma k} u_{v,\sigma k+q} \mathrm{e}^{-\mathrm{i}(E_{c,k}+E_{v,-k-q})t} \gamma_{c,k,\sigma,0} \gamma_{v,-q-k,\bar{\sigma},0} \\ & + \sigma u^*_{c,\sigma k} v_{v,\sigma(k-q)} \mathrm{e}^{\mathrm{i}(E_{c,k}+E_{v,q-k})t} \gamma^\dagger_{v,q-k,\bar{\sigma},0} \gamma^\dagger_{c,k,\sigma,0} \Big). \end{aligned} \tag{5.102}$$

Finally the coefficient

$$\begin{aligned} Z_q \equiv \sum_{k,\sigma} \chi_{q,k,\sigma} \Bigg( & \frac{n_{v,k-q,\sigma} - n_{c,k,\sigma}}{\tilde{w}_{-q} + E_{c,k} - E_{v,k-q} + \mathrm{i}\eta} + \frac{n_{v,k-q,\sigma} - n_{c,k,\sigma}}{\tilde{w}_q - E_{c,k} + E_{v,k-q} + \mathrm{i}\eta} \\ & + \frac{1 - n_{v,q-k,\bar{\sigma}} - n_{c,k,\sigma}}{\tilde{w}_q - E_{c,k} - E_{v,k-q} + \mathrm{i}\eta} + \frac{1 - n_{v,q-k,\bar{\sigma}} - n_{c,k,\sigma}}{\tilde{w}_{-q} + E_{c,k} + E_{v,k-q} + \mathrm{i}\eta} \Bigg) \end{aligned} \tag{5.103}$$

controls the emission of entangled photon pairs and is therefore in the center of interest. There are four nearby resonances which describe four physical transitions. They are schematically depicted in figure 5.6. In process number one an unpaired electron in the conduction band makes a transition to the valence band where it stays unpaired. The second process describes a Cooper pair being split up in the conduction band, then one of the electrons goes to the valence band under photon emission and recombines to a Cooper pair with another unpaired valence electron. The third process is like the second process with the difference that the electron that goes to the valence band stays unpaired (Fig. 5.2). Finally, the fourth process is an unpaired conduction electron going to the valence band where it pairs. This process leads to an emission of a photon with the highest energy compared to the other four processes, because in addition to the gap it contains the energy of two times the Cooper pair binding energy (Fig. 5.3). At zero temperature there are no excitations present in the system. Therefore we can understand the photon pair production process as a combination of process three and four. This effectively corresponds to a transition of a Cooper pair from the conduction to the valence band under the emission of a photon pair. The intermediate state an excited quasiparticle in each band can be considered as a virtual intermediate state with an extremely short lifetime. Maybe this explains why the observed recombination time is reduced by a factor of two in the experiments we discussed in section 2.1.3. Another consequence is that the energy of the two photons in a pair is not the same but slightly different. The difference is roughly 4 times the induced order parameter. This however is a very small effect compared to the total photon energy which is of the order of the gap in the semiconductor. In numbers this means a frequency mismatch of 0.001%. The various recombination processes have also been discussed in a related context by Recher *et.al.* [RNK10] who came to similar conclusions.

Wrapping it up we have shown that due to induced superconductivity the effective Hamiltonian looks similar to a superposition of a photon pump and a parametric amplifier. This allows to speculate that the system is a source of squeezed light which we will investigate further in section 5.3. In addition we have discussed how a Cooper pair emits a photon pair and found that the frequencies of the emitted photons are slightly different.

### 5.2.7. Zero temperature limit

The coefficients $X_q$, $Y_q(t)$ and $Z_q$ are quite complicated. To gain more physical insight we discuss the zero temperature, $T = 0$, limit. We also assume an isotropic superconducting

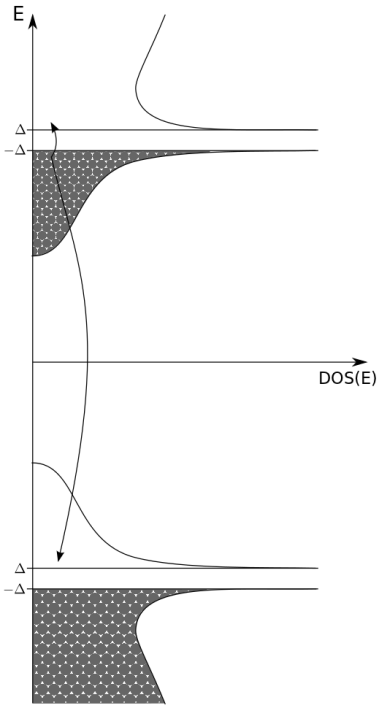


Figure 5.2.: Conduction band Cooper pair is split up

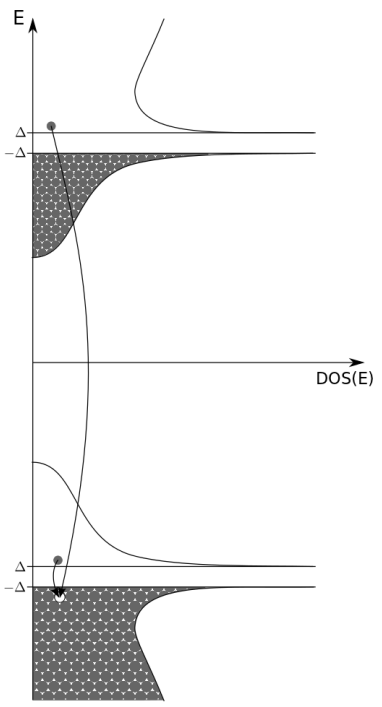


Figure 5.3.: Valence band Cooper pair is formed

gap and and that we can neglect the photon momentum compared to the electron momentum. We find that all the coefficients of the Bogoliubov transforms that appear in $X$, $Y$ and $Z$ come in products of $u$ and $v$. Hence, we can exploit that $u$ and $v$ only have a small overlap in the vicinity of the fermi surface which allows the evaluation of the sums over electron momenta if we assume that the momentum dependence of all functions are smooth on the scale of the overlap. By $k_F$ we denote the Fermi momentum, at which $\xi_{k_F} = 0$. Finally we assume that the induced order parameters are roughly equal in the conduction and in the valence band $|\Delta_c| \approx |\Delta_v| \equiv |\Delta|$. Using all those approximations and executing the momentum summations we find

$$\begin{aligned}
X_q &= 2\pi|\Delta|\left(\frac{1}{\tilde{w}_q - 2|\Delta| + \mathrm{i}\eta} + \frac{1}{\tilde{w}_q - 2|\Delta| - \mathrm{i}\eta} - \frac{1}{\tilde{w}_q + 2|\Delta| - \mathrm{i}\eta} - \frac{1}{\tilde{w}_q + 2|\Delta| + \mathrm{i}\eta}\right), \\
Y(t) &= 2\pi|\Delta| \sum_\sigma \sigma \left(\mathrm{e}^{-2\mathrm{i}|\Delta|t}\gamma_{c,k_F,0}\gamma_{v,-k_F,\bar{\sigma},0} + \mathrm{e}^{2\mathrm{i}|\Delta|t}\gamma^\dagger_{v,-k_F,\bar{\sigma},0}\gamma^\dagger_{c,k_F,\sigma,0}\right), \\
Z_q &= 2\pi|\Delta|\left(\frac{1}{\tilde{w}_q - 2|\Delta| + \mathrm{i}\eta} + \frac{1}{\tilde{w}_q + 2|\Delta| + \mathrm{i}\eta}\right).
\end{aligned} \tag{5.104}$$

From this simplified coefficients we can read of that only processes that involve Cooper pairs are allowed at zero temperature. Quasiparticles occur only in pairs in virtual intermediate states which is natural, since there are no excitations in a superconductor at zero temperature. We will make use of these simplified coefficients later in the next section, when we investigate the squeezing of the emitted light.

## 5.3. Source of squeezed light

The goal of this section is to show that a superconductor-light emitting diode-superconductor heterostructure is a source of squeezed light. We restrict ourself to two mode squeezed

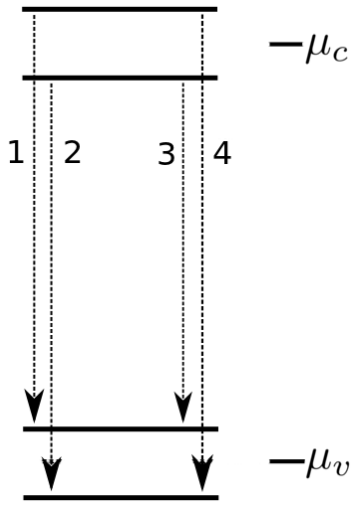


Figure 5.4.: The four resonances of the effective photon Hamiltonian

light for simplicity and note that the generalization to multi-mode squeezing is possible. In analogy to [SZ97] we introduce collective creation and annihilation operators $a_q$ and $a_q^\dagger$ with

$$a_q(t) \equiv \frac{1}{\sqrt{2}}\big(b_q(t) + b_{-q}(t)\big), \qquad a_q^\dagger(t) \equiv \frac{1}{\sqrt{2}}\big(b_q^\dagger(t) + b_{-q}^\dagger(t)\big). \tag{5.105}$$

All operators are in the rotated frame $b_H(t) = \mathrm{e}^{-\mathrm{i}wt}b(t)$ since we are interested in the properties of the quadrature amplitudes $A_q$ and $B_q$. For brevity we drop the time arguments. Next we define the quadrature amplitudes for these operators that we introduced in section 3.4 and get

$$A_q = \frac{1}{2}\Big(a_q^\dagger + a_q\Big), \qquad B_q = \frac{1}{2\mathrm{i}}\Big(a_q^\dagger - a_q\Big). \tag{5.106}$$

As discussed in section 3.4 squeezing is, if the variance of one of one of the quadrature amplitudes is smaller than the other one. For minimal uncertainty states this would mean $(\Delta A_q)^2 < 1/4$ or $(\Delta B_q)^2 < 1/4$. In the rest of this section we proof that our model leads to such squeezed light. We begin by calculating the variances

$$\begin{aligned}(\Delta A_q)^2 &\equiv \langle A_q^2\rangle - \langle A_q\rangle^2 \\ &= \frac{1}{4}\big\langle a_q^\dagger a_q + a_q a_q^\dagger + a_q^\dagger a_q^\dagger + a_q a_q\big\rangle - \big\langle a_q + a_q^\dagger\big\rangle.\end{aligned} \tag{5.107}$$

Assuming we are in a number state which is truncated at a finite number the second term vanishes (not so in a coherent state). From the general structure of the effective Hamiltonian we see that terms such as $b_q^\dagger b_{-q}$ or $b_q b_q$ can not have a finite expectation value for $q \neq 0$ (momentum conservation). Hence,

$$(\Delta A_q)^2 = \frac{1}{4}\big\langle b_q^\dagger b_q + b_{-q}^\dagger b_{-q} + 1 + b_q b_{-q} + b_q^\dagger b_{-q}^\dagger\big\rangle. \tag{5.108}$$

Since we assume that all (real) photons are absorbed by our detector the first two terms vanish since they count the number of photons in the system. The derivation of $(\Delta B_q)^2$ goes along the same line of arguments and we only state the final result:

$$(\Delta A_q)^2 = \frac{1}{4}\Big(1 + 2\mathrm{Re}\big\langle b_q b_{-q}\big\rangle\Big), \qquad (\Delta B_q)^2 = \frac{1}{4}\Big(1 - 2\mathrm{Re}\big\langle b_q b_{-q}\big\rangle\Big). \tag{5.109}$$

We immediately see two things. First, the system without squeezing would be in a minimal uncertainty state and second that if $\mathrm{Re}\langle b_q b_{-q}\rangle \neq 0$ there is squeezing. It is easily understood that the unsqueezed system is in a minimal uncertainty state, since all photons exit the system immediately and the unsqueezed vacuum is a coherent state with zero amplitude. What is left to show is that the real part of the anomalous expectation value $\langle b_q b_{-q}\rangle$ is non zero. To do that we calculate the Heisenberg photon operator in the rotating frame using the effective Hamiltonian. The Heisenberg equation of motion reads

$$\begin{aligned}\dot{b}_{H,q}(t) &= \mathrm{i}\big[\big(H_{\mathrm{eff}}\big)_H, b_{H,q}\big] \\ &= -\mathrm{i}\Big(w_q + |g|^2\mathrm{e}^{2\eta t}X_q\Big)b_{H,q}(t) - \mathrm{i}g^*\mathrm{e}^{\eta t}\mathrm{e}^{-\mathrm{ieV}t}Y_q^\dagger(t) \\ &\quad + \mathrm{i}g\sum_{q_1}\mathrm{e}^{\eta t}\mathrm{e}^{\mathrm{ieV}t}[Y_{q_1}(t), b_{H,q}(t)]b_{H,q_1}(t) \\ &\quad + \mathrm{i}g^*\mathrm{e}^{\eta t}\mathrm{e}^{-\mathrm{ieV}t}\sum_{q_1} b^\dagger_{H,q_1}(t)[Y^\dagger_{q_1}(t), b_{H,q}(t)] \\ &\quad + (g^*)^2\mathrm{e}^{2\eta t}\mathrm{e}^{-2\mathrm{ieV}t}(Z_q^* + Z_{-q}^*)b^\dagger_{H,-q}(t). \end{aligned} \tag{5.110}$$

Next we go to the rotating frame $b_{H,q}(t) \equiv \mathrm{e}^{-\mathrm{i}w_q t}b_q(t)$. Formal integration $\int_{t_0}^t \mathrm{d}t'$ and recursive substitution lead to

$$b_q(t) = b_{q,0} - g^*\mathcal{Y}_q^\dagger(t) + \mathrm{i}|g|^2\frac{\mathrm{e}^{2\eta t}}{2\eta}M_q(t)b_{q,0} - (g^*)^2Z_q^*\frac{\mathrm{e}^{2\mathrm{i}(\tilde{w}_q - \mathrm{i}\eta)t}}{\tilde{w}_q - \mathrm{i}\eta}b^\dagger_{-q,0} + O(|g|^3), \tag{5.111}$$

where $\tilde{w}_q \equiv w_q - \mathrm{eV}$. As before we used the approximation $|k+q| \approx |k|$. The coefficients

$$\begin{aligned}M_q(t) \equiv \sum_k \Bigg[&\alpha_k\frac{n_{c,k} - n_{v,k}}{\tilde{w}_q - E_{c,k} + E_{v,k} + \mathrm{i}\eta} - \beta_k\frac{n_{c,k} - n_{v,k}}{\tilde{w}_q + E_{c,k} - E_{v,k} + \mathrm{i}\eta} \\ &+ \delta_k\frac{1 - n_{c,k} - n_{v,k}}{\tilde{w}_q + E_{c,k} + E_{v,k} + \mathrm{i}\eta} - \zeta_k\frac{1 - n_{c,k} - n_{v,k}}{\tilde{w}_q - E_{c,k} - E_{v,k} + \mathrm{i}\eta}\Bigg]\end{aligned} \tag{5.112}$$

and

$$\begin{aligned}Z_q^* \equiv \sum_{k,\sigma}\chi^*_{q,k,\sigma}\Bigg(&\frac{n_{v,k-q,\sigma} - n_{c,k,\sigma}}{\tilde{w}_{-q} + E_{c,k} - E_{v,k-q} - \mathrm{i}\eta} + \frac{n_{v,k-q,\sigma} - n_{c,k,\sigma}}{\tilde{w}_q - E_{c,k} + E_{v,k-q} - \mathrm{i}\eta} \\ &+ \frac{1 - n_{v,q-k,\bar{\sigma}} - n_{c,k,\sigma}}{\tilde{w}_q - E_{c,k} - E_{v,k-q} - \mathrm{i}\eta} + \frac{1 - n_{v,q-k,\bar{\sigma}} - n_{c,k,\sigma}}{\tilde{w}_{-q} + E_{c,k} + E_{v,k-q} - \mathrm{i}\eta}\Bigg)\end{aligned} \tag{5.113}$$

are simple c-numbers. On the other hand

$$\begin{aligned}\mathcal{Y}_q^\dagger(t) \equiv \sum_{k,\sigma}\Bigg(&u_{c,k}u^*_{v,k}\frac{\mathrm{e}^{\mathrm{i}(\tilde{w}_q - E_{c,k} + E_{v,k} - \mathrm{i}\eta)t}}{\tilde{w}_q - E_{c,k} + E_{v,k} - \mathrm{i}\eta}\gamma^\dagger_{v,k-q,\sigma,0}\gamma_{c,k,\sigma,0} \\ &- v_{c,k}v^*_{v,k}\frac{\mathrm{e}^{\mathrm{i}(\tilde{w}_q + E_{c,k} - E_{v,k} - \mathrm{i}\eta)t}}{\tilde{w}_q + E_{c,k} - E_{v,k} - \mathrm{i}\eta}\gamma^\dagger_{c,k,\sigma,0}\gamma_{v,k+q,\sigma,0} \\ &+ \sigma v_{c,k}u^*_{v,k}\frac{\mathrm{e}^{\mathrm{i}(\tilde{w}_q + E_{c,k} + E_{v,k} - \mathrm{i}\eta)t}}{\tilde{w}_q + E_{c,k} + E_{v,k} - \mathrm{i}\eta}\gamma_{v,-q-k,\bar{\sigma},0}\gamma_{c,k,\sigma,0} \\ &+ \sigma u_{c,k}v^*_{v,k}\frac{\mathrm{e}^{\mathrm{i}(\tilde{w}_q - E_{c,k} - E_{v,k} - \mathrm{i}\eta)t}}{\tilde{w}_q - E_{c,k} - E_{v,k} - \mathrm{i}\eta}\gamma^\dagger_{c,k,\sigma,0}\gamma^\dagger_{v,q-k,\bar{\sigma},0}\Bigg)\end{aligned} \tag{5.114}$$

does contain fermionic operators. With this preparation we are in the position to calculate the anomalous expectation value in the rotating frame. We find

$$\Big\langle b_q b_{-q}\Big\rangle = (g^*)^2\big\langle\mathcal{Y}_q^\dagger(t)\mathcal{Y}^\dagger_{-q}(t)\big\rangle - (g^*)^2Z_q^*\frac{\mathrm{e}^{2\mathrm{i}(\tilde{w}_q - \mathrm{i}\eta)t}}{\tilde{w}_q - \mathrm{i}\eta}, \tag{5.115}$$

where

$$\langle \mathcal{Y}_q^\dagger(t)\mathcal{Y}_{-q}^\dagger(t)\rangle = \sum_{k,\sigma}\Bigg( -\chi_k^*(n_{v,k-q,\sigma}-n_{c,k,\sigma})\frac{\mathrm{e}^{2\mathrm{i}(\tilde{w}_q-\mathrm{i}\eta)t}}{(\tilde{w}_q-\mathrm{i}\eta)^2-(E_{c,k}-E_{v,k})^2} + \chi_k^*(1-n_{v,k,\bar{\sigma}}-n_{c,k,\sigma})\frac{\mathrm{e}^{2\mathrm{i}(\tilde{w}_q-\mathrm{i}\eta)t}}{(\tilde{w}_q-\mathrm{i}\eta)^2-(E_{c,k}+E_{v,k})^2}\Bigg). \quad (5.116)$$

We find that the two terms in (5.115) look alike but with opposite signs. The contribution from the term containing $Z^*$ is twice as large as from the other one, so they do not cancel. We note at this place, that even if they would cancel, squeezing survives. The reason is that the latter term in (5.115) is proportional to $(1+n_{ph})$ while the first term is independent of the number of photons in the system. Therefore, if we modify the detector and lift the constraint of zero photons in the system, the two terms can't cancel and there must be squeezing. In the zero temperature limit and with the same approximations as in section 5.2.7 we can write down a simple analytic expression for the anomalous expectation value

$$\Big\langle b_q b_{-q}\Big\rangle = \frac{2\pi|g|^2|\Delta|\,\mathrm{e}^{2\mathrm{i}(\tilde{w}_q-\mathrm{i}\eta)t}}{(2|\Delta|)^2-(\tilde{w}_q-\mathrm{i}\eta)^2}\mathcal{N}_F\mathrm{e}^{-\mathrm{i}\varphi}. \quad (5.117)$$

Here $\varphi$ is the initial time-independent phase difference between the superconducting. For simplicity the phase of the coupling constant has also been absorbed into $\varphi$. The most interesting case is the resonant case. At resonance the rotating AC-Josephson phase due to the bias voltage compensates the combined dynamical phase of both photon modes. Investigating the resonance requires some care, since otherwise, one gets the false impression that the squeezing increases with decreasing order parameters. At this point we use our results from section 5.1.5 where we found that higher order corrections give the photons a finite lifetime $(2\Gamma)^{-1} \sim (2|g|^2\mathcal{N}_F)^{-1}$ and lead to a small frequency shift $\Sigma$. Though we have not explicitly done this calculations with superconductors we are confident that there will be a similar effect. The reason is, that the virtual photons have the energy of the semiconductor gap and are thus not suppressed by the induced superconductor gaps $|\Delta|$. We introduce an effective density of states $\rho$ and write for the superconductor $\Gamma \sim \rho|g|^2$. In the limit of $|\Delta| \to 0$ we know $\rho \to \mathcal{N}_F$. Presumably $\rho$ will be larger than $\mathcal{N}_F$, since the density of states in the vicinity, but outside of the superconductor gap is larger than $\mathcal{N}_F$. Hence, our resonance condition is $\tilde{w}_q - \Sigma = 0$ and we find

$$\mathrm{Re}\Big\langle b_q b_{-q}\Big\rangle = \frac{2\pi|g|^2}{(2|\Delta|)^2+(\rho|g|^2)^2}|\Delta|\,\mathcal{N}_F\cos(\varphi). \quad (5.118)$$

On first sight it looks as if the squeezing could be controlled by the relative phase $\mathrm{e}^{-\mathrm{i}\arg(\chi)}$ between the superconductors at initial time $t_0$. And in fact the squeezing of a particular choice of quadrature amplitudes can be controlled in such a way, but not the squeezing in general. If we picture the squeezing as an uncertainty ellipse (Fig. 5.5), this phase simply rotates it. Hence, if we choose pair of quadrature amplitudes in such a way that the axes of the ellipse fall together with the quadrature axes the squeezing is independent of $\mathrm{e}^{-\mathrm{i}\arg(\chi)}$. We also notice, that off resonance the squeezing ellipse would rotate with time. Assuming the quadrature amplitudes correspond to the main axes the result at resonance is

$$(\Delta A_q)^2 = \frac{1}{4}\Big(1+\frac{4\pi|\Delta|\mathcal{N}_F}{(2|\Delta|/|g|)^2+(\rho|g|)^2}\Big) > \frac{1}{4},$$
$$(\Delta B_q)^2 = \frac{1}{4}\Big(1-\frac{4\pi|\Delta|\mathcal{N}_F}{(2|\Delta|/|g|)^2+(\rho|g|)^2}\Big) < \frac{1}{4}. \quad (5.119)$$

It is encouraging that the squeezing is robust against the variation of individual parameters and remains finite as long as there is a finite induced order parameter $|\Delta|$. There are

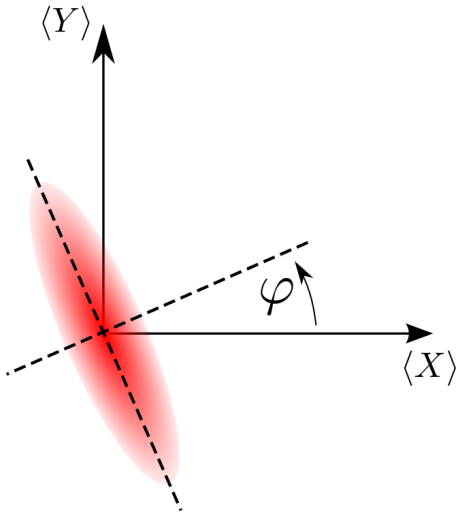


Figure 5.5.: Squeezing ellipse

two competing effects that are controlled by the coupling strength. On the one hand the creation of photon pairs and on the other hand the level broadening of the photons. Hence, there exist a value for the coupling constant $g_{\max} = \sqrt{2|\Delta|/\rho}$ for which the squeezing reaches it's maximal value $\mathcal{N}_F/\rho$. Changing the density of states or the induced gap only shifts the position of the maximum. To conclude our discussion we make an estimate of

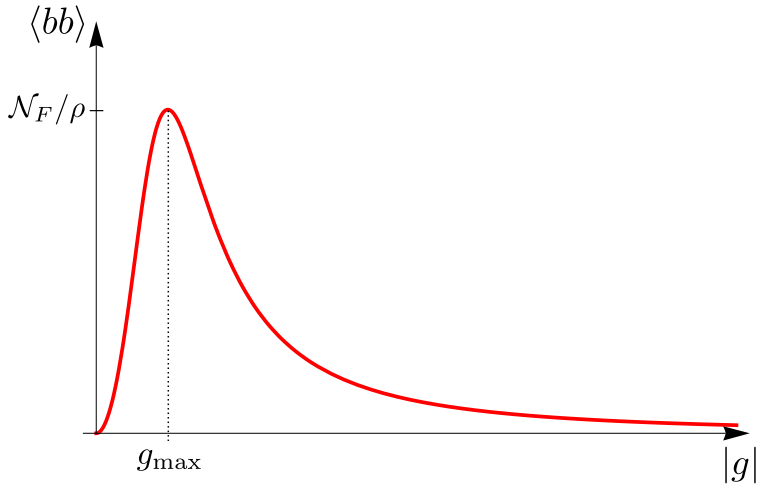


Figure 5.6.: Amount of squeezing for realistic set of parameters

the squeezing efficiency. As a system size we assume a cube of edge length $L = 100nm$.

- semiconductor gap $E_g \sim 10^4 K$
- induced gap $|\Delta| \sim 1K$
- dipole coupling $g \sim 1K$
- electron density of states $\mathcal{N}_F \sim 50/K \triangleq 10^{-3}/(\mathrm{eV}a_0^3)$
- photon level broadening $\Gamma \sim |g|^2 \mathcal{N}_F \sim 10^4 K$

The maximum is at a very weak coupling of $0.2K$. At a more realistic dipole coupling strength of $1K$ the squeezing effect is still at about 8%.

Summarizing we have studied the variance in the quadrature amplitudes of the light that is emitted from our setup. We found that there is squeezing and that this effect is robust. We also showed that the relative phase between the superconductors can be used to rotate the orientation of the uncertainty ellipse in quadrature amplitude space.

# 6. Summary and conclusion

In this thesis we investigated photon emission from a superconductor-light emitting diode-superconductor heterostructure. We modeled the light emitting diode with a direct band gap model. The bias voltage was included by introducing separate chemical potentials to the conduction- and valence band electrons. We accounted for the proximity induced superconductivity by BCS type leads and used Bogoliubov transformation to diagonalize the non-interacting part of the problem. To simplify the analysis and focus on the salient new features, we placed our setup in a detector that absorbs all photons. Hence, we didn't have to consider induced photon emission and photon absorption. In addition, this also guaranteed that the system reaches a stationary state.

We began the analysis of the model in section 5.1, by calculating the spontaneous photon emission, or luminescence $L^{\text{em}}$, of a normal light emitting diode without superconductivity. To do that we used the Keldysh formalism, which is suitable to describe nonequilibrium problems in a consistent diagrammatic way. We calculated the leading and the next to leading order in the coupling constant and finally summed up an infinite series of diagrams in the random phase approximation (PRA). We found that the higher order corrections gave a finite lifetime to the photons and lead to a small frequency shift. The luminescence that we calculated in RPA is

$$L^{\text{em, (RPA)}} \approx 2\pi|g|^2\overline{\mathcal{N}_{ph}}(\Delta\epsilon)\sum_k n_{c,k}(1-n_{v,k}), \tag{6.1}$$

which is similar in structure to the leading order contribution. Instead of the photon density of states at the semiconductor gap $\Delta\epsilon$, what enters is a smeared density of states. This is a consequence of the finite photon lifetime. We concluded the section by a toy calculation where we replaced the two band model by a two level model. The next to leading order contribution to the luminescence diverged, and we solved this via extensive resummations of diagrams in RPA. This corrections in turn lead to a finite photon life-time and hence finite level width. The final result turned out to be qualitatively similar to the photon emission in the two band model.

In section 5.2 we used Heisenberg's equations of motion to derive an expression that we call effective photon Hamiltonian. It is strictly speaking not a Hamiltonian in the true sense of the word. It is however an expression that allows to calculate the photon operators in the Heisenberg picture up to second order in the coupling constant. The advantage of the effective Hamiltonian is that one immediately sees clearly the properties of the emitted

photons. We found that the effective photon Hamiltonian

$$\begin{aligned}\big(H_{\text{eff}}\big)_H \equiv &\sum_q (w_q + |g|\mathrm{e}^{2\eta t} X_q) b^\dagger_{H,q} b_{H,q} \\ &+ \sum_q \Big( g\mathrm{e}^{\eta t}\mathrm{e}^{\mathrm{ieV}t} Y_q(t) b_{H,q} + g^*\mathrm{e}^{\eta t}\mathrm{e}^{-\mathrm{ieV}t} b^\dagger_{H,q} Y^\dagger_q(t)\Big) \\ &+ \sum_q \Big( g^2\mathrm{e}^{2\eta t}\mathrm{e}^{2\mathrm{ieV}t} Z_q b_{H,-q} b_{H,q} + (g^*)^2\mathrm{e}^{2\eta t}\mathrm{e}^{-2\mathrm{ieV}t} Z^\dagger_q b^\dagger_{H,q} b^\dagger_{H,-q}\Big), \end{aligned} \tag{6.2}$$

consists of three parts, each with distinct physical meaning. The first part is the free photon Hamiltonian with a real valued frequency correction that is second order in the coupling constant. The second part has the structure of a photon pump. Unlike $X$ and $Z$ the coefficient $Y$ does contain fermionic quasiparticle operators, which is a necessary evil. In principle it is possible to integrate out fermionic operators completely using the Keldysh technique, but the nonequilibrium nature leads to terms that contain photon operators at different times and on different branches of the Keldysh contour. These terms can not be interpreted in the framework of an effective Hamiltonian and therefore are non-intuitive. The last term in equation (6.2) couples two photon modes with a rotating phase. Such an expression suggests, that the system acts as a parametric amplifier, and hence leads to squeezing of the photon states. The coefficient $Z$ is a number that is proportional to the squared induced order parameter, and therefore this term is entirely due to superconductivity. It vanishes in the normal conducting state.

A detailed analysis of the coefficient $Z$ at zero temperature gave us further insight into the nature of the microscopic processes which lead to the production of photon pairs. We concluded that the photon pair emission consists of two steps. First a Cooper pair is broken into two quasiparticles. One of them goes to the valence band and emits a photon. The system is now in a virtual intermediate state. The remaining quasiparticle follows quickly, and tunnels to the valence band, where it forms a Cooper pairs with the other quasiparticle. There are two consequences. First, the emitted photons have a slightly different energy. The energy of the first photon is slightly smaller than the energy of the second photon. This might cause dephasing, but we note that the ratio of induced order parameter to the semiconductor gap is very small, about $10^{-5}$. And second, it might explain, why the time for luminescent electron-hole recombination doubled in the experiment which we discussed in section 2.1.3. Due to superconductivity two electrons now recombine with two holes in the same time in which there was only one recombination in the normal conducting case.

Finally, in section 5.3, we used the effective Hamiltonian to calculate the variance in the quadrature amplitudes $A$ and $B$. We found that the squeezing is given by

$$(\Delta A_q)^2 = \frac{1}{4}\Big(1 + 2\mathrm{Re}\big\langle b_q b_{-q}\big\rangle\Big), \qquad (\Delta B_q)^2 = \frac{1}{4}\Big(1 - 2\mathrm{Re}\big\langle b_q b_{-q}\big\rangle\Big). \tag{6.3}$$

We gave arguments as to why the squeezing is robust against variation of parameters such as the electron density of states $\mathcal{N}_F$ or the size of the induced oder parameter $|\Delta|$. It is given by

$$\mathrm{Re}\langle b_q b_{-q}\rangle = \frac{2|\Delta|\,\mathcal{N}_F\,\cos(\varphi)}{\big(2|\Delta|/|g|\big)^2 + (\rho|g|)^2}. \tag{6.4}$$

The denominator combines two competing effects, the production of photons and the finite photon lifetime $(2\Gamma)^{-1} = (2\rho|g|^2)^{-1}$, that is due to the coupling to the leads. Hence, as long as there is induced superconductivity, there exists a critical value of the coupling constant $g_{\max} = \sqrt{2|\Delta|/\rho}$ where the squeezing is maximal and given by $\mathcal{N}_F/\rho$.

We conclude that a superconductor-light emitting diode-superconductor heterostructure is indeed a strong candidate for a generic source of squeezed light. Especially the high efficiency, which we estimate to be around 8%, makes this setup very interesting. As a next step we propose to study how the system behaves in a resonator and how squeezed light can be extracted from the whole system for actual applications. The conceptual framework we laid out in this thesis forms the foundation for this investigations.

# 7. Deutsche Zusammenfassung

## 7.1. Motivation

Wenn zwei gut verstandene Materialien oder Technologien zusammenkommen, entstehen oft ganz neue Eigenschaften und Phänomene. Eines der bekanntesten Beispiele ist der elektrische Schwingkreis. Er besteht aus einem Kondensator und einer Spule und besitzt Eigenschaften, welche keines der beiden Teile einzeln aufweisen kann. Oder, um es mit Aristoteles zu sagen: "Das Ganze ist mehr als die Summe seiner Teile."

Zwei der interessantesten Materialien sind Halbleiter und Supraleiter. Halbleiter sind die Grundlage unserer modernen Informationstechnologie. Sie sind das Rohmaterial für Transistoren, Dioden, MOSFETs und vieler andere elementare Bausteine moderner Elektronik. Computer, Handys, Fernbedienungen und unzählige andere elektrische Geräte sind aus diesen Bausteinen zusammengesetzt. Einer der grundlegendsten Bausteine ist die Diode. Sie besteht aus einem n-dotiertem und einem p-dotiertem Halbleiter. Wenn die Bandstruktur im Bereich der Kontaktfläche einen direkten Bandübergang hat, dann kann ein Elektron das vom Leitungsband der n-dotierten Seite in das Valenzband der p-dotierten Seite tunnelt, ein Photon aussenden [Rou07]. (Der umgekehrte Prozess ist die Grundlage von Solarzellen.) Eine Leuchtdiode ist also eine künstliche Kopplung zwischen Elektronen und Photonen. Im Gegensatz zu Halbleitern sind Supraleiter im Alltag (noch) nicht sehr präsent. Sie werden jedoch schon heute als Grundlage vieler zukünftiger Technologien gehandelt. In der Medizin sind sie schon heute unverzichtbarer Bestandteil von Magnetresonanztomographen. Supraleiter haben viele faszinierende Eigenschaften, von denen die widerstandsfreie Leitung nur die bekannteste ist. Sie schirmen Magnetfelder ab, und zeigen quantenmechanisches Verhalten auf makroskopischen Längenskalen. Der Grundzustand eines Supraleiters wurde 1957 durch Bardeen, Cooper, und Schrieffer beschrieben [BCS57]. Es ist ein makroskopischer, kohärenter Zustand, der sich über den gesamten Supraleiter erstreckt. Er besteht aus einer Überlagerung gebundener Elektronenpaare, die Cooper-Paare genannt werden. Einer der beeindruckendsten Effekte ist, dass diese Cooper-Paare unter günstigen Umständen aus dem Supraleiter in ein nicht supraleitendes Material tunneln können. Dort haben sie eine endliche Lebensdauer, die lang genug sein kann, sodass das zuvor nicht supraleitende Material ebenfalls supraleitend wird. Man nennt dieses Phänomen Proximity-Effekt. Diese Materialien besitzen dann eine Mischung aus ihren ursprünglichen Eigenschaften und den Eigenschaften des Supraleiters.

Die Entdeckung des Proximity-Effekts hat einen wahren Goldrausch auf die Suche von interessanten Supraleiter-Nicht Supraleiter Heterostrukturen ausgelöst. Die vermutlich

wichtigste Erfindung in diesem Zusammenhang sind Josephson-Kontakte [Jos62]. Sie bestehen aus zwei Supraleitern, die durch eine dünne Isolationsschicht voneinander getrennt sind. Josephson-Kontakte sind die Grundlage von hochpräzisen Magnetfeldmessgeräten, genannt SQUID.

Lange Zeit wurden ausschließlich rein elektrische Systeme untersucht. Vor ungefähr zehn Jahren kamen dann erste Überlegungen auf, was passieren würde, wenn man Supraleiter mit Leuchtdioden zusammen bringt. Angenommen die Cooper-Paare können tief genug in die Leuchtdiode tunneln und dort lange genug überleben, koppeln sie dann an die ausgesendeten Photonen und falls ja, in welcher Weise? Welche außergewöhnlichen Eigenschaften würde das so entstehende Licht haben? Auf den ersten Blick würde man vielleicht kohärentes Licht erwarten, ähnlich wie das eines Lasers, weil Supraleiter auch durch einen kohärenten Zustand beschrieben werden. Allerdings ist Laserlicht ein kohärenter *Ein*-Photonenzustand während Supraleiter durch einen kohärenten *Zwei*-Elektronenzustand beschrieben werden. In der Literatur über Quantenoptik findet sich das Konzept eines kohärenten Zwei-Photonenzustandes unter dem Namen "Squeezed Light" oder gequetschtes Licht. Das Konzept von gequetschten Zuständen geht auf Schrödinger [Sch26] zurück. Betrachtet man ein Paar konjugierter Variablen, dann muss das Produkt ihrer Varianzen der Heisenbergschen Unschärferelation genügen. Ist die Unschärfe nicht gleichmäßig auf beide Variablen verteilt, so sagt man das System befindet sich bezüglich dieser Variablen in einem gequetschtem Zustand. In Analogie zu Ort- und Impulsvariable in einem Oszillator kann man das elektrische Feld von Licht durch ein Paar von konjugierten Variablen, die sogenannten Quadratur Amplituden, beschreiben. Diese sind nicht eindeutig festgelegt und können durch einen Winkel parametrisiert werden. Wenn nun bei wenigstens einer Wahl dieser Quadratur Amplituden die Unschärfe nicht gleichmäßig verteilt ist, dann spricht man von gequetschtem Licht. Man kann das Ganze veranschaulichen, indem man den Zustand in einem Diagramm aufträgt, in dem ein Paar von Quadratur Amplituden die Achsen bildet. Bei ungequetschtem Licht stellt die Varianz in diesem zweidimensionalen Raum einen Kreis dar, bei gequetschtem Licht eine Ellipse. Die erste ausführliche Behandlung von gequetschtem Licht stammt von Klauder aus dem Jahr 1968 [KS68]. Das große Interesse setzte jedoch erste zwanzig Jahre später ein, als Hochpräzisions Messgeräte, wie zum Beispiel Interferometer, eine Auflösung von der Größenordnung der Quantenfluktuationen erreicht hatten. Die Reduktion dieser Fluktuationen wurde damit zum Schlüsselelement, um noch bessere Auflösungen zu erreichen. Genau diese Reduktion kann mit gequetschtem Licht erreicht werden. Das Problem ist jedoch, dass es bis zum heutigen Tag unseres Wissens nach keine direkte Quelle für gequetschtes Licht gibt. Die populärste Methode um gequetschtes Licht herzustellen is die sogenannte spontane parametrische Abwärtskonversion. Bei dieser wird ein nichtlineares optisches Medium verwendet, um aus einem gewöhnlichen Laserstrahl gequetschtes Licht zu erzeugen. Leider ist der Wirkungsgrad der parametrische Abwärtskonversion extrem gering.

In dieser Arbeit schlagen wir vor, dass eine Leuchtdiode mit zwei supraleitenden Kontakten eine Quelle für gequetschtes Licht sein könnte. Eiich Hanamura hat 2002 ein ähnliches Setup im Zusammenhang mit einer erhöhten Leuchteffizienz vorgeschlagen [Han02]. Außerdem vermutete er, dass solch ein System eine Quelle verschränkter Photonenpaare sein könnte. Die erste experimentelle Realisierung einer Leuchtdiode mit einem supraleitendem Kontakt [HTA$^+$08] bestätigte die von Hanamura vorhergesagte erhöhte Leuchteffizienz und zeigte damit, dass die Anwesenheit von Cooper-Paaren sich tatsächlich auf die Photonenproduktion auswirkt. Dieses Experiment wiederum hat weitere theoretische Arbeiten motiviert [ASTH09], [RNK10], [HNK09] und [GHN11]. Das von uns untersuchte Setup haben wir in Abbildung 7.1 skizziert.

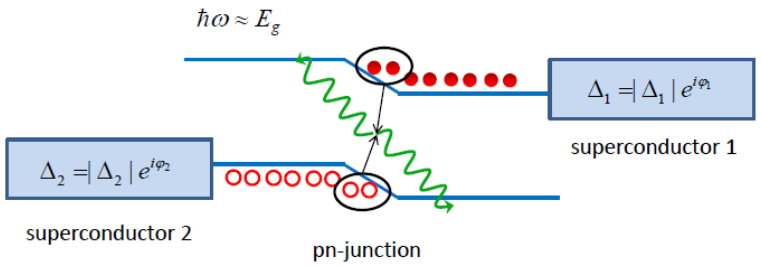


Figure 7.1.: Leuchtdiode mit zwei supraleitenden Kontakten

## 7.2. Modell

Da wir uns vor Allem für die Photonen interessieren, genügt es die Region in der Mitte der Leuchtdiode zu beschreiben, denn nur dort entstehen Photonen. Dieser Bereich kann durch ein effektives zwei Bändermodell mit direktem Bandübergang beschrieben werden. Den Kopplungsterm haben wir so gewählt, dass ausschließlich Prozesse erlaubt sind, die mit Photonenemission oder Photonenabsorption einhergehen. Die angelegte Vorspannung $V$, die zum Betreiben einer Leuchtdiode notwendig ist, beschreiben wir durch individuelle chemische Potentiale für Leitungs- und Valenzelektronen. Die Differenz der Beiden entspricht der Vorspannung. Durch die supraleitenden Kontakte werden Ordnungsparameter in beide Bänder induziert. Das führt zu Termen, wie sie aus der BCS Theorie bekannt sind. Als nächstes Diagonalisieren wir den nicht wechselwirkenden Teil des Systems mit Hilfe von Bogoliubov Transformationen. Zusätzlich versetzen wir unser Setup zu in einen Photonendetektor der alle Photonen, die die Leuchtdiode aussendet, sofort absorbiert. Als Folge dessen findet keine induzierte Photonenemission und keine Photonenabsorption statt. Dadurch vereinfachen sich die Rechnungen und es ist garantiert, dass das System einen stationären Zustand einnehmen kann.

## 7.3. Auswertung

Zunächst berechnen wir die spontane Photonenemissionsrate einer normalen Leuchtdiode störungstheoretisch. Dazu verwenden wir den Keldysh Formalismus, der eine diagrammatische Beschreibung von nichtgleichgewichts Physik erlaubt. Wir untersuchen die Relevanz von Korrekturen über die führenden Ordnung hinaus. Dazu summieren wir eine unendliche Folge von Diagrammen in der randome phase approximation (RPA) auf. Wir finden, dass die Photonen dadurch eine kleine Frequenzverschiebung $\Sigma$ erfahren und eine endliche Lebensdauer $(2\Gamma)^{-1}$ erhalten. Die Photonenemissionsrate

$$L^{\text{em, (RPA)}} \approx 2\pi|g|^2\overline{\mathcal{N}_{ph}}(\Delta\epsilon)\sum_k n_{c,k}(1-n_{v,k}) \tag{7.1}$$

ändert sich im Vergleich zur führenden Ordnung nur darin, dass die ursprüngliche Zustandsdichte der Photonen $\mathcal{N}_{ph}$ etwas ausgeschmiert wird. Wir beenden die Untersuchung der normalen LED mit einer Vergleichsrechnung, in der wir das zwei Bändermodell durch ein zwei Niveau System ersetzen. In führender Ordnung ist die Photonenemissionsrate qualitativ wie beim Bändermodell, jedoch treten in der nächst höheren Ordnung Divergenzen auf. Wir lösen dieses Problem durch aufwändiges Summieren von Diagrammen in der randome phase approximation. Schlussendlich finden wir eine effektive Verbreiterung der Elektron Level, was die Divergenzen aufhebt. Das Endergebnis ist dann wieder dem des zwei Bändermodells ähnlich.

Im zweiten Teil der Auswertung benutzen wir die Heisenbergschen Bewegungsgleichungen, um einen Ausdruck herzuleiten, den wir effektiven Photon-Hamiltonian nennen. Streng

genommen handelt es sich dabei zwar um keinen Hamiltonian, aber er ermöglicht es uns die Photonenoperatoren im Heisenberg Bild störungstheoretisch bis zur zweiten Ordnung in der Kopplungskonstante abzuleiten. Der Vorteil dieses effektiven Photon Hamiltonian liegt darin, dass man an ihm direkt ablesen kann, welche Eigenschaften die Photonen besitzen. Der effektive Photon-Hamiltonian

$$\begin{aligned}\big(H_{\text{eff}}\big)_H \equiv &\sum_q (w_q + |g|\mathrm{e}^{2\eta t} X_q) b^\dagger_{H,q} b_{H,q} \\ &+ \sum_q \Big( g\mathrm{e}^{\eta t}\mathrm{e}^{\mathrm{ieV}t} Y_q(t) b_{H,q} + g^*\mathrm{e}^{\eta t}\mathrm{e}^{-\mathrm{ieV}t} b^\dagger_{H,q} Y^\dagger_q(t)\Big) \\ &+ \sum_q \Big( g^2\mathrm{e}^{2\eta t}\mathrm{e}^{2\mathrm{ieV}t} Z_q b_{H,-q} b_{H,q} + (g^*)^2\mathrm{e}^{2\eta t}\mathrm{e}^{-2\mathrm{ieV}t} Z^\dagger_q b^\dagger_{H,q} b^\dagger_{H,-q}\Big), \end{aligned} \tag{7.2}$$

besteht aus drei Teilen. Der erste Teil ist das freie Photonenbad zusammen mit einer kleinen Frequenzverschiebung. Der Koeffizient $X_q$ ist eine reale Zahl. Der zweite Term hat die Form einer Photonenpumpe. Im Gegensatz zu $X_q$ und $Z_q$ enthält der Koeffizient $Y_q$ noch fermionische Operatoren. Dies ist ein notwendiges Übel. Zwar ist es im Prinzip möglich die Fermionen - zum Beispiel mit dem Keldysh Pfadintegral Formalismus - komplett auszuintegrieren. Allerdings resultiert daraus ein Ausdruck, bei dem Photon Operatoren an unterschiedlichen Orten auf der Keldysh Zeitkontur liegen. Ein solcher Ausdruck kann nicht mehr als effektiver Photon Hamiltonian interpretiert werden. Der letzte Term ist der interessanteste. Er existiert ausschließlich wegen der induzierten Supraleitung. Er koppelt zwei Photon Moden mit einer rotierenden Phase. In der Literatur ist das als parametrischer Verstärker bekannt, und führt zur Produktion von gequetschtem Licht.

Im dritten Teil der Auswertung benutzen wir den effektiven Hamiltonian um die Varianz in den Quadratur Amplituden, die wir $A$ und $B$ nennen, herzuleiten. Wir finden

$$(\Delta A_q)^2 = \frac{1}{4}\Big(1 + 2\mathrm{Re}\big\langle b_q b_{-q}\big\rangle\Big), \qquad (\Delta B_q)^2 = \frac{1}{4}\Big(1 - 2\mathrm{Re}\big\langle b_q b_{-q}\big\rangle\Big). \tag{7.3}$$

Das bedeutet, dass das ausgesendete Licht gequetscht ist, falls $\mathrm{Re}\big\langle b_q b_{-q}\big\rangle \neq 0$. Unsere Rechnung ergibt, dass dies der Fall ist, solange die induzierte Supraleitung nicht verschwindet $|\Delta| \neq 0$. Die Stärke der Quetschung ist durch

$$\mathrm{Re}\langle b_q b_{-q}\rangle = \frac{2|\Delta|\,\mathcal{N}_F\,\cos(\varphi)}{\big(2|\Delta|/|g|\big)^2 + (\rho|g|)^2} \tag{7.4}$$

gegeben. Im Nenner konkurrieren zwei Prozesse, die beide von der Größe der Kopplungskonstante $g$ abhängen. Zum einen die Produktion von Photonenpaaren und zum anderen die endliche Lebensdauer der Photonen. Als Folge dessen gibt es einen Wert der Kopplungskonstante $g_{\max} = \sqrt{2|\Delta|/\rho}$ bei der das emittierte Licht maximal, mit $\mathcal{N}_F/\rho$, gequetscht wird.

## 7.4. Schlussfolgerungen und Ausblick

Zusammenfassend schlussfolgern wir, dass eine Leuchtdiode mit supraleitenden Kontakten ein heißer Kandidat für eine Quelle gequetschten Lichtes ist. Insbesondere die hohe Effizienz, die wir im Bereich von bis zu 8% sehen, macht diesen Vorschlag besonders interessant. Als nächsten Schritt möchten wir untersuchen, wie sich das Setup in einen Resonator verhält und wie gequetschtes Licht aus diesem Resonator extrahiert werden kann. Die in dieser Arbeit vorgestellten theoretischen Überlegungen und Techniken bilden die Grundlage für diese weiteren Studien.

# 8. Acknowledgements

First of all I would like to thank Professor Dr. Jörg Schmalian for giving me the opportunity to write my Diploma thesis in his group. I want to thank him for his advice and guidance, for being there when I needed him and for making this time extraordinary by giving me the opportunity to visit the APS March meeting in Boston and Professor Dr. Vekhter at Louisiana state university.

I want to thank Professor Dr. Kurt Busch, who agreed to review my thesis.

I'm am very grateful to Professor Dr. Ilya Vekhter for inviting me to visit him in the USA and for his guidance and expertise.

A big thank you goes to many other people at the TKM. My roommates Ulf Briskot, Nikolaos Kainaris, Patrik Hlobil, Pablo Schad, Mathias Scheurer, Michael Schneider, Tobias Sproll, David Wendland and Philip Wollfarth for the nice atmosphere and support. Elio König, Stephane Ngo Dinh, Peter Orth, Christian Seiler, Michael Schütt and Sergey Syzranov for fruitful discussions and advice.

I'm very thankful to Roswitha Schrempp, who took care of everything when it came to organization and administration. Among many other things she helped me to organize my participation at the Bad Herrenalb summer school and the APS March meeting.

On the way to my Diploma I had lots of support by my study mates and friends Kathrin Ender, Jörg Gramich Kristina Hönes, Bastian Kern, Jonathan Müller, Robert Schittny, Michael Walz, Christian Wiese, and Nicolas Vogt for which I am very grateful. Very special thanks go to Simon Ketterer who was there since the beginning. Together we mastered countless exercises and lab reports, without him, it would not have been the same.

Most of all I want to thank my family and my girlfriend who always supported me, believed in me and gave me their love.

# Bibliography


[Alt10] A. Altland, Condensed matter field theory . Cambridge University Press, 2010.

[ASTH09] Y. Asano, I. Suemune, H. Takayanagi, and E. Hanamura, "Luminescence of a Cooper Pair," Physical Review Letters 103, 187001 (2009)., May 2009. [Online]. Available: http://arxiv.org/abs/0905.1182v1;http://arxiv.org/pdf/0905.1182v1

[BCS57] J. Bardeen, L. N. Cooper, and J. R. Schrieffer, "Theory of Superconductivity," Phys. Rev., vol. 108, no. 5, pp. 1175–1204, Dec. 1957. [Online]. Available: http://prola.aps.org/abstract/PR/v108/i5/p1175_1

[BF04] H. Bruus and K. Flensberg, Many-Body Quantum Theory in Condensed Matter Physics. Oxford Graduate Texts, 2004.

[BW70] D. Burnham and D. Weinberg, "Observation of simultaneity in parametric production of optical photon pairs," Phys. Rev. Lett., vol. 25, no. 84, 1970.

[CS85] C. Caves and B. Schumaker, "New formalism for two-photon quantum optics. I. Quadrature phases and squeezed states," Physical Review A, vol. 31, no. 5, p. 3068, 1985.

[GHN11] F. Godschalk, F. Hassler, and Y. V. Nazarov, "Proposal for an optical laser producing light at half the Josephson frequency," Phys. Rev. Lett. 107, 073901 (2011), Sep. 2011. [Online]. Available: http://arxiv.org/abs/1010.5960v2;http://arxiv.org/pdf/1010.5960v2

[GM65] J. Giordmaine and R. Miller, "Tunable coherent parametric oscillation in LiNbOs at optical frequencies," Phys. Rev. Lett, vol. 14, no. 24, 1965.

[GZ99] A. Gulian and G. Zharkov, Nonequilibrium electrons and phonons in superconductors. Kluwer Acade- mic/Plenum Publishers, 1999.

[Han02] E. Hanamura, "Superradiance from p-n Junction of Hole- and Electron-Superconductors," Phys Stat Sob B, vol. 234, no. 1, 2002.

[HNK09] F. Hassler, Y. V. Nazarov, and L. P. Kouwenhoven, "Quantum manipulation in a Josephson LED," Nanotechnology 21, 274004 (2010), Nov. 2009. [Online]. Available: http://arxiv.org/abs/0911.5100v1;http://arxiv.org/pdf/0911.5100v1

[HTA+08] Y. Hayashi, K. Tanaka, T. Akazaki, M. Jo, H. Kumano, and I. Suemune, "Superconductor-based Light Emitting Diode: Demonstration of Role of Cooper Pairs in Radiative Recombination Processes ," Applied Physics Express, vol. 1, 2008.

[ITA+10] R. Inoue, H. Takayanagi, T. Akazaki, K. Tanaka, and I. Suemune, "Transport characteristics of a superconductor-based LED ," Supercond. Sci. Technol., vol. 23, 2010.

[Jos62] B. Josephson, "Possible new effects in superconductive tunnelling," Physics Letters, 1962.

[KB62] L. P. Kadanoff and G. Baym, Quantum Statistical Mechanics. New York: Benjamin, 1962.

[Kel65] L. V. Keldysh, "Diagram technique for nonequilibrium processes," Soviet Phys. JETP, vol. 20, pp. 1018–26, 1965. [Online]. Available: http://www.bibsonomy.org/bibtex/284c4417a258ee057b982f59c57a3be2c/brouder

[Kha09] F. Khanna, Thermal quantum field theory: algebraic aspects and applications. World Scientific Pub Co Inc, 2009.

[KL09] A. Kamenev and A. Levchenko, "Keldysh technique and non-linear sigma-model: basic principles and applications," Advances in Physics 58, 197 (2009), Apr. 2009. [Online]. Available: http://arxiv.org/abs/0901.3586v3;http://arxiv.org/pdf/0901.3586v3

[KRB09] N. Kwong, G. Rupper, and R. Binder, "Self-consistent T-matrix theory of semiconductor light-absorption and luminescence ," Physical Review B, vol. 79, 2009.

[KS68] J. Klauder and E. Sudarshan, Fundamentals of Quantum Optics, 1968.

[Lan76] D. C. Langreth, "Linear and nonlinear response theory with application," in Linear and Nonlinear Electron Transport in Solids, J. T. Devreese and V. E. van Doren, Eds. New York: Plenum Press, 1976. [Online]. Available: http://www.bibsonomy.org/bibtex/2867a9f66d09b2ea56220b9b2dbce7e2d/bronckobuster

[Mah90] G. D. Mahan, Many-Particle Physics. New York: Plenum, 1990.

[PF05] X. Pang and Y. Feng, Quantum Mechanics In Nonlinear Systems. World Scientific Publishing Company, 2005.

[Ram07] J. Rammer, Quantum field theory of Non-equilibrium States. Cambridge: Cambridge University Press, 2007.

[RNK10] P. Recher, Y. V. Nazarov, and L. P. Kouwenhoven, "Josephson light-emitting diode." Phys. Rev. Lett., vol. 104, no. 15, p. 156802, Apr. 2010.

[Rou07] H. Round, "A note on carborundum," Electrical World, 1907.

[SAT+06] I. Suemune, T. Akazaki, K. Tanaka, M. Jo, K. Uesugi, M. Endo, H. Kumano, E. Hanamura, H. Takayanagi, M. Yamanishi, and H. Kan, "Superconductor-Based Quantum-Dot Light-Emitting Diodes: Role of Cooper Pairs in Generating Entangled Photon Pairs," Japanese Journal of Applied Physics, vol. 45, no. 12, 2006.

[SC85] B. Schumaker and C. Caves, "New formalism for two-photon quantum optics. II. Mathematical foundation and compact notation," Physical Review A, vol. 31, no. 5, p. 3093, 1985.

[Sch26] E. Schödinger, "Der stetige Ubergang von der Mikro- zur Makromechanik," Naturwissenschaften, vol. 14, pp. 664–666, 1926.

[SHK+10] I. Suemune, Y. Hayashi, S. Kuramitsu, K. Tanaka, T. Akazaki, E. Hanamura, S. Odashima, and H. Kumano, "A Cooper-Pair Light-Emitting Diode: Temperature Dependence of Both Quantum Efficiency and Radiative Recombination Lifetime ," Applied Physics Express, vol. 3, 2010.

[SKH+11] H. Sasakura, S. Kuramitsu, Y. Hayashi, K. Tanaka, T. Akazaki, E. Hanamura, R. Inoue, H. Takayanagi, Y. Asano, C. Hermannstädter, H. Kumano, and I. Suemune, "Enhanced photon generation in a Nb/n-InGaAs/p-InP superconductor/semiconductor-diode light emitting device." Phys. Rev. Lett., vol. 107, no. 15, p. 157403, Oct. 2011.

[SZ97] M. O. Scully and M. S. Zubairy, Quantum Optics. Cambridge University Press, 1997.

[TIA+10] H. Takayanagi, R. Inoue, T. Akazaki, K. Tanaka, and I. Suemune, "Superconducting transport in an LED with Nb electrodes," Physica C, vol. 470, 2010.

[Yue76] H. Yuen, "Two-photon coherent states of the radiation field," Physical Review A, vol. 13, no. 6, p. 2226, 1976.

[Zag98] A. Zagoskin, Quantum theory of many-body systems: techniques and applications, ser. Graduate texts in contemporary physics. New York: Springer-Verlag, 1998.

# Appendix

## A. Formalism

### A.1. Nambu Formalism

The BCS ground state state mixes electrons and holes. Hence, a natural way to reformulate the BCS theory is the so called particle-hole or Nambu formalism [Alt10] p271f and [BF04] p335f. We follow the convention in this books and define

$$\hat{\Psi}_k \equiv \begin{pmatrix} c_{\mathbf{k}\uparrow} \\ c^\dagger_{-\mathbf{k}\downarrow} \end{pmatrix}, \qquad \hat{\Psi}^\dagger_k \equiv \begin{pmatrix} c^\dagger_{\mathbf{k}\uparrow} & c_{-\mathbf{k}\downarrow} \end{pmatrix}. \tag{A.1}$$

In this formalism the Hamiltonian is a two by two matrix

$$H_{\mathrm{BCS}} - \mu N = \sum_{\mathbf{k}} \hat{\Psi}^\dagger_k \begin{pmatrix} \xi_k & -\Delta_{\mathbf{k}} \\ -\Delta^*_{\mathbf{k}} & -\xi_{-k} \end{pmatrix} \Psi_k + \sum_{\mathbf{k}} \xi_k. \tag{A.2}$$

In the following we will ignore the additive constant $\sum_{\mathbf{k}} \xi_k$. In addition we assume that the dispersion relation is isotropic in momentum space $\xi_{\mathbf{k}} = \xi_{|\mathbf{k}|} = \xi_k$. The generic way to introduce superconductivity to systems which are well understood in the non superconducting case is therefore to introduce a matrix structure for the Green's functions [BF04] p336 and [Ram07] p226f. If this formalism is applied carefully the structure of the non superconducting equations carries over to the superconducting case. We have to take great care when doing this step since unlike scalars matrices do not commute and hence in all previous derivations no commutations must have occurred. In addition, anomalous expectation values can become finite. Specifically we mean expectation values that contain a product of two annihilation or creation operators of the same species. We choose the following convention for the matrix structure of the Nambu Green's functions:

$$\begin{aligned} \hat{G}^{\mathrm{T}}_{\mathbf{k}}(t,t') &\equiv -\mathrm{i}\hat{\tau}_3 \langle T \hat{\Psi}_{\mathbf{k}}(t) \hat{\Psi}^\dagger_{\mathbf{k}}(t') \rangle \\ &= -\mathrm{i}\hat{\tau}_3 \begin{pmatrix} \langle T \hat{c}_{\mathbf{k}\uparrow}(t) c^\dagger_{\mathbf{k}\uparrow}(t') \rangle & \langle T \hat{c}_{\mathbf{k}\uparrow}(t) c_{-\mathbf{k}\downarrow}(t') \rangle \\ \langle T \hat{c}^\dagger_{-\mathbf{k}\downarrow}(t) c^\dagger_{\mathbf{k}\uparrow}(t') \rangle & \langle T \hat{c}^\dagger_{-\mathbf{k}\downarrow}(t) c_{-\mathbf{k}\downarrow}(t') \rangle \end{pmatrix} \\ &= \begin{pmatrix} G^T_{\mathbf{k}}(\mathbf{k},t,t') & F^T_{\mathbf{k}}(\mathbf{k},t,t') \\ -\tilde{F}^T_{\mathbf{k}}(\mathbf{k},t,t') & -\tilde{G}^T_{\mathbf{k}}(\mathbf{k},t,t') \end{pmatrix} \end{aligned} \tag{A.3}$$

The two anomalous Green's functions $F^T$ and $\tilde{F}^T$ are often called Gorkov Green's functions. The appear due to superconductivity and vanish in a normal conductor. Next we derive the explicit expressions for the free Green's functions using the equations of motion technique. First we calculate a set of commutators

$$\begin{aligned} &[c^\dagger_{\mathbf{k}'\sigma'} c_{\mathbf{k}'\sigma'}, c_{\mathbf{k}\sigma}] = -\delta_{\mathbf{k}\mathbf{k}'}\delta_{\sigma\sigma'} c_{\mathbf{k}\sigma} && [c^\dagger_{\mathbf{k}'\sigma'} c_{\mathbf{k}'\sigma'}, c^\dagger_{\mathbf{k}\sigma}] = +\delta_{\mathbf{k}\mathbf{k}'}\delta_{\sigma\sigma'} c^\dagger_{\mathbf{k}\sigma} \\ &[c^\dagger_{\mathbf{k}'\uparrow} c^\dagger_{-\mathbf{k}'\downarrow}, c_{\mathbf{k}\uparrow}] = -\delta_{\mathbf{k}\mathbf{k}'} c^\dagger_{-\mathbf{k}\downarrow} && [c^\dagger_{\mathbf{k}'\uparrow} c^\dagger_{-\mathbf{k}'\downarrow}, c_{-\mathbf{k}\downarrow}] = +\delta_{\mathbf{k}\mathbf{k}'} c^\dagger_{\mathbf{k}\uparrow} \\ &[c_{-\mathbf{k}'\downarrow} c_{\mathbf{k}'\uparrow}, c^\dagger_{\mathbf{k}\uparrow}] = +\delta_{\mathbf{k}\mathbf{k}'} c_{-\mathbf{k}\downarrow} && [c_{-\mathbf{k}'\downarrow} c_{\mathbf{k}'\uparrow}, c^\dagger_{-\mathbf{k}\downarrow}] = -\delta_{\mathbf{k}\mathbf{k}'} c_{\mathbf{k}\uparrow}, \end{aligned} \tag{A.4}$$

and note that all other commutators are either not needed or vanish. By taking the time derivative with respect to one of the time variables the equations we find the equations of motion which are coupled equations that can easily be decoupled and solved in the case of a homogeneous state:

$$\begin{aligned}\partial_t g^{\mathrm{T}}_{\mathbf{k}}(t) &= -\mathrm{i}\delta(t) - \mathrm{i}\xi_k g^{\mathrm{T}}_{\mathbf{k}}(t) + \mathrm{i}\Delta_{\mathbf{k}}\tilde{g}^{\mathrm{T}}_{\mathbf{k}}(t),\\ \partial_t \tilde{g}^{\mathrm{T}}_{\mathbf{k}}(t) &= +\mathrm{i}\xi_k \tilde{g}^{\mathrm{T}}_{\mathbf{k}}(t) + \mathrm{i}\Delta^*_{\mathbf{k}} f^{\mathrm{T}}_{\mathbf{k}}(t).\end{aligned} \tag{A.5}$$

We find the solution of these coupled differential equations systematically by going to frequency space and solving the resulting algebraic system of equations:

$$\begin{aligned}g^{\mathrm{T}}_{\mathbf{k}}(w) &= \frac{w+\xi_k}{w^2-(\xi_k^2+|\Delta_{\mathbf{k}}|^2)},\\ \tilde{f}^{\mathrm{T}}_{\mathbf{k}}(w) &= \frac{-\Delta^*_{\mathbf{k}}}{w^2-(\xi_k^2+|\Delta_{\mathbf{k}}|^2)}.\end{aligned} \tag{A.6}$$

An analogous calculation leads to the other two Green's functions that appear in the Nambu formalism. See for example [BF04] p336. These equations are lacking the boundary conditions that are usually described by shifting the poles of the Green's functions slightly into the upper or lower imaginary plane. However, there is a straight forward way to fix this. From the Lehmann representation we can see that the time-ordered Green's function can be composed of the retarded and the advanced Green's function $G^{\mathrm{T}}(w) = G^A(w)\theta(-w) + G^R(w)\theta(w)$. The poles of the advanced Green's function are by definition all in the upper half of the complex plane and the poles of the retarded in the lower half plane. Summarizing these results and noting that in a finite gap superconductor $E_{\mathbf{k}} = \sqrt{\xi_k^2 + |\Delta_{\mathbf{k}}|^2} > 0$, we find

$$\hat{G}^{\mathrm{T}}_{\mathbf{k}}(,w) = \frac{1}{(w-E_{\mathbf{k}}+\mathrm{i}0^+)(w+E_{\mathbf{k}}-\mathrm{i}0^+)}\begin{pmatrix} w+\xi_k & -\Delta_{\mathbf{k}} \\ \Delta^*_{\mathbf{k}} & -w+\xi_k\end{pmatrix}. \tag{A.7}$$

([GZ99] p25) the following relations hold:

$$\begin{aligned}\hat{G}^R(1,1') &= \theta(t-t')\Big(\hat{G}^{>}(1,1') - \hat{G}^{<}(1,1')\Big),\\ \hat{G}^A(1,1') &= -\theta(t'-t)\Big(\hat{G}^{>}(1,1') - \hat{G}^{<}(1,1')\Big),\\ \hat{G}^K(1,1') &= \hat{G}^{>}(1,1') + \hat{G}^{<}(1,1').\end{aligned} \tag{A.8}$$

To sharpen the physical understanding is worth mentioning the following representation:

$$G^{\mathrm{T}}_{\mathbf{k}}(w) = \frac{|u_{\mathbf{k}}|^2}{w-E_{\mathbf{k}}+\mathrm{i}0^+} + \frac{|v_{\mathbf{k}}|^2}{w+E_{\mathbf{k}}-\mathrm{i}0^+}. \tag{A.9}$$

Here $u_{\mathbf{k}}$ and $v_{\mathbf{k}}$ are the parameters of the BCS ground state giving a direct connection to physical quantities [Zag98] p174. All results generalize to the finite temperature case. The derivation is not given here but straightforward. In fact it is in some way easier than the zero temperature case, since it avoids the poles on the real axis. To make the connection between the Green's function derived in the finite temperature Matsubara formalism and the real time Green's function the concept of analytic continuation is applied. This leads to the retarded and advanced real time Green's functions. In a final step we find the time-ordered Green's function. Further details can for example be found in [Zag98]. The

Green's functions read

$$G^{\mathrm{T}}_{\mathbf{k}}(w,T) = \mathcal{P}\Big(\frac{|u_{\mathbf{k}}|^2}{w-E_{\mathbf{k}}} + \frac{|v_{\mathbf{k}}|^2}{w+E_{\mathbf{k}}}\Big) \\ - \mathrm{i}\pi\Big(1-2n_F(E_{\mathbf{k}},T)\Big)\Big(|u_{\mathbf{k}}|^2\delta(w-E_{\mathbf{k}}) - |v_{\mathbf{k}}|^2\delta(w+E_{\mathbf{k}})\Big) \\ = G^{\mathrm{T}}_{\mathbf{k}}(w,T=0) + 2\pi\mathrm{i}n_F(E_{\mathbf{k}},T)\Big(|u_{\mathbf{k}}|^2\delta(w-E_{\mathbf{k}}) - |v_{\mathbf{k}}|^2\delta(w+E_{\mathbf{k}})\Big),$$

$$\tilde{F}^{\mathrm{T}}_{\mathbf{k}}(w,T) = \tilde{F}^{\mathrm{T}}_{\mathbf{k}}(w,T=0) \\ - \frac{\Delta^*_{\mathbf{k}}(T)}{w+\xi_{\mathbf{k}}}2\pi\mathrm{i}n_F(E_{\mathbf{k}},T)\Big(|u_{\mathbf{k}}|^2\delta(w-E_{\mathbf{k}}) - |v_{\mathbf{k}}|^2\delta(w+E_{\mathbf{k}})\Big). \qquad \text{(A.10)}$$

The derivation of the retarded, advanced, lesser and greater Green's functions for superconductors in equilibrium is straightforward and follows directly from the expression of the time ordered Green's function, by shifting both poles to the lower complex half-space. We find

$$G^R_{\mathbf{k}}(w) = \frac{|u_{\mathbf{k}}|^2}{w-E_{\mathbf{k}}+\mathrm{i}0^+} + \frac{|v_{\mathbf{k}}|^2}{w+E_{\mathbf{k}}+\mathrm{i}0^+},$$

$$G^A_{\mathbf{k}}(w) = \frac{|u_{\mathbf{k}}|^2}{w-E_{\mathbf{k}}-\mathrm{i}0^+} + \frac{|v_{\mathbf{k}}|^2}{w+E_{\mathbf{k}}-\mathrm{i}0^+}. \qquad \text{(A.11)}$$

From these three Green's functions we obtain the lesser and greater Green's function:

$$G^<_{\mathbf{k}}(w) = G^{\mathrm{T}}_{\mathbf{k}}(w) - G^R_{\mathbf{k}}(w) = 2\pi\mathrm{i}\,|v_{\mathbf{k}}|^2\delta(w+E_{\mathbf{k}}), \\ G^>_{\mathbf{k}}(w) = G^{\mathrm{T}}_{\mathbf{k}}(w) - G^A_{\mathbf{k}}(w) = -2\pi\mathrm{i}\,|u_{\mathbf{k}}|^2\delta(w-E_{\mathbf{k}}). \qquad \text{(A.12)}$$

By the same procedure we can derive the anomalous Green's functions:

$$\tilde{F}^{\mathrm{T}}_{\mathbf{k}}(w) = \frac{-2E_{\mathbf{k}}u_{\mathbf{k}}v^*_{\mathbf{k}}}{(w-E_{\mathbf{k}}+\mathrm{i}0^+)(w+E_{\mathbf{k}}-\mathrm{i}0^+)}, \\ \tilde{F}^R_{\mathbf{k}}(w) = \frac{-2E_{\mathbf{k}}u_{\mathbf{k}}v^*_{\mathbf{k}}}{(w-E_{\mathbf{k}}+\mathrm{i}0^+)(w+E_{\mathbf{k}}+\mathrm{i}0^+)}, \\ \tilde{F}^A_{\mathbf{k}}(w) = \frac{-2E_{\mathbf{k}}u_{\mathbf{k}}v^*_{\mathbf{k}}}{(w-E_{\mathbf{k}}-\mathrm{i}0^+)(w+E_{\mathbf{k}}-\mathrm{i}0^+)},$$

$$\tilde{F}^<_{\mathbf{k}}(w) = 2\pi\mathrm{i}\,u_{\mathbf{k}}v^*_{\mathbf{k}}\delta(w-E_{\mathbf{k}}), \\ \tilde{F}^>_{\mathbf{k}}(w) = 2\pi\mathrm{i}\,u_{\mathbf{k}}v^*_{\mathbf{k}}\delta(w+E_{\mathbf{k}}). \qquad \text{(A.13)}$$

## A.2. Keldysh-Schwinger formalism

Neither the $T=0$ nor the Matsubara formalism can describe non-equilibrium physics. To see that we consider an external potential, which depends on time. Such a perturbation pumps energy into or sucks energy out of the system. Therefore the state at $t\to\infty$ is generally qualitatively different from the initial state, regardless whether the perturbation is turned off after a while or not. Linear response theory is an option to describe such non-equilibrium physics, but only in linear order of perturbation theory [Zag98]. In 1965 Keldysh introduced what he called "A graph technique analogous to the usual Feynman technique in field theory [...] for calculating Green's functions for particles in a statistical system which under the action of an external field deviates to any arbitrary extent from

the state of thermodynamic equilibrium." [Kel65]. With this technique we can evaluate arbitrary non-equilibrium situations at both zero and finite temperature. The power of the Keldysh technique is that it is topological equivalent to the usual zero temperature and finite temperature equilibrium formalisms. This means that the structure of all equations and therefore the Feynman diagrams are equivalent. The core idea of the Keldysh formalism is to promote all integrations over the time axis to integrations over a time contour which starts a certain point in time $t_0$ where the system is noninteracting and in equilibrium. Then it goes sufficiently into the future and then returns to the very same point it started from. By sufficiently we mean past all times of interest. If initial conditions are not important the starting point can be sent to the infinite past. Assuming a

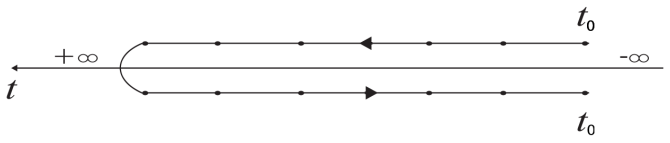


Figure A.1.: Keldysh contour slightly altered from [KL09]

general Hamiltonian $\mathcal{H} = H + V_{\text{ex}} = H_0 + H_{\text{int}} + V_{\text{ex}}$ with interaction $H_{\text{int}}$ and an external perturbation $V_{\text{ex}}$, the equilibrium statistical operator $\rho$ at the initial time $t_0$ is given by

$$\rho(t_0) = \frac{\mathrm{e}^{-\beta H_0}}{\mathrm{Tr}(\mathrm{e}^{-\beta H_0})}. \tag{A.14}$$

It's time evolution can be described by a unitary operator where T denotes the time ordering operator:

$$\rho(t > t_0) = U(t, t_0)\rho(t_0)U^\dagger(t, t_0), \qquad U(t, t') = \mathrm{T}\exp\left(-\mathrm{i}\int_{t'}^{t} \mathrm{d}\tilde{t}\,\mathcal{H}(\tilde{t})\right). \tag{A.15}$$

In the following we denote the Heisenberg picture with a subindex $\mathcal{H}$ and the interaction picture - which is the Heisenberg picture with respect to $H_0$ by subindex $H_0$. Further we choose the point where Heisenberg, Schrödinger and the interaction picture coincide to be $t_0$. Now we can express average values of operators by

$$\langle A\rangle(t) = \mathrm{Tr}(\rho(t)A_S) = \mathrm{Tr}(\rho(t_0)A_{\mathcal{H}}(t)). \tag{A.16}$$

It can be shown that an analogous expression of the conversion between Heisenberg and interaction picture as in the equilibrium situation is given by

$$O_{\mathcal{H}}(t) = \mathrm{T}_C\left[\exp\left(-\mathrm{i}\int_C \mathrm{d}s\,(H_{\text{int}} + V_{\text{ex}})_{H_0}(s)\right) O_{H_0}(t)\right], \tag{A.17}$$

where $T_C$ denote time order along the contour. For a proof of the relation shown above we refer for example to [Ram07]. The Green's function generalizes to

$$\begin{aligned} G_C(1,1') &= -\mathrm{i}\langle \mathrm{T}_C(\psi_{\mathcal{H}}(1)\psi^\dagger_{\mathcal{H}}(1'))\rangle = -\mathrm{i}\frac{\mathrm{Tr}\big(\mathrm{e}^{-\beta H}\,\mathrm{T}_C(\psi_{\mathcal{H}}(1)\psi^\dagger_{\mathcal{H}}(1'))\big)}{\mathrm{Tr}(\mathrm{e}^{-\beta H})} \\ &= -\mathrm{i}\frac{\mathrm{Tr}\big(\mathrm{e}^{-\beta H}\mathrm{T}_C\left(\exp\left[-\mathrm{i}\int_C \mathrm{d}s\,(H_{\text{int}} + V_{\text{ex}})_{H_0}(s)\right](\psi_{H_0}(1)\psi^\dagger_{H_0}(1'))\right)\big)}{\mathrm{Tr}(\mathrm{e}^{-\beta H})}, \end{aligned} \tag{A.18}$$

where 1 is a set of quantum numbers and time $t$. From this expression of the Green's function the topological equivalence to the equilibrium formalism is obvious. If we are not interested in transient phenomena or physics on times scales as short as the collision time,

which are due to interaction, we can sent $t_0$ to minus infinity and the statistical operator reduces to the free, unperturbed version. For a detailed discussion see for example [Ram07] page 91ff. The Green's function then simplifies to

$$G_C(1,1') = -\mathrm{i}\mathrm{Tr}\big(\mathrm{e}^{-\beta H_0}\mathrm{T}_C\left(\exp\left[-\mathrm{i}\int_C \mathrm{d}s\,(H_{\mathrm{int}}+V_{\mathrm{ex}})_{H_0}(s)\right](\psi_{H_0}(1)\psi^\dagger_{H_0}(1'))\right). \quad \text{(A.19)}$$

In this expression all the weighting factors are quadratic in the fields. Now we can employ straightforward perturbation theory and use Wick's theorem to break strings of operators down to statistical averages over pairs of operators, averaged over the free system (Gaussian products). This leads to Dyson equations that are structurally equivalent to the equilibrium case. However, the two Dyson equations

$$\begin{aligned} G &= G_0 + G_0 \otimes \Pi \otimes G, \\ G &= G_0 + G \otimes \Pi \otimes G_0, \end{aligned} \quad \text{(A.20)}$$

which are equivalent in the equilibrium case aren't equivalent in the non-equilibrium case. From their difference we can derive the quantum kinetic equation. In principle this is all that we need to describe non-equilibrium systems. However, often it is desirable to use real time instead of complex time to allow for physical insight. We can achieve this by splitting the contour integral into a forward and a backward time integral. Since the operators can lie either on the forward or on the backward contour we have to introduce so called Keldysh indices that label the time arguments. The index 1 stands for operators on the forward part of the time contour and 2 for operators on the backward part of the contour. The natural way to write Keldysh Green's functions in the real time formalism is therefore a two by two matrix structure. Hence, summations over Keldysh indices naturally translates into matrix multiplications. The minus signs in the second row of the Green's function matrix

$$G_C(s,s') \to \underline{G}(t,t') \equiv \begin{pmatrix} G_{11}(t,t') & G_{12}(t,t') \\ -G_{21}(t,t') & -G_{22}(t,t') \end{pmatrix} \quad \text{(A.21)}$$

account for the minus sign associated with the backwards contour. With this convention the structure of the Dyson equations

$$\begin{aligned} \underline{\underline{G}} &= \underline{\underline{G_0}} + \underline{\underline{G_0}}\,\underline{\underline{\Pi}}\,\underline{\underline{G}}, \\ \underline{\underline{G}} &= \underline{\underline{G_0}} + \underline{\underline{G}}\,\underline{\underline{\Pi}}\,\underline{\underline{G_0}}, \end{aligned} \quad \text{(A.22)}$$

remains unaltered. Note that each matrix multiplication implies a convolution over the time and space variables. In the matrix structure $G_{ij}$ the line index i refers to the first and the column index j to the second time argument. The usual names related with these matrix elements are time-ordered, anti-time-ordered, lesser and greater Green's function

$$\begin{aligned} G_{11}(1,1') &= G^{\mathrm{T}}(1,1') = -\mathrm{i}\langle \mathrm{T}\psi(1)\psi^\dagger(1')\rangle, \\ G_{21}(1,1') &= G^{>}(1,1') = -\mathrm{i}\langle \psi(1)\psi^\dagger(1')\rangle, \\ G_{12}(1,1') &= G^{<}(1,1') = \pm\mathrm{i}\langle \psi^\dagger(1')\psi(1)\rangle, \\ G_{22}(1,1') &= G^{\tilde{\mathrm{T}}}(1,1') = -\mathrm{i}\langle \tilde{\mathrm{T}}\psi(1)\psi^\dagger(1')\rangle. \end{aligned} \quad \text{(A.23)}$$

Here, the upper signs are for fermions and the lower signs for bosons. Since matrices do in general not commute, it is clear the the two Dyson equations are in general not equivalent. Often it is convenient to rotate the above representation in Keldysh space by $\pi/4$, such that it can be represented by the more intuitive retarded, advanced and one new, the so

called Keldysh Green's function $G^K$. This representation is sometimes called the RAK or real representation

$$G^{\mathrm{RAK}} \equiv U\underline{\underline{G}}U^\dagger, \qquad G^{\mathrm{RAK}} = \begin{pmatrix} G^R & G^K \\ 0 & G^A \end{pmatrix}, \qquad U \equiv \frac{1}{\sqrt{2}}\begin{pmatrix} 1 & -1 \\ 1 & 1 \end{pmatrix}. \tag{A.24}$$

Since the retarded and the advanced Green's function do not contain any information about the statistics, it follows that all information related to non-equilibrium must be encoded in the Keldysh Green's function

$$\begin{aligned} G^R(1,2) &= G^{\mathrm{T}}(1,2) - G^<(1,2) = G^>(1,2) - G^{\tilde{\mathrm{T}}}(1,2), \\ G^A(1,2) &= G^{\mathrm{T}}(1,2) - G^>(1,2) = G^<(1,2) - G^{\tilde{\mathrm{T}}}(1,2), \\ G^K(1,2) &= G^<(1,2) + G^>(1,2) = G^{\mathrm{T}}(1,2) + G^{\tilde{\mathrm{T}}}(1,2). \end{aligned} \tag{A.25}$$

Here R stands for retarded, A for advanced and K for Keldysh. This Keldysh Green's function contains all information about the non equilibrium. In the rotated Keldysh space the Dyson equations has the same structure:

$$\begin{aligned} G^{\mathrm{RAK}} &= g^{\mathrm{RAK}}\Pi^{\mathrm{RAK}}G^{\mathrm{RAK}}, \\ G^{\mathrm{RAK}} &= G^{\mathrm{RAK}}\Pi^{\mathrm{RAK}}g^{\mathrm{RAK}}. \end{aligned} \tag{A.26}$$

As before each matrix multiplication implies a convolution over the time and space variables. A nice property about the RAK representation is that all matrices are in triangular shape:

$$\Pi^{\mathrm{RAK}} = \begin{pmatrix} \Pi^R & \Pi^K \\ 0 & \Pi^A \end{pmatrix}. \tag{A.27}$$

This is inherited by the self energy matrix. Another advantage is the particular simple form of the Dyson equations for the retarded and advanced Green's function

$$\begin{aligned} G^R &= G_0^R + G_0^R\Pi^R G^R, \\ G^A &= G_0^A + G_0^A\Pi^A G^A, \\ G^K &= G_0^K + G_0^R\Pi^R G^K + G_0^R\Pi^K G^A + G_0^K\Pi^A G^A. \end{aligned} \tag{A.28}$$

In the case of a stationary homogeneous system which can be described by a non-equilibrium distribution function, the free Green's functions are given by the following equations. The common abbreviation to denote the infinitesimal imaginary part of the propagators is $0^+ \equiv \lim_{\eta\to 0^+}\eta$. The delta distributions have also to be interpreted in this fashion $\pi\delta(x) = \lim_{\eta\to 0^+}\eta/(x^2+\eta^2)$. As a simplification to the eye we denote the free Green's functions by lower-case letters $g_{\mathbf{k}}$. Below we show a collection:

$$\begin{aligned} g_{\mathbf{k}}^{\mathrm{T}}(w) &= \frac{1}{w-(\epsilon_{\mathbf{k}}-\mu)+\mathrm{i}0^+} \pm 2\pi\mathrm{i}n_{\mathbf{k}}\delta(w-(\epsilon_{\mathbf{k}}-\mu)), \\ g_{\mathbf{k}}^<(w) &= \pm 2\pi\mathrm{i}n_{\mathbf{k}}\delta(w-(\epsilon_{\mathbf{k}}-\mu)), \\ g_{\mathbf{k}}^>(w) &= -2\pi\mathrm{i}(1\mp n_{\mathbf{k}})\delta(w-(\epsilon_{\mathbf{k}}-\mu)), \\ g_{\mathbf{k}}^{\tilde{\mathrm{T}}}(w) &= -\frac{1}{w-(\epsilon_{\mathbf{k}}-\mu)-\mathrm{i}0^+} \pm 2\pi\mathrm{i}n_{\mathbf{k}}\delta(w-(\epsilon_{\mathbf{k}}-\mu)), \\ g_{\mathbf{k}}^R(w) &= \frac{1}{w-(\epsilon_{\mathbf{k}}-\mu)+\mathrm{i}0^+}, \\ g_{\mathbf{k}}^A(w) &= \frac{1}{w-(\epsilon_{\mathbf{k}}-\mu)-\mathrm{i}0^+}, \\ g_{\mathbf{k}}^K(w) &= -2\pi\mathrm{i}(1\mp 2n_{\mathbf{k}})\delta(w-(\epsilon_{\mathbf{k}}-\mu)). \end{aligned} \tag{A.29}$$

## A.3. Nambu and Keldysh formalisms combined

The Nambu and the Keldysh formalism can be combined to describe non-equilibrium superconducting systems. This is done by a tensorial product between the two matrix spaces. Namely each component of the Keldysh space becomes a two by two matrix. The total dimension of the Green's function is therefore 4x4. We choose the book by Jorgen Rammer [Ram07] p225-230 to provide the formal basis. In all equations convolution that goes along with matrix multiplications is implicitly assumed:

$$\hat{G}_c(1,1') = -\mathrm{i}\hat{\tau}_3\langle \mathrm{T}_c\, \hat{\Psi}(1)\hat{\Psi}^\dagger(1')\rangle,$$

$$\begin{aligned}
\hat{G}^{\mathrm{T}}(1,1') &= -\mathrm{i}\hat{\tau}_3\langle \mathrm{T}\, \hat{\Psi}(1)\hat{\Psi}^\dagger(1')\rangle,\\
\hat{G}^{<}(1,1') &= +\mathrm{i}\hat{\tau}_3\langle \hat{\Psi}^\dagger(1')\hat{\Psi}(1)\rangle,\\
\hat{G}^{>}(1,1') &= -\mathrm{i}\hat{\tau}_3\langle \hat{\Psi}(1)\hat{\Psi}^\dagger(1')\rangle,\\
\hat{G}^{\tilde{\mathrm{T}}}(1,1') &= -\mathrm{i}\hat{\tau}_3\langle \tilde{\mathrm{T}}\, \hat{\Psi}(1)\hat{\Psi}^\dagger(1')\rangle,
\end{aligned}$$

$$\begin{aligned}
\hat{G}^{R}(1,1') &= -\mathrm{i}\theta(t-t')\hat{\tau}_3\Big\langle \Big\{ \hat{\Psi}(1), \hat{\Psi}^\dagger(1') \Big\} \Big\rangle,\\
\hat{G}^{A}(1,1') &= +\mathrm{i}\theta(t'-t)\hat{\tau}_3\Big\langle \Big\{ \hat{\Psi}(1), \hat{\Psi}^\dagger(1') \Big\} \Big\rangle,\\
\hat{G}^{K}(1,1') &= -\mathrm{i}\hat{\tau}_3\Big\langle \Big[ \hat{\Psi}(1), \hat{\Psi}^\dagger(1') \Big] \Big\rangle.
\end{aligned} \tag{A.30}$$

Here $\hat{\tau}_3$ denotes the third Pauli matrix acting on the Nambu space. Introducing the Pauli matrix leads to Dyson equations with the same structure as in the non-superconducting case:

$$\begin{aligned}
(\underline{\underline{\hat{G}_0}}^{-1}\, \underline{\underline{\hat{G}}})(1,1') &= \delta(1-1') + (\underline{\underline{\hat{\Sigma}}}\, \underline{\underline{\hat{G}}})(1,1'),\\
(\underline{\underline{\hat{G}}}\, \underline{\underline{\hat{G}_0}}^{-1})(1,1') &= \delta(1-1') + (\underline{\underline{\hat{\Sigma}}}\, \underline{\underline{\hat{G}}})(1,1'),
\end{aligned}$$

$$\begin{aligned}
(G_0^{-1}\, G^{R/A})(1,1') &= \delta(1-1') + (\Sigma^{R/A}\, G^{R/A})(1,1'),\\
(G_0^{-1}\, G^{K})(1,1') &= (\Sigma^{R}\, G^{K})(1,1') + (\Sigma^{K}\, G^{A})(1,1').
\end{aligned} \tag{A.31}$$

The pairing interaction leads to off-diagonal elements in the Nambu space:

$$\hat{H}_0 = \begin{pmatrix} H_0 & 0 \\ 0 & H_0^* \end{pmatrix}, \qquad \hat{\Sigma}_{\mathrm{BCS}} = \begin{pmatrix} 0 & -\Delta \\ \Delta^* & 0 \end{pmatrix}. \tag{A.32}$$

In a homogeneous system which is in a stationary state the derivation of the free Green's functions is straightforward. First we calculate the equations of motion for the Bogoliubon creation and destruction operators $\gamma^\dagger$ and $\gamma$:

$$\begin{aligned}
\dot{\gamma}_{\mathbf{k}\uparrow}(t) &= \mathrm{i}[H_{\mathrm{BCS}}, \gamma_{\mathbf{k}\uparrow}](t) = -\mathrm{i}E_{\mathbf{k}}(\gamma_{\mathbf{k}\uparrow})_S,\\
\dot{\gamma}^\dagger_{\mathbf{k}\uparrow}(t) &= \mathrm{i}[H_{\mathrm{BCS}}, \gamma^\dagger_{\mathbf{k}\uparrow}](t) = \mathrm{i}E_{\mathbf{k}}(\gamma^\dagger_{\mathbf{k}\uparrow})_S,
\end{aligned}$$

$$\begin{aligned}
\gamma_{\mathbf{k}\uparrow}(t) &= \mathrm{e}^{-\mathrm{i}E_{\mathbf{k}}t}(\gamma_{\mathbf{k}\uparrow})_S,\\
\gamma^\dagger_{\mathbf{k}\uparrow}(t) &= \mathrm{e}^{\mathrm{i}E_{\mathbf{k}}t}(\gamma^\dagger_{\mathbf{k}\uparrow})_S.
\end{aligned} \tag{A.33}$$

The time where the Heisenberg and the Schrödinger picture coincide shall be $t = 0$. With this and the Bogoliubov transformation we obtain all the free Green's functions by equation

of motion technique:

$$\begin{aligned}
\mathrm{i}g^{\mathrm{T}}_{\mathbf{k}\uparrow\uparrow}(t) &= \langle \mathrm{T}c_{\mathbf{k}\uparrow}(t)c^{\dagger}_{\mathbf{k}\uparrow}(0)\rangle, \\
&= \langle \mathrm{T}(u_{\mathbf{k}}\gamma_{\mathbf{k}\uparrow}(t) - v_{\mathbf{k}}\gamma^{\dagger}_{-\mathbf{k}\downarrow}(t))(u^{*}_{\mathbf{k}}\gamma^{\dagger}_{\mathbf{k}\uparrow}(0) - v^{*}_{\mathbf{k}}\gamma_{-\mathbf{k}\downarrow}(0))\rangle, \\
&= \theta(t)\Big(|u_{\mathbf{k}}|^2\mathrm{e}^{-\mathrm{i}E_{\mathbf{k}}t}(1-n_{\mathbf{k}}) + |v_{\mathbf{k}}|^2\mathrm{e}^{\mathrm{i}E_{\mathbf{k}}t}n_{-\mathbf{k}}\Big) \\
&\quad - \theta(-t)\Big(|u_{\mathbf{k}}|^2\mathrm{e}^{-\mathrm{i}E_{\mathbf{k}}t}n_{\mathbf{k}} + |v_{\mathbf{k}}|^2\mathrm{e}^{\mathrm{i}E_{\mathbf{k}}t}(1-n_{-\mathbf{k}})\Big)
\end{aligned}$$

$$\begin{aligned}
g^{\mathrm{T}}_{\mathbf{k}\uparrow\uparrow}(w) &= |u_{\mathbf{k}}|^2\left\{\frac{n_{\mathbf{k}\uparrow}}{w - E_{\mathbf{k}} - \mathrm{i}0^{+}} + \frac{1-n_{\mathbf{k}\uparrow}}{w - E_{\mathbf{k}} + \mathrm{i}0^{+}}\right\} \\
&\quad + |v_{\mathbf{k}}|^2\left\{\frac{n_{-\mathbf{k}\downarrow}}{w + E_{\mathbf{k}} + \mathrm{i}0^{+}} + \frac{1-n_{-\mathbf{k}\downarrow}}{w + E_{\mathbf{k}} - \mathrm{i}0^{+}}\right\}, \\
\tilde{g}^{\mathrm{T}}_{\mathbf{k}\downarrow\downarrow}(w) &= |u_{\mathbf{k}}|^2\left\{\frac{n_{-\mathbf{k}\downarrow}}{w + E_{\mathbf{k}} + \mathrm{i}0^{+}} + \frac{1-n_{-\mathbf{k}\downarrow}}{w + E_{\mathbf{k}} - \mathrm{i}0^{+}}\right\} \\
&\quad + |v_{\mathbf{k}}|^2\left\{\frac{n_{\mathbf{k}\uparrow}}{w - E_{\mathbf{k}} - \mathrm{i}0^{+}} + \frac{1-n_{\mathbf{k}\uparrow}}{w - E_{\mathbf{k}} + \mathrm{i}0^{+}}\right\}.
\end{aligned} \tag{A.34}$$

Form this two equations we see that the particle and hole Green's functions only differ by an interchanging of $|u_{\mathbf{k}}|^2$ and $|v_{\mathbf{k}}|^2$. By the same method we obtain the retarded and the advanced Green's function:

$$\begin{aligned}
g^{R}_{\mathbf{k}\uparrow\uparrow}(w) &= \frac{|u_{\mathbf{k}}|^2}{w - E_{\mathbf{k}} + \mathrm{i}0^{+}} + \frac{|v_{\mathbf{k}}|^2}{w + E_{\mathbf{k}} + \mathrm{i}0^{+}}, \\
g^{A}_{\mathbf{k}\uparrow\uparrow}(w) &= \frac{|u_{\mathbf{k}}|^2}{w - E_{\mathbf{k}} - \mathrm{i}0^{+}} + \frac{|v_{\mathbf{k}}|^2}{w + E_{\mathbf{k}} - \mathrm{i}0^{+}}.
\end{aligned} \tag{A.35}$$

There are several ways to derive the lesser and greater Green's functions. One is analogous to the calculations shown above. The most elegant way is probably to extract them directly from the time ordered Green's function by spectral decomposition:

$$G^{\mathrm{T}}_{\mathbf{k}}(w) = \int_{-\infty}^{\infty}\frac{\mathrm{d}w}{2\pi\mathrm{i}}\left\{\frac{G^{<}_{\mathbf{k}}(w')}{w - w' - \mathrm{i}0^{+}} - \frac{G^{>}_{\mathbf{k}}(w')}{w - w' + \mathrm{i}0^{+}}\right\}. \tag{A.36}$$

This idea is from [GZ99] p86f.. Comparison gives the desired functions:

$$\begin{aligned}
g^{<}_{\mathbf{k}}(w) &= +2\pi\mathrm{i}\Big(|u_{\mathbf{k}}|^2 n_{\mathbf{k}}\delta(w - E_{\mathbf{k}}), \\
&\quad + |v_{\mathbf{k}}|^2(1-n_{-\mathbf{k}})\delta(w + E_{\mathbf{k}})\Big), \\
g^{>}_{\mathbf{k}}(w) &= -2\pi\mathrm{i}\Big(|u_{\mathbf{k}}|^2(1-n_{\mathbf{k}})\delta(w - E_{\mathbf{k}}) + |v_{\mathbf{k}}|^2 n_{-\mathbf{k}}\delta(w + E_{\mathbf{k}})\Big).
\end{aligned} \tag{A.37}$$

To conclude, we state the anomalous Green's functions:

$$\begin{aligned}
f^{\mathrm{T}}_{\mathbf{k}}(w) &= u_{\mathbf{k}}v_{\mathbf{k}}\left\{\frac{(1-n_{\mathbf{k}})}{w - E_{\mathbf{k}} + \mathrm{i}0^{+}} - \frac{(n_{-\mathbf{k}})}{w + E_{\mathbf{k}} + \mathrm{i}0^{+}} + \frac{n_{\mathbf{k}}}{w - E_{\mathbf{k}} - \mathrm{i}0^{+}} - \frac{(1-n_{-\mathbf{k}})}{w + E_{\mathbf{k}} - \mathrm{i}0^{+}}\right\}, \\
\tilde{f}^{\mathrm{T}}_{\mathbf{k}}(w) &= u^{*}_{\mathbf{k}}v^{*}_{\mathbf{k}}\left\{\frac{(1-n_{\mathbf{k}})}{w - E_{\mathbf{k}} + \mathrm{i}0^{+}} - \frac{(n_{-\mathbf{k}})}{w + E_{\mathbf{k}} + \mathrm{i}0^{+}} + \frac{n_{\mathbf{k}}}{w - E_{\mathbf{k}} - \mathrm{i}0^{+}} - \frac{(1-n_{-\mathbf{k}})}{w + E_{\mathbf{k}} - \mathrm{i}0^{+}}\right\},
\end{aligned}$$

$$
\begin{aligned}
f^R_{\mathbf{k}}(w) &= u_{\mathbf{k}} v_{\mathbf{k}} \left\{ \frac{1}{w - E_{\mathbf{k}} + \mathrm{i}0^+} - \frac{1}{w + E_{\mathbf{k}} + \mathrm{i}0^+} \right\}, \\
\tilde{f}^R_{\mathbf{k}}(w) &= u^*_{\mathbf{k}} v^*_{\mathbf{k}} \left\{ \frac{1}{w - E_{\mathbf{k}} + \mathrm{i}0^+} - \frac{1}{w + E_{\mathbf{k}} + \mathrm{i}0^+} \right\}, \\
f^A_{\mathbf{k}}(w) &= u_{\mathbf{k}} v_{\mathbf{k}} \left\{ \frac{1}{w - E_{\mathbf{k}} - \mathrm{i}0^+} - \frac{1}{w + E_{\mathbf{k}} - \mathrm{i}0^+} \right\}, \\
\tilde{f}^A_{\mathbf{k}}(w) &= u^*_{\mathbf{k}} v^*_{\mathbf{k}} \left\{ \frac{1}{w - E_{\mathbf{k}} - \mathrm{i}0^+} - \frac{1}{w + E_{\mathbf{k}} - \mathrm{i}0^+} \right\}, \\
f^<_{\mathbf{k}}(w) &= 2\pi \mathrm{i}\, u_{\mathbf{k}} v_{\mathbf{k}} \Big\{ n_{\mathbf{k}} \delta(w - E_{\mathbf{k}}) - (1 - n_{\mathbf{k}}) \delta(w + E_{\mathbf{k}}) \Big\}, \\
\tilde{f}^<_{\mathbf{k}}(w) &= 2\pi \mathrm{i}\, u^*_{\mathbf{k}} v^*_{\mathbf{k}} \Big\{ n_{\mathbf{k}} \delta(w - E_{\mathbf{k}}) - (1 - n_{-\mathbf{k}}) \delta(w + E_{\mathbf{k}}) \Big\}, \\
f^>_{\mathbf{k}}(w) &= -2\pi \mathrm{i}\, u_{\mathbf{k}} v_{\mathbf{k}} \Big\{ (1 - n_{\mathbf{k}}) \delta(w - E_{\mathbf{k}}) - n_{-\mathbf{k}} \delta(w + E_{\mathbf{k}}) \Big\}, \\
\tilde{f}^>_{\mathbf{k}}(w) &= -2\pi \mathrm{i}\, u^*_{\mathbf{k}} v^*_{\mathbf{k}} \Big\{ (1 - n_{\mathbf{k}}) \delta(w - E_{\mathbf{k}}) - n_{-\mathbf{k}} \delta(w + E_{\mathbf{k}}) \Big\}.
\end{aligned}
\tag{A.38}
$$

# B. Luminescence

## B.1. Dyson Equations

The general Dyson equations [Mah90] are

$$\begin{aligned} G^< &= \Big(1 + G^R\Pi^R\Big)g^<\Big(1 + \Pi^A G^A\Big) + G^R\Pi^< G^A, \\ G^> &= \Big(1 + G^R\Pi^R\Big)g^>\Big(1 + \Pi^A G^A\Big) + G^R\Pi^> G^A, \\ G^A &= g^A\Big(1 + \Pi^A G^A\Big), \\ G^R &= g^R\Big(1 + \Pi^R G^R\Big). \end{aligned} \tag{B.1}$$

In the case of stationarity and the assumptions that the system could be described by a set of distribution functions at some point in the past, the Dyson equations simplify to

$$\begin{aligned} G^A &= \frac{1}{(g^A)^{-1} - \Pi^A}, \\ G^R &= \frac{1}{(g^R)^{-1} - \Pi^R}, \\ G^< &= g^< + G^R\Pi^< G^A, \\ G^> &= g^> + G^R\Pi^> G^A. \end{aligned} \tag{B.2}$$

## B.2. Photon propagator

In this subsection we derive the photon propagator in detail. In a normal light emitting diode only processes with an equal number of fermion creation and destruction operators contribute. They are proportional to $|g|^{2n}$. In a superconductor-normal conductor mixed phase also contributions proportional to $g^{2m}|g|^{2n}$ would contribute but are not discussed here. We also exploit that all diagrams that are not fully connected chancel in the Keldysh formalism. We start with the very general perturbative expansion of the photon propagator

$$D_{qq'}(t_1, t_2) \equiv -\mathrm{i}\sum_{n=0}\frac{(-\mathrm{i})^n}{n!}\int_C \mathrm{d}s_1 ... \mathrm{d}s_1 \left\langle \hat{T}_c\, H^{\mathrm{int}}_{H_0}(s_1)...H^{\mathrm{int}}_{H_0}(s_n) b_q(t_1) b^\dagger_{q'}(t_2)\right\rangle. \tag{B.3}$$

The leading contribution in the coupling constant is

$$\begin{aligned} D^{(1)}_{qq'}(t_1, t_2) &= \frac{\mathrm{i}}{2}\int_C \mathrm{d}s_1 \mathrm{d}s_2 \left\langle \hat{T}_c\, H^{\mathrm{int}}_{H_0}(s_1) H^{\mathrm{int}}_{H_0}(s_2) b_q(t_1) b^\dagger_{q'}(t_2)\right\rangle \\ &= \frac{\mathrm{i}}{2}\int_C \mathrm{d}s_1 \mathrm{d}s_2 \Bigg\langle \hat{T}_c \sum_{k_1, q_1}\Big(g c^\dagger_{k_1}(s_1) v_{k_1-q_1}(s_1) b_{q_1}(s_1) + g^* v^\dagger_{k_1-q_1}(s_1) c_{k_1}(s_1) b^\dagger_{q_1}(s_1)\Big)\times \\ &\qquad \times \sum_{k_2, q_2}\Big(g c^\dagger_{k_2}(s_2) v_{k_2-q_2}(s_2) b_{q_2}(s_2) + g^* v^\dagger_{k_2-q_2}(s_2) c_{k_2}(s_2) b^\dagger_{q_2}(s_2)\Big) b_q(t_1) b^\dagger_{q'}(t_2)\Bigg\rangle. \end{aligned}$$

Using Wick's theorem of contraction we find

$$D^{(1)}_{qq'}(t_1, t_2) = -\mathrm{i}|g|^2 \sum_k \int_C \mathrm{d}s_{1,2}\, d_q(t_1, s_1) g^c_k(s_1, s_2) g^v_{k-q}(s_2, s_1) d_q(s_2, t_2)\delta_{qq'}. \tag{B.4}$$

Next we go to real time, assume stationarity, Fourier transform and find

$$\begin{aligned} D_q^{R,(1)}(t,t') &= \int \mathrm{d}t_{1,2}\, d_q^R(t,t_1)\Pi_q^{R,(1)}(t_1,t_2)d_q^R(t_2,t'), \\ D_q^{R,(1)}(w) &= d_q^R(w)\Pi_q^{R,(1)}(w)d_q^R(w) \\ &= |g|^2\Big(\frac{1}{w-w_q+\mathrm{i}0^+}\Big)^2\sum_k \frac{n_{v,k-q}-n_{c,k}}{w+\epsilon_{v,k-q}-\epsilon_{c,k}+\mathrm{i}0^+}. \end{aligned} \tag{B.5}$$

The randome phase corrected photon propagator is just one step away. We preform the geometric row and find

$$D_q^R(w) = \frac{1}{w-w_q+\mathrm{i}0^+ - |g|^2\sum_k \frac{n_{v,k-q}-n_{c,k}}{w-\epsilon_{c,k}+\epsilon_{v,k-q}+2\mathrm{i}0^+}} \equiv \frac{1}{w-w_q-\Sigma_{ph}^R-\mathrm{i}\Gamma_{ph}^R}. \tag{B.6}$$

In order to derive the luminescence we need the imaginary part

$$\mathrm{Im}\big(D_q^R(w)\big) = \frac{\Gamma_{ph}^R}{(w-w_q-\Sigma_{ph}^R)^2+(\Gamma_{ph}^R)^2}, \tag{B.7}$$

where $\Gamma_{ph}^R$ is

$$\begin{aligned} \Gamma_{ph}^R(w) &= \mathrm{Im}\Big(\sum_k \frac{n_{v,k}-n_{c,k}}{w-\epsilon_{c,k}+\epsilon_{v,k}+2\mathrm{i}0^+}\Big) \\ &= -\pi\int \mathrm{d}\epsilon\, \mathcal{N}_F(\epsilon)\Big(n_F(\epsilon_{v,0}-\epsilon-\mu_v)-n_F(\epsilon_{c,0}+\epsilon-\mu_c)\Big)\delta(w-\Delta\epsilon-2\epsilon). \end{aligned} \tag{B.8}$$

## B.3. Photon self energy

We find the first order photon self energy by comparing the first order photon propagator with the the Dyson equation:

$$\begin{aligned} D_q^{(1)}(t_1,t_2) &= -\mathrm{i}|g|^2\sum_{k_1}\int_C \mathrm{d}s_{1,2}\, d_q(t_1,s_1)g_{k_1}^c(s_1,s_2)g_{k_1-q}^v(s_2,s_1)d_q(s_2,t_2) \\ &\equiv \int_C \mathrm{d}s_1\mathrm{d}s_2\; d_q(t_1,s_1)\Pi_{ph,q}^{(1)}(s_1,s_2)d_q(s_2,t_2). \end{aligned} \tag{B.9}$$

The leading order self energy is

$$\Pi_{ph,q}^{(1)}(s_1,s_2) = -\mathrm{i}|g|^2\sum_k g_k^c(s_1,s_2)g_{k-q}^v(s_2,s_1) = \quad . \tag{B.10}$$

The second order photon self energy can be extracted from the second order photon propagator and so forth. Next we going to real time, assume stationarity

$$\Pi_{ph,q,ab}^{(1)}(t_1,t_2) = -\mathrm{i}|g|^2\sum_k g_{k,ab}^c(t_1-t_2)g_{k-q,ba}^v(t_2-t_1) \tag{B.11}$$

and Fourier transform

$$\Pi_{ph,q,ab}^{(1)}(w) = -\mathrm{i}|g|^2\sum_k \int \frac{\mathrm{d}w_1}{2\pi}\; g_{k,ab}^c(w_1)g_{k-q,ba}^v(w_1-w). \tag{B.12}$$

What we are really interested in are the explicit expressions for time ordered, lesser and retarded self energy:

$$\begin{aligned}
\Pi^{(1)}_{ph,q,11}(w) &= -\mathrm{i}|g|^2 \sum_k \int \frac{\mathrm{d}w_1}{2\pi}\; g^c_{k,11}(w_1) g^v_{k-q,11}(w_1 - w) \\
&= -\mathrm{i}|g|^2 \sum_k \int \frac{\mathrm{d}w_1}{2\pi} \left( \frac{1}{w_1 - \epsilon_{c,k} + \mathrm{i}0^+} + \frac{n_{c,k}}{w_1 - \epsilon_{c,k} - \mathrm{i}0^+} + \frac{-n_{c,k}}{w_1 - \epsilon_{c,k} + \mathrm{i}0^+} \right) \times \\
&\times \left( \frac{1}{w_1 - w - \epsilon_{v,k-q} + \mathrm{i}0^+} + \frac{n_{v,k-q}}{w_1 - w - \epsilon_{v,k-q} - \mathrm{i}0^+} + \frac{-n_{v,k-q}}{w_1 - w - \epsilon_{v,k-q} + \mathrm{i}0^+} \right) \\
&= -|g|^2 \sum_k \left( \frac{n_{v,k-q}(1 - n_{c,k})}{w - \epsilon_{c,k} + \epsilon_{v,k-q} + 2\mathrm{i}0^+} + \frac{-n_{c,k}(1 - n_{v,k-q})}{w - \epsilon_{c,k} + \epsilon_{v,k-q} - 2\mathrm{i}0^+} \right),
\end{aligned}$$

$$\begin{aligned}
\Pi^{(1)}_{ph,q,12}(w) &= -\mathrm{i}|g|^2 \sum_k \int \frac{\mathrm{d}w_1}{2\pi}\; g^c_{k,12}(w_1) g^v_{k-q,21}(w_1 - w) \\
&= -\mathrm{i}|g|^2 \sum_k \int \frac{\mathrm{d}w_1}{2\pi} \Big( 2\pi \mathrm{i} n_{c,k} \delta(w_1 - \epsilon_{c,k}) \Big) \Big( -2\pi\mathrm{i}(1 - n_{v,k-q}) \delta(w_1 - w - \epsilon_{v,k-q}) \Big) \\
&= -2\pi\mathrm{i}|g|^2 \sum_k n_{c,k}(1 - n_{v,k-q}) \delta(w - \epsilon_{c,k} + \epsilon_{v,k-q}), \\
\Pi^{R(1)}_{ph,q}(w) &= \Pi^{(1)}_{ph,q,11}(w) - \Pi^{(1)}_{ph,q,12}(w) \\
&= -|g|^2 \sum_k \left( \frac{n_{v,k-q}(1 - n_{c,k})}{\epsilon_{c,k} - w - \epsilon_{v,k-q} - \mathrm{i}0^+} + \frac{-n_{c,k}(1 - n_{v,k-q})}{\epsilon_{c,k} - w - \epsilon_{v,k-q} + \mathrm{i}0^+} \right) \\
&\quad + 2\mathrm{i}|g|^2 \sum_k n_{c,k}(1 - n_{v,k-q}) \frac{0^+}{(w + \epsilon_{v,k-q} - \epsilon_{c,k})^2 + (0^+)^2} \\
&= |g|^2 \sum_k \frac{n_{v,k-q} - n_{c,k}}{(w + \epsilon_{v,k-q} - \epsilon_{c,k} + \mathrm{i}0^+)}.
\end{aligned} \tag{B.13}$$

We can even show that the lesser self energy has no higher order corrections to the lesser photon self energy due to our constraint $D^<_q = 0$ of no photons in the system. All we use other than that are the simplified Dyson equations (B.2) and get

$$\begin{aligned}
\Pi^<_q(w) &= -\mathrm{i}|g|^2 \sum_k \int \frac{\mathrm{d}w_1}{2\pi}\, G^<_{c,k}(w_1) G^>_{v,k-q}(w_1 - w), \\
G^<_{c,k}(w) &= G^R_{c,k}(w) \Pi^<_{c,k}(w) G^A_{c,k}(w), \\
G^>_{v,k}(w) &= G^R_{v,k}(w) \Pi^>_{v,k}(w) G^A_{v,k}(w), \\
\Pi^<_{c,k}(w) &= \mathrm{i}|g|^2 \sum_q \int \frac{\mathrm{d}w_1}{2\pi}\, G^<_{v,k-q}(w_1) D^<_q(w - w_1) = 0, \\
\Pi^>_{v,k}(w) &= \mathrm{i}|g|^2 \sum_q \int \frac{\mathrm{d}w_1}{2\pi}\, G^>_{c,k+q}(w_1) D^<_q(w - w_1) = 0, \\
\Rightarrow \Pi^<_q(w) &= -\mathrm{i}|g|^2 \sum_k \int \frac{\mathrm{d}w_1}{2\pi}\, g^<_{c,k}(w_1) g^>_{v,k-q}(w_1 - w) = \Pi^{<(1)}_{ph,q}(w)
\end{aligned} \tag{B.14}$$

## B.4. Electron propagators

The derivation of the electron operators follows the very same procedure as the photon propagator. Therefore, we only state the results:

$$G^{(1)}_{c,k}(t_1,t_2) = \mathrm{i}|g|^2 \sum_q \int_C \mathrm{d}s_1\mathrm{d}s_2\, g_{c,k}(t_1,s_1) g_{v,k-q}(s_1,s_2) d_q(s_1,s_2) g_{c,k}(s_2,t_2),$$
$$G^{(1)}_{v,p}(t_1,t_2) = \mathrm{i}|g|^2 \sum_q \int_C \mathrm{d}s_1\mathrm{d}s_2\, g_{v,p}(t_1,s_1) g_{c,p+q}(s_1,s_2) d_q(s_2,s_1) g_{v,p}(s_2,t_2). \quad \text{(B.15)}$$

# C. Special case: Two level system

## C.1. Luminescence

The detailed steps to arrive at the final result are:

$$
\begin{aligned}
L^{\mathrm{em,RPA+}} &= 2|g|^2\, n_c(1-n_v)\int_0^{\Lambda} \mathrm{d}w_q \mathcal{N}_{ph}(w_q) \frac{\frac{|g|^2}{\Gamma}(\frac{1}{2}-n_v+n_c)}{(\epsilon_c-\epsilon_v-w_q)^2+\left(\frac{|g|^2}{\Gamma}(\frac{1}{2}-n_v+n_c)\right)^2}, \\
&= 2|g|^2\, n_c(1-n_v)\frac{1}{\Delta\epsilon}\int_0^{\Lambda} \mathrm{d}w_q \mathcal{N}_{ph}(w_q) \frac{\frac{\frac{1}{2}-n_v+n_c}{\pi(1-n_v)\,\Delta\epsilon N_{ph}(\Delta\epsilon)}}{\left(1-\frac{w_q}{\Delta\epsilon}\right)^2+\left(\frac{\frac{1}{2}-n_v+n_c}{\pi(1-n_v)\,\Delta\epsilon N_{ph}(\Delta\epsilon)}\right)^2}, \\
&\approx 2|g|^2\, n_c(1-n_v)\mathcal{N}_{ph}(\Delta\epsilon)\int_0^{\frac{\Lambda}{\Delta\epsilon}} \mathrm{d}x \frac{\frac{\frac{1}{2}-n_v+n_c}{\pi(1-n_v)\,\Delta\epsilon N_{ph}(\Delta\epsilon)}}{(1-x)^2+\left(\frac{\frac{1}{2}-n_v+n_c}{\pi(1-n_v)\,\Delta\epsilon N_{ph}(\Delta\epsilon)}\right)^2}, \\
&= 2\pi|g|^2\, n_c(1-n_v)\mathcal{N}_{ph}(\Delta\epsilon)\left[\frac{1}{2}+\frac{1}{\pi}\arctan\left(\pi\,\Delta\epsilon N_{ph}(\Delta\epsilon)\frac{1-n_v}{1-n_v+n_c-\frac{1}{2}}\right)\right]. \qquad \text{(C.1)}
\end{aligned}
$$

## C.2. Photon propagator

In RPA using the already RPA resumed photon self energy we find

$$
\begin{aligned}
D^{\mathrm{RPA+}}(w) &= \frac{1}{(d^R)^{-1}-\Pi_{ph}^{\mathrm{RPA+}}}, \\
&= \frac{1}{w-w_q-|g|^2\left[\frac{1}{w+\tilde{\epsilon}_v-\tilde{\epsilon}_c+\mathrm{i}(\Gamma_c+\Gamma_v)}+\frac{-n_c}{w+\tilde{\epsilon}_v-\epsilon_c+\mathrm{i}\Gamma_v}+\frac{-(1-n_v)}{w+\epsilon_v-\tilde{\epsilon}_c+\mathrm{i}\Gamma_c}\right]}, \\
&\approx \frac{1}{w-w_q-|g|^2\left[\frac{1}{w_q+\epsilon_v-\epsilon_c+2\mathrm{i}\Gamma}+\frac{-1+n_v-n_c}{w_q+\epsilon_v-\epsilon_c+\mathrm{i}\Gamma}\right]}. \qquad \text{(C.2)}
\end{aligned}
$$

## C.3. Photon self energy

The RPA resumed retarded photon self energy that is calculated using RPA resumed electron propagators reads:

$$
\begin{aligned}
\Pi_{ph}^{R,\mathrm{RPA+}}(w) = -\mathrm{i}|g|^2 \int \frac{\mathrm{d}w_1}{2\pi} \Big[ & G_c^{T,\mathrm{RPA}}(w_1)G_v^{T,\mathrm{RPA}}(w_1-w) \\
& - G_c^{<,\mathrm{RPA}}(w_1)G_v^{>,\mathrm{RPA}}(w_1-w)\Big]. \qquad \text{(C.3)}
\end{aligned}
$$

In order to evaluate this expression we use general relations between the various types of Green's functions

$$
\begin{aligned}
G_c^T G_v^T - G_c^< G_v^> &= (G_c^R+G_c^<)(G_v^A+G_v^>) - G_c^< G_v^> \\
&= G_c^R G_v^A + G_c^< G_v^A + G_c^R G_v^> \\
&= G_c^R G_v^A + g_c^< G_v^A + G_c^R g_v^> \qquad \text{(C.4)}
\end{aligned}
$$

to rewrite equation (C.3). The nice feature of this new form is that the lesser conduction electron and the greater valence electron Green's function do not acquire higher order

corrections. The physical reason is the absence of photons. Hence, we find

$$\Pi_{ph}^{R,\mathrm{RPA}+}(w) = -\mathrm{i}|g|^2 \int \frac{\mathrm{d}w_1}{2\pi} \Big[ G_c^{R,\mathrm{RPA}}(w_1) G_v^{A,\mathrm{RPA}}(w_1 - w) + g_c^<(w_1) G_v^{A,\mathrm{RPA}}(w_1 - w) + G_c^{R,\mathrm{RPA}}(w_1) g_v^>(w_1 - w) \Big]. \tag{C.5}$$

For clarity we evaluate the individual contributions step by step:

$$\begin{aligned}
\int \frac{\mathrm{d}w_1}{2\pi}\, G_c^{R,\mathrm{RPA}}(w_1) G_v^{A,\mathrm{RPA}}(w_1 - w) &= \int \frac{\mathrm{d}w_1}{2\pi}\, \frac{1}{w_1 - \tilde{\epsilon}_c + \mathrm{i}\Gamma_c} \frac{1}{w_1 - w - \tilde{\epsilon}_v - \mathrm{i}\Gamma_v} \\
&= \frac{\mathrm{i}}{w + \tilde{\epsilon}_v - \tilde{\epsilon}_c + \mathrm{i}(\Gamma_c + \Gamma_v)},
\end{aligned}$$

$$\begin{aligned}
\int \frac{\mathrm{d}w_1}{2\pi}\, g_c^<(w_1) G_v^{A,\mathrm{RPA}}(w_1 - w) &= \int \frac{\mathrm{d}w_1}{2\pi}\, 2\pi \mathrm{i} n_c \delta(w_1 - \epsilon_c) \frac{1}{w_1 - w - \tilde{\epsilon}_v - \mathrm{i}\Gamma_v} \\
&= \frac{-\mathrm{i}n_c}{w + \tilde{\epsilon}_v - \epsilon_c + \mathrm{i}\Gamma_v},
\end{aligned}$$

$$\begin{aligned}
\int \frac{\mathrm{d}w_1}{2\pi}\, G_c^{R,\mathrm{RPA}}(w_1) g_v^>(w_1 - w) &= \int \frac{\mathrm{d}w_1}{2\pi}\, \frac{1}{w_1 - \tilde{\epsilon}_c + \mathrm{i}\Gamma_c} (-2\pi\mathrm{i})(1 - n_v) \delta(w_1 - w - \epsilon_v) \\
&= \frac{-\mathrm{i}(1 - n_v)}{w + \epsilon_v - \tilde{\epsilon}_c + \mathrm{i}\Gamma_c}.
\end{aligned} \tag{C.6}$$

All together the result is

$$\Pi_{ph}^{R,\mathrm{RPA}+}(w) = |g|^2 \left[ \frac{1}{w + \tilde{\epsilon}_v - \tilde{\epsilon}_c + \mathrm{i}(\Gamma_c + \Gamma_v)} + \frac{-n_c}{w + \tilde{\epsilon}_v - \epsilon_c + \mathrm{i}\Gamma_v} + \frac{-(1 - n_v)}{w + \epsilon_v - \tilde{\epsilon}_c + \mathrm{i}\Gamma_c} \right]. \tag{C.7}$$

## C.4. Electron Propagators

Next we include randome phase corrections:

$$\begin{aligned}
G_c^{R,\mathrm{RPA}}(w) &= \frac{1}{(g_c^R)^{-1} - \Pi_c^{R(1)}} \\
&= \frac{1}{(w - \epsilon_c + \mathrm{i}0^+) + |g|^2 (1 - n_v) \Big( \int \mathrm{d}w_q \frac{\mathcal{N}_{ph}(w_q)}{w_q - w + \epsilon_v} + \mathrm{i}\pi N_{ph}(w - \epsilon_v) \Big)},
\end{aligned}$$

$$\begin{aligned}
G_c^{A,\mathrm{RPA}}(w) &= \frac{1}{(g_c^A)^{-1} - \Pi_c^{A(1)}} \\
&= \frac{1}{(w - \epsilon_c - \mathrm{i}0^+) + |g|^2 (1 - n_v) \Big( \int \mathrm{d}w_q \frac{\mathcal{N}_{ph}(w_q)}{w_q - w + \epsilon_v} - \mathrm{i}\pi N_{ph}(w - \epsilon_v) \Big)},
\end{aligned}$$

$$G_c^{<,\mathrm{RPA}}(w) = g_c^<(w) + \Big( G_c^{R,\mathrm{RPA}} \Pi_c^{<(1)} G_c^{A,\mathrm{RPA}} \Big)(w) = g_c^<(w). \tag{C.8}$$

For further calculations an approximation of the above expression is useful. Assuming that $N_{ph} \sim w_q^\gamma$ with $\gamma > 0$, allows an approximation of the real part of the self energy

as a small constant $\Sigma_c^R \sim |g|^2$ that is absorbed in the conduction electron level energy $\tilde{\epsilon}_c = \epsilon_c + \Sigma_c^R$. Obviously this neglects the nontrivial $w$-dependence. However since $\gamma > 0$ the expression is finite and positive. Since it amounts only to a small ($\sim |g|^2$) shift in the energy level, the qualitative physics should remain unaltered. Also the infinitesimal imaginary part in the denominator can be neglected, since the self energy provides a finite imaginary contribution to the denominator. The retarded propagator reads

$$G_c^{R,\mathrm{RPA}}(w) \approx \frac{1}{(w-\tilde{\epsilon}_c) - \mathrm{i}\pi|g|^2(1-n_v)\,N_{ph}(w-\epsilon_v)}. \tag{C.9}$$

Also, from the above equation it is clear that the imaginary part is only important, if $(w-\tilde{\epsilon}_c) \leq \pi|g|^2(1-n_v)\,N_{ph}(w-\epsilon_v)$, since the coupling constant is assumed to be small, this is only a small interval which allows to approximate the photon density of states a constant and therefore the imaginary part of the self energy also is a constant $\Gamma_c^R$. To avoid confusion a positive constants are introduced: $\Sigma_c \equiv -\Sigma_c^R = -\Sigma_c^A$ and $\Gamma_c \equiv -\Gamma_c^R = \Gamma_c^A$. Hence

$$\begin{aligned} G_c^{R,\mathrm{RPA}}(w) &\approx \frac{1}{(w-\tilde{\epsilon}_c) - \mathrm{i}\pi|g|^2(1-n_v)\,N_{ph}(\tilde{\epsilon}_c-\epsilon_v)} \\ &\equiv \frac{1}{w-\tilde{\epsilon}_c - \mathrm{i}\Gamma_c^R} \equiv \frac{1}{w-\tilde{\epsilon}_c+\mathrm{i}\Gamma_c}. \end{aligned} \tag{C.10}$$

The same approximation can be made for the valence electron propagator

$$\begin{aligned} G_c^{A,\mathrm{RPA}}(w) &\approx \frac{1}{(w-\tilde{\epsilon}_c) + \mathrm{i}\pi|g|^2(1-n_v)\,N_{ph}(\tilde{\epsilon}_c-\epsilon_v)} \\ &\equiv \frac{1}{w-\tilde{\epsilon}_c - \mathrm{i}\Gamma_c^A} \equiv \frac{1}{w-\tilde{\epsilon}_c-\mathrm{i}\Gamma_c}. \end{aligned} \tag{C.11}$$

Using the same approximations as for the conduction band, the valence band propagators read

$$\begin{aligned} G_v^{R,\mathrm{RPA}}(w) &= \frac{1}{(g_v^R)^{-1} - \Pi_v^R} = \frac{1}{(w-\epsilon_v+\mathrm{i}0^+) - |g|^2 n_c\Big(\int \mathrm{d}w_q \frac{\mathcal{N}_{ph}(w_q)}{w_q+w-\epsilon_c} - \mathrm{i}\pi N_{ph}(\epsilon_c-w)\Big)} \\ &\approx \frac{1}{w-\tilde{\epsilon}_v - \mathrm{i}\Gamma_v^R}, \\ G_v^{A,\mathrm{RPA}}(w) &= \frac{1}{(g_v^A)^{-1} - \Pi_v^A} = \frac{1}{(w-\epsilon_v-\mathrm{i}0^+) - |g|^2 n_c\Big(\int \mathrm{d}w_q \frac{\mathcal{N}_{ph}(w_q)}{w_q+w-\epsilon_c} + \mathrm{i}\pi N_{ph}(\epsilon_c-w)\Big)} \\ &\approx \frac{1}{w-\tilde{\epsilon}_v - \mathrm{i}\Gamma_v^A}, \\ G_c^{>,\mathrm{RPA}}(w) &= g_c^>(w) + \Big(G_c^{R,\mathrm{RPA}}\Pi_c^{>(1)}G_c^{A,\mathrm{RPA}}\Big)(w) = g_c^>(w). \end{aligned} \tag{C.12}$$

## C.5. Electron self energies

In this subsection we give a detailed derivation of the explicit expressions for the conduction and valence electron self energies. The derivation is analogous to the photon self energy calculations. We begin with comparing the first order conduction electron propagator with the Dyson equation:

$$\begin{aligned} G_c^{(1)}(t_1,t_2) &= \mathrm{i}|g|^2 \sum_{q_1} \int_C \mathrm{d}s_1\mathrm{d}s_2\, g^c(t_1,s_1)g^v(s_1,s_2)d(q_1;s_1,s_2)g^c(s_2,t_2) \\ &\equiv \int_C \mathrm{d}s_1\mathrm{d}s_2\; g^c(t_1,s_1)\Pi_c^{(1)}(s_1,s_2)g^c(s_2,t_2). \end{aligned} \tag{C.13}$$

The self energy on the Keldysh contour is thus

$$\Pi_c^{(1)}(s_1, s_2) = \mathrm{i}|g|^2 \sum_q g^v(s_1, s_2) d(q; s_1, s_2). \tag{C.14}$$

Assuming stationarity and going to real time allows us to use Fourier transformation:

$$\begin{aligned}\Pi_{c,ab}^{(1)}(t_1 - t_2) &= \mathrm{i}|g|^2 \sum_q \int g_{ab}^v(t_1 - t_2) d_{ab}(q; t_1 - t_2), \\ \Pi_{c,ab}^{(1)}(w) &= \mathrm{i}|g|^2 \sum_q \int \frac{\mathrm{d}w_1}{2\pi}\, g_{ab}^v(w_1) d_{ab}(q, w - w_1)\end{aligned} \tag{C.15}$$

All that is left to do is to plug in the explicit expressions for the free Green's functions (5.21). The algebra is sketched in the following lines:

$$\begin{aligned}\Pi_c^{T,(1)}(w) &= \mathrm{i}|g|^2 \sum_q \int \frac{\mathrm{d}w_1}{2\pi}\, g_{11}^v(w_1) d_{11}(q, w - w_1) \\ &= \mathrm{i}|g|^2 \int \mathrm{d}w_q \mathcal{N}_{ph}(w_q) \int \frac{\mathrm{d}w_1}{2\pi} \left( \frac{1 - n_v}{w_1 - \epsilon_v + \mathrm{i}0^+} + \frac{n_v}{w_1 - \epsilon_v - \mathrm{i}0^+} \right) \left( \frac{1}{w - w_1 - w_q + \mathrm{i}0^+} \right) \\ &= -|g|^2 \int \mathrm{d}w_q \mathcal{N}_{ph}(w_q) \left( \frac{1 - n_v}{w_q - w + \epsilon_v - 2\mathrm{i}0^+} \right), \\ \Pi_c^{<,(1)}(w) &= \mathrm{i}|g|^2 \sum_q \int \frac{\mathrm{d}w_1}{2\pi}\, g_{12}^v(w_1) d_{12}(q, w - w_1) = 0, \\ \Pi_c^{>,(1)}(w) &= \mathrm{i}|g|^2 \sum_q \int \frac{\mathrm{d}w_1}{2\pi}\, g_{21}^v(w_1) d_{21}(q, w - w_1) \\ &= \mathrm{i}|g|^2 \int \mathrm{d}w_q \mathcal{N}_{ph}(w_q) \int \frac{\mathrm{d}w_1}{2\pi} \Big( -2\pi\mathrm{i}(1 - n_v)\delta(w_1 - \epsilon_v) \Big) \Big( -2\pi\mathrm{i}\delta(w - w_1 - w_q) \Big) \\ &= -2\pi\mathrm{i}|g|^2 \mathcal{N}_{ph}(w - \epsilon_v)(1 - n_v), \\ \Pi_c^{\tilde{T},(1)}(w) &= \mathrm{i}|g|^2 \sum_q \int \frac{\mathrm{d}w_1}{2\pi}\, g_{22}^v(w_1) d_{22}(q, w - w_1) \\ &= \mathrm{i}|g|^2 \int \mathrm{d}w_q \mathcal{N}_{ph}(w_q) \int \frac{\mathrm{d}w_1}{2\pi} \left( \frac{n_v - 1}{w_1 - \epsilon_v - \mathrm{i}0^+} + \frac{-n_v}{w_1 - \epsilon_v + \mathrm{i}0^+} \right) \times \\ &\qquad \times \left( \frac{-1 - n_{ph}}{w - w_1 - w_q - \mathrm{i}0^+} + \frac{n_{ph}}{w - w_1 - w_q + \mathrm{i}0^+} \right) \\ &= |g|^2 \int \mathrm{d}w_q \mathcal{N}_{ph}(w_q) \left( \frac{1 + n_{ph} - n_v - n_v n_{ph}}{\epsilon_v - w + w_q + 2\mathrm{i}0^+} + \frac{n_v n_{ph}}{\epsilon_v - w + w_q - 2\mathrm{i}0^+} \right).\end{aligned} \tag{C.16}$$

All derivations of the valence electron propagators are analogous to the conduction electron propagators. We only state the results:

$$\begin{aligned}\Pi_v^{T,(1)}(w) &= -|g|^2 \int \mathrm{d}w_q \mathcal{N}_{ph}(w_q) \left( \frac{n_c}{\epsilon_c - w - w_q + 2\mathrm{i}0^+} \right), \\ \Pi_v^{<,(1)}(w) &= 2\pi\mathrm{i}|g|^2 \mathcal{N}_{ph}(\epsilon_c - w) n_c, \\ \Pi_v^{>,(1)}(w) &= \mathrm{i}|g|^2 \sum_q \int \frac{\mathrm{d}w_1}{2\pi}\, g_{21}^c(w_1) d_{12}(q, w_1 - w) = 0.\end{aligned} \tag{C.17}$$

## D. Source of squeezed light

This section contains detailed calculations complimentary to section 5.3. We begin with the derivation of the photon operator in the rotating frame. The equation of motion reads

$$\begin{aligned}
\dot{b}_{H,q}(t) &= \mathrm{i}\big[\big(H_{\mathrm{eff}}\big)_H, b_{H,q}\big] \\
&= -\mathrm{i}\Big(w_q + |g|^2\mathrm{e}^{2\eta t}X_q\Big)b_{H,q}(t) - \mathrm{i}g^*\mathrm{e}^{\eta t}\mathrm{e}^{-\mathrm{ieV}t}Y_q^\dagger(t) \\
&\quad + \mathrm{i}g\sum_{q_1}\mathrm{e}^{\eta t}\mathrm{e}^{\mathrm{ieV}t}[Y_{q_1}(t), b_{H,q}(t)]b_{H,q_1}(t) \\
&\quad + \mathrm{i}g^*\mathrm{e}^{\eta t}\mathrm{e}^{-\mathrm{ieV}t}\sum_{q_1}b_{H,q_1}^\dagger(t)[Y_{q_1}^\dagger(t), b_{H,q}(t)] \\
&\quad + (g^*)^2\mathrm{e}^{2\eta t}\mathrm{e}^{-2\mathrm{ieV}t}(Z_q^* + Z_{-q}^*)b_{H,-q}^\dagger(t). \qquad \text{(D.1)}
\end{aligned}$$

Next we go to the rotating frame $b_{H,q}(t) \equiv \mathrm{e}^{-\mathrm{i}w_q t}b_q(t)$ and find

$$\begin{aligned}
\dot{b}_q(t) &= -\mathrm{i}|g|^2\mathrm{e}^{2\eta t}X_q b_q(t) - \mathrm{i}g^*\mathrm{e}^{\eta t}Y_q^\dagger(t)\mathrm{e}^{-\mathrm{ieV}t}\mathrm{e}^{\mathrm{i}w_q t} \\
&\quad + \mathrm{i}g\sum_{q_1}\mathrm{e}^{\eta t}\mathrm{e}^{\mathrm{ieV}t}[Y_{q_1}(t), b_q(t)]b_{q_1}(t)\mathrm{e}^{-\mathrm{i}w_{q_1}t} \\
&\quad + \mathrm{i}g^*\mathrm{e}^{\eta t}\mathrm{e}^{-\mathrm{ieV}t}\sum_{q_1}b_{q_1}^\dagger(t)\mathrm{e}^{\mathrm{i}w_{q_1}t}[Y_{q_1}^\dagger(t), b_q(t)] \\
&\quad + (g^*)^2\mathrm{e}^{2\eta t}\mathrm{e}^{-2\mathrm{ieV}t}(Z_q^* + Z_{-q}^*)b_{-q}^\dagger(t)\mathrm{e}^{2\mathrm{i}w_q t} \\
&= -\mathrm{i}|g|^2\mathrm{e}^{2\eta t}X_q b_q(t) - \mathrm{i}g^*\mathrm{e}^{\eta t}\mathrm{e}^{\mathrm{i}(w_q-\mathrm{eV})t}Y_q^\dagger(t) \\
&\quad + \mathrm{i}g\sum_{q_1}\mathrm{e}^{\eta t}\mathrm{e}^{-\mathrm{i}(w_{q_1}-\mathrm{eV})t}[Y_{q_1}(t), b_q(t)]b_{q_1}(t) \\
&\quad + \mathrm{i}g^*\mathrm{e}^{\eta t}\sum_{q_1}\mathrm{e}^{\mathrm{i}(w_{q_1}-\mathrm{eV})t}b_{q_1}^\dagger(t)[Y_{q_1}^\dagger(t), b_q(t)] \\
&\quad + (g^*)^2\mathrm{e}^{2\eta t}\mathrm{e}^{2\mathrm{i}(w_q-\mathrm{eV})t}(Z_q^* + Z_{-q}^*)b_{-q}^\dagger(t). \qquad \text{(D.2)}
\end{aligned}$$

Formal integration $\int_{t_0}^t \mathrm{d}t'$ and recursive substitution lead to

$$\begin{aligned}
b_q(t) &= b_{q,0} - \mathrm{i}|g|^2X_q b_{q,0}\int_{t_0}^t \mathrm{d}t'\,\mathrm{e}^{2\eta t'} - \mathrm{i}g^*\int_{t_0}^t \mathrm{d}t'\,\mathrm{e}^{\eta t'}\mathrm{e}^{\mathrm{i}(w_q-\mathrm{eV})t'}Y_q^\dagger(t') \\
&\quad + \mathrm{i}g\sum_{q_1}\int_{t_0}^t \mathrm{d}t'\,\mathrm{e}^{\eta t'}\mathrm{e}^{-\mathrm{i}(w_{q_1}-\mathrm{eV})t'}[Y_{q_1}(t'), b_q(t')]b_{q_1}(t') \\
&\quad + \mathrm{i}g^*\sum_{q_1}\int_{t_0}^t \mathrm{d}t'\,\mathrm{e}^{\eta t'}\mathrm{e}^{\mathrm{i}(w_{q_1}-\mathrm{eV})t'}b_{q_1}^\dagger(t')[Y_{q_1}^\dagger(t'), b_q(t')] \\
&\quad + (g^*)^2(Z_q^* + Z_{-q}^*)b_{-q,0}^\dagger\int_{t_0}^t \mathrm{d}t'\,\mathrm{e}^{2\eta t'}\mathrm{e}^{2\mathrm{i}(w_q-\mathrm{eV})t'} + O(|g|^3) \\
&= b_{q,0} - \mathrm{i}g^*\int_{t_0}^t \mathrm{d}t'\,\mathrm{e}^{\eta t'}\mathrm{e}^{\mathrm{i}(w_q-\mathrm{eV})t'}Y_q^\dagger(t') + O(|g|^2) \qquad \text{(D.3)}
\end{aligned}$$

Recursive iteration gives

$$\begin{aligned}
b_q(t) &= b_{q,0} - \mathrm{i}|g|^2X_q b_{q,0}\int_{t_0}^t \mathrm{d}t'\,\mathrm{e}^{2\eta t'} - \mathrm{i}g^*\int_{t_0}^t \mathrm{d}t'\,\mathrm{e}^{\eta t'}\mathrm{e}^{\mathrm{i}(w_q-\mathrm{eV})t'}Y_q^\dagger(t') \\
&\quad + |g|^2\sum_{q_1}\int_{t_0}^t \mathrm{d}t'\,\mathrm{e}^{\eta t'}\mathrm{e}^{-\mathrm{i}(w_{q_1}-\mathrm{eV})t'}\int_{t_0}^{t'} \mathrm{d}t''\,\mathrm{e}^{\eta t''}\mathrm{e}^{\mathrm{i}(w_q-\mathrm{eV})t''}[Y_{q_1}(t'), Y_q^\dagger(t'')]b_{q_1}(t') \\
&\quad - \mathrm{i}(g^*)^2(Z_q^* + Z_{-q}^*)b_{-q,0}^\dagger\int_{t_0}^t \mathrm{d}t'\,\mathrm{e}^{2\eta t'}\mathrm{e}^{2\mathrm{i}(w_q-\mathrm{eV})t'} + O(|g|^3). \qquad \text{(D.4)}
\end{aligned}$$

We then go back into the Heisenberg picture

$$
\begin{aligned}
b_{H,q}(t) = b_{q,0}\mathrm{e}^{-\mathrm{i}w_q t} &- \mathrm{i}|g|^2\mathrm{e}^{2\eta t}X_q b_{q,0}\int_{t_0}^{t}\mathrm{d}t'\,\mathrm{e}^{-\mathrm{i}w_q t}\\
&- \mathrm{i}g^*\int_{t_0}^{t}\mathrm{d}t'\,\mathrm{e}^{\eta t'}\mathrm{e}^{\mathrm{i}(w_q-\mathrm{eV})t'}Y_q^\dagger(t')\mathrm{e}^{-\mathrm{i}w_q t}\\
&+ |g|^2\int_{t_0}^{t}\mathrm{d}t'\,\mathrm{e}^{\eta t'}\mathrm{e}^{-\mathrm{i}(w_q-\mathrm{eV})t'}\int_{t_0}^{t'}\mathrm{d}t''\,\mathrm{e}^{\eta t''}\mathrm{e}^{\mathrm{i}(w_q-\mathrm{eV})t''}[Y_q(t'),Y_q^\dagger(t'')]b_q(t')\mathrm{e}^{-\mathrm{i}w_q t}\\
&- \mathrm{i}(g^*)^2(Z_q^*+Z_{-q}^*)b_{-q,0}^\dagger\int_{t_0}^{t}\mathrm{d}t'\,\mathrm{e}^{2\eta t'}\mathrm{e}^{2\mathrm{i}(w_q-\mathrm{eV})t'}\mathrm{e}^{-\mathrm{i}w_q t}+O(|g|^2). \qquad \text{(D.5)}
\end{aligned}
$$

The commutator of the $Y$ operators is given by

$$
\begin{aligned}
[Y_{q_1}(t_1),Y_{q_2}^\dagger(t_2)] = \sum_{k,k_1,\sigma,\sigma_1}\Bigg[\Bigg(&u_{c,\sigma k}^* u_{v,\sigma(k-q_1)}\mathrm{e}^{\mathrm{i}(E_{c,k}-E_{v,k-q_1})t_1}\gamma_{c,k,\sigma,0}^\dagger\gamma_{v,k-q_1,\sigma,0}\\
&- v_{c,\sigma k}^* v_{v,\sigma(k+q_1)}\mathrm{e}^{-\mathrm{i}(E_{c,k}-E_{v,(k+q_1)})t_1}\gamma_{v,(k+q_1),\sigma,0}^\dagger\gamma_{c,k,\sigma,0}\\
&+ \sigma v_{c,\sigma k}^* u_{v,\sigma(k+q_1)}\mathrm{e}^{-\mathrm{i}(E_{c,k}+E_{v,-k-q_1})t_1}\gamma_{c,k,\sigma,0}\gamma_{v,-k-q_1,\bar\sigma,0}\\
&+ \sigma u_{c,\sigma k}^* v_{v,\sigma(k-q_1)}\mathrm{e}^{\mathrm{i}(E_{c,k}+E_{v,q_1-k})t_1}\gamma_{v,q_1-k,\bar\sigma,0}^\dagger\gamma_{c,k,\sigma,0}^\dagger\Bigg),\\
&\Bigg(u_{c,\sigma_1 k_1}u_{v,\sigma_1(k_1-q_2)}^*\mathrm{e}^{-\mathrm{i}(E_{c,k_1}-E_{v,k_1-q_2})t_2}\gamma_{v,k_1-q_2,\sigma_1,0}^\dagger\gamma_{c,k_1,\sigma_1,0}\\
&- v_{c,\sigma_1 k_1}v_{v,\sigma_1(k_1+q_2)}^*\mathrm{e}^{\mathrm{i}(E_{c,k_1}-E_{v,(k_1+q_2)})t_2}\gamma_{c,k_1,\sigma_1,0}^\dagger\gamma_{v,(k_1+q_2),\sigma_1,0}\\
&+ \sigma_1 v_{c,\sigma_1 k_1}u_{v,\sigma_1(k_1+q_2)}^*\mathrm{e}^{\mathrm{i}(E_{c,k_1}+E_{v,-k_1-q_2})t_2}\gamma_{v,-k_1-q_2,\bar\sigma_1,0}^\dagger\gamma_{c,k_1,\sigma_1,0}^\dagger\\
&+ \sigma_1 u_{c,\sigma_1 k_1}v_{v,\sigma_1(k_1-q_2)}^*\mathrm{e}^{-\mathrm{i}(E_{c,k_1}+E_{v,q_2-k_1})t_2}\gamma_{c,k_1,\sigma_1,0}\gamma_{v,q_2-k_1,\bar\sigma_1,0}\Bigg)\Bigg]\delta_{q_1,q_2}\\
= \sum_{k,\sigma}\Bigg[&|u_{c,\sigma k}|^2|u_{v,\sigma(k-q)}|^2(n_{c,k,\sigma}-n_{v,k-q,\sigma})\mathrm{e}^{\mathrm{i}(E_{c,k}-E_{v,k-q})(t_1-t_2)}\\
&- |v_{c,\sigma k}|^2|v_{v,\sigma(k+q)}|^2(n_{c,k,\sigma}-n_{v,k+q,\sigma})\mathrm{e}^{-\mathrm{i}(E_{c,k}-E_{v,k+q})(t_1-t_2)}\\
&+ |v_{c,\sigma k}|^2|u_{v,\sigma(k+q)}|^2(1-n_{c,k,\sigma}-n_{v,-k-q,\bar\sigma})\mathrm{e}^{-\mathrm{i}(E_{c,k}+E_{v,-k-q})(t_1-t_2)}\\
&- |u_{c,\sigma k}|^2|v_{v,\sigma(k-q)}|^2(1-n_{c,k,\sigma}-n_{v,q-k,\bar\sigma})\mathrm{e}^{\mathrm{i}(E_{c,k}+E_{v,q-k})(t_2-t_1)}\Bigg]\delta_{q_1,q_2}\\
= \sum_{k,\sigma}\Bigg[&\alpha_{q,k,\sigma}(n_{c,k,\sigma}-n_{v,k-q,\sigma})\mathrm{e}^{\mathrm{i}(E_{c,k}-E_{v,k-q})(t_1-t_2)}\\
&- \beta_{-q,k,\sigma}(n_{c,k,\sigma}-n_{v,k+q,\sigma})\mathrm{e}^{-\mathrm{i}(E_{c,k}-E_{v,k+q})(t_1-t_2)}\\
&+ \delta_{-q,k,\sigma}(1-n_{c,k,\sigma}-n_{v,-k-q,\bar\sigma})\mathrm{e}^{-\mathrm{i}(E_{c,k}+E_{v,-k-q})(t_1-t_2)}\\
&- \zeta_{q,k,\sigma}(1-n_{c,k,\sigma}-n_{v,q-k,\bar\sigma})\mathrm{e}^{\mathrm{i}(E_{c,k}+E_{v,q-k})(t_2-t_1)}\Bigg]\delta_{q_1,q_2} \qquad \text{(D.6)}
\end{aligned}
$$

Here we have used Greek letters

$$\begin{aligned}
\alpha_{q,k,\sigma} &\equiv |u_{c,\sigma k}|^2 |u_{v,\sigma(k-q)}|^2, \\
\beta_{q,k,\sigma} &\equiv |v_{c,\sigma k}|^2 |v_{v,\sigma(k-q)}|^2, \\
\chi_{q,k,\sigma} &\equiv u^*_{c,\sigma k} v^*_{c,\sigma k} u_{v,\sigma(k-q)} v_{v,\sigma(k-q)}, \\
\delta_{q,k,\sigma} &\equiv |v_{c,\sigma k}|^2 |u_{v,\sigma(k-q)}|^2, \\
\zeta_{q,k,\sigma} &\equiv |u_{c,\sigma k}|^2 |v_{v,\sigma(k-q)}|^2,
\end{aligned} \tag{D.7}$$

to write the various combinations of coherence factors in a compact way. We continue with the evaluation of the equation of motion

$$\begin{aligned}
&\int_{t_0}^{t} \mathrm{d}t_1 \, \mathrm{e}^{\eta t_1} \mathrm{e}^{-\mathrm{i}(w_q - \mathrm{eV})t_1} \int_{t_0}^{t_1} \mathrm{d}t_2 \, \mathrm{e}^{\eta t_2} \mathrm{e}^{\mathrm{i}(w_q - \mathrm{eV})t_2} [Y_q(t_1), Y_q^\dagger(t_2)] - \mathrm{i} X_q \int_{t_0}^{t} \mathrm{d}t' \, \mathrm{e}^{2\eta t'} \\
&= \mathrm{i} \frac{\mathrm{e}^{2\eta t}}{2\eta} \sum_{k,\sigma} \Bigg[ \alpha_{q,k,\sigma} (n_{c,k,\sigma} - n_{v,k-q,\sigma}) \frac{1}{w_q - \mathrm{eV} - E_c + E_v + \mathrm{i}\eta} \\
&\qquad - \beta_{-q,k,\sigma} (n_{c,k,\sigma} - n_{v,k+q,\sigma}) \frac{1}{w_q - \mathrm{eV} + E_c - E_v + \mathrm{i}\eta} \\
&\qquad + \delta_{-q,k,\sigma} (1 - n_{c,k,\sigma} - n_{v,-k-q,\bar{\sigma}}) \frac{1}{w_q - \mathrm{eV} + E_c + E_v + \mathrm{i}\eta} \\
&\qquad - \zeta_{q,k,\sigma} (1 - n_{c,k,\sigma} - n_{v,q-k,\bar{\sigma}}) \frac{1}{w_q - \mathrm{eV} - E_c - E_v + \mathrm{i}\eta}, \Bigg]
\end{aligned} \tag{D.8}$$

approximate $|k| \gg |q|$ and write $\tilde{w}_q \equiv w_q - \mathrm{eV}$ to get

$$\begin{aligned}
&\approx \mathrm{i} \frac{\mathrm{e}^{2\eta t}}{2\eta} \sum_{k} \Bigg[ \alpha_k \frac{n_{c,k} - n_{v,k}}{\tilde{w}_q - E_c + E_v + \mathrm{i}\eta} - \beta_k \frac{n_{c,k} - n_{v,k}}{\tilde{w}_q + E_c - E_v + \mathrm{i}\eta} \\
&\qquad + \delta_k \frac{1 - n_{c,k} - n_{v,k}}{\tilde{w}_q + E_c + E_v + \mathrm{i}\eta} - \zeta_k \frac{1 - n_{c,k} - n_{v,k}}{\tilde{w}_q - E_c - E_v + \mathrm{i}\eta} \Bigg].
\end{aligned} \tag{D.9}$$

All together the result is

$$\begin{aligned}
b_q(t) \approx b_{q,0} &- g^* \sum_{k,\sigma} \Bigg( u_{c,k} u^*_{v,k} \frac{\mathrm{e}^{\mathrm{i}(\tilde{w}_q - E_c + E_v - \mathrm{i}\eta)t}}{\tilde{w}_q - E_c + E_v - \mathrm{i}\eta} \gamma^\dagger_{v,k-q,\sigma,0} \gamma_{c,k,\sigma,0} \\
&\qquad - v_{c,k} v^*_{v,k} \frac{\mathrm{e}^{\mathrm{i}(\tilde{w}_q + E_c - E_v - \mathrm{i}\eta)t}}{\tilde{w}_q + E_c - E_v - \mathrm{i}\eta} \gamma^\dagger_{c,k,\sigma,0} \gamma_{v,k+q,\sigma,0} \\
&\qquad + \sigma v_{c,k} u^*_{v,k} \frac{\mathrm{e}^{\mathrm{i}(\tilde{w}_q + E_c + E_v - \mathrm{i}\eta)t}}{\tilde{w}_q + E_c + E_v - \mathrm{i}\eta} \gamma_{v,-q-k,\bar{\sigma},0} \gamma_{c,k,\sigma,0} \\
&\qquad + \sigma u_{c,k} v^*_{v,k} \frac{\mathrm{e}^{\mathrm{i}(\tilde{w}_q - E_c - E_v - \mathrm{i}\eta)t}}{\tilde{w}_q - E_c - E_v - \mathrm{i}\eta} \gamma^\dagger_{c,k,\sigma,0} \gamma^\dagger_{v,q-k,\bar{\sigma},0} \Bigg) \\
&+ \mathrm{i}|g|^2 \frac{\mathrm{e}^{2\eta t}}{2\eta} \sum_{k} \Bigg[ \alpha_k \frac{n_{c,k} - n_{v,k}}{\tilde{w}_q - E_c + E_v + \mathrm{i}\eta} - \beta_k \frac{n_{c,k} - n_{v,k}}{\tilde{w}_q + E_c - E_v + \mathrm{i}\eta} \\
&\qquad + \delta_k \frac{1 - n_{c,k} - n_{v,k}}{\tilde{w}_q + E_c + E_v + \mathrm{i}\eta} - \zeta_k \frac{1 - n_{c,k} - n_{v,k}}{\tilde{w}_q - E_c - E_v + \mathrm{i}\eta} \Bigg] b_{q,0} \\
&- (g^*)^2 Z_q^* \frac{\mathrm{e}^{2\mathrm{i}(\tilde{w}_q - \mathrm{i}\eta)t}}{\tilde{w}_q - \mathrm{i}\eta} b^\dagger_{-q,0} + O(|g|^3).
\end{aligned} \tag{D.10}$$

For clarity we introduce the operator $\mathcal{Y}_q$ that contains all fermionic contributions and the c-valued parameter $M_q$:

$$b_q(t) = b_{q,0} - g^* \mathcal{Y}_q^\dagger(t) + \mathrm{i}|g|^2 \frac{\mathrm{e}^{2\eta t}}{2\eta} M_q(t) b_{q,0} - (g^*)^2 Z_q^* \frac{\mathrm{e}^{2\mathrm{i}(\tilde{w}_q - \mathrm{i}\eta)t}}{\tilde{w}_q - \mathrm{i}\eta} b_{-q,0}^\dagger + O(|g|^2). \tag{D.11}$$

The anomalous expectation value reads

$$\begin{aligned}\left\langle b_q b_{-q} \right\rangle &= (g^*)^2 \langle \mathcal{Y}_q^\dagger(t) \mathcal{Y}_q^\dagger(t) \rangle - (g^*)^2 Z_q^* \frac{\mathrm{e}^{2\mathrm{i}(\tilde{w}_q - \mathrm{i}\eta)t}}{\tilde{w}_q - \mathrm{i}\eta} \langle b_{-q,0}^\dagger b_{-q,0} + b_{q,0} b_{q,0}^\dagger \rangle \\ &= (g^*)^2 \langle \mathcal{Y}_q^\dagger(t) \mathcal{Y}_{-q}^\dagger(t) \rangle - (g^*)^2 Z_q^* \frac{\mathrm{e}^{2\mathrm{i}(\tilde{w}_q - \mathrm{i}\eta)t}}{\tilde{w}_q - \mathrm{i}\eta}. \end{aligned} \tag{D.12}$$

The first term is explicitly given by

$$\begin{aligned}\langle \mathcal{Y}_q^\dagger(t) \mathcal{Y}_{-q}^\dagger(t) \rangle = \sum_{k,\sigma} \Bigg( &- \chi_k (n_{v,k-q,\sigma} - n_{c,k,\sigma}) \frac{\mathrm{e}^{2\mathrm{i}(\tilde{w}_q - \mathrm{i}\eta)t}}{(\tilde{w}_q - \mathrm{i}\eta)^2 - (E_c - E_v)^2} \\ &+ \chi_k (1 - n_{v,k,\bar{\sigma}} - n_{c,k,\sigma}) \frac{\mathrm{e}^{2\mathrm{i}(\tilde{w}_q - \mathrm{i}\eta)t}}{(\tilde{w}_q - \mathrm{i}\eta)^2 - (E_c + E_v)^2} \Bigg). \end{aligned} \tag{D.13}$$

If we use the same approximations as in section 5.2.7 we find

$$\langle \mathcal{Y}_q^\dagger(t) \mathcal{Y}_{-q}^\dagger(t) \rangle = 2\pi\Delta \mathrm{e}^{\mathrm{i}\arg(\chi)} \frac{\mathrm{e}^{2\mathrm{i}(\tilde{w}_q - \mathrm{i}\eta)t}}{(\tilde{w}_q - \mathrm{i}\eta)^2 - (2\Delta)^2},$$

$$Z_q = 2\pi\Delta \mathrm{e}^{\mathrm{i}\arg(\chi)} \left( \frac{1}{\tilde{w}_q - 2\Delta + \mathrm{i}\eta} + \frac{1}{\tilde{w}_q + 2\Delta + \mathrm{i}\eta} \right), \tag{D.14}$$

and finally

$$\left\langle b_q b_{-q} \right\rangle = 2\pi (g^*)^2 \Delta \mathrm{e}^{\mathrm{i}\arg(\chi)} \frac{1}{(2\Delta)^2 - (\tilde{w}_q - \mathrm{i}\eta)^2} \mathrm{e}^{2\mathrm{i}(\tilde{w}_q - \mathrm{i}\eta)t}. \tag{D.15}$$